X-RAY DIFFRACTION STUDIES OF SILICON AND MERCURY COMPLEXES WITH ORGANIC LIGANDS

A Thesis

presented by

Valerie Anne Brookeman, B.Sc.

to the

University of St. Andrews

in application for the Degree

of Doctor of Philosophy.

DECLARATION

I hereby declare that this thesis has been composed by me, is a record of work done by me, and has not previously been presented for a Higher Degree.

The work was carried out in the research laboratories of the Physics Department, St. Salvator's College, University of St. Andrews, under the supervision of Dr. R.C.G. Killean.

Valerie A. Brookeman

CAREER

In July 1965 I graduated with 1st class B.Sc. honours in Physics at St. Salvator's College, University of St. Andrews. In October 1965 with the award of a Science Research Council studentship I was enrolled under general Ordinance 12 as a research student in the Physics Department, University of St. Andrews. In October 1966 I was transferred to Ordinance 16 as a candidate for the degree of Ph.D.

CERTIFICATE

I certify that Valerie Anne Brookeman (née Bain),B.Sc., has spent nine terms at research work in the Physical Laboratory of St. Salvator's College, University of St. Andrews, under my direction, that she has fulfilled the conditions of Ordinance No. 16 (St. Andrews) and that she is qualified to submit the accompanying thesis in application for the Degree of Doctor of Philosophy.

Research Supervisor.

Acknowledgements

The author's thanks are due to Dr. R.C.G. Killean and Dr. D.F. Grant for guidance, advice and discussion. She also wishes to thank Professor J.F. Allen, F.R.S. for his encouragement and the research facilities, and Dr. D. Calvert and Dr. M. Webster for preparing the crystals and for their interest and help. The author is grateful to the staff of the Computing Laboratory for their help with the use of the IBM 1620 computer and to Mrs. Janice Page for her assistance with the photographic work and the preparation of the diagrams and tables.

Contents

1. THEORY

1.1 Introduction

The purpose of crystal structure analysis by x-ray diffraction is to postulate a molecular structure whose diffraction spectra match the experimentally obtained set. The principles used are essentially those of physical optics since the x-ray diffraction pattern obtained is the Fourier transform of the object, and a subsequent inverse transform of the diffraction pattern will give the image.

The diffraction pattern is a map of the reciprocal lattice of the crystal; a plane [h,k,l] in real space diffracts x-rays to form the reflection (h,k,l) in reciprocal space, the reciprocal lattice vector $\underline{h}(h,k,l)$ being normal to the plane [h,k,l] of the crystal lattice and of magnitude 1/d where d is the spacing of (h,k,l) planes in the real lattice.

The cyclic nature may be represented schematically as follows:

object	$\longrightarrow$	diffraction pattern	$\longrightarrow$	image
real space	$\longrightarrow$	reciprocal space	$\longrightarrow$	real space
$\rho(\underline{r})$	$\longrightarrow$	$F(\underline{h}) = T[\rho(\underline{r})]$	$\longrightarrow$	$\rho(\underline{r}) = T^{-1}[F(\underline{h})]$

$\underline{r}(x,y,z)$ = vector in real space

$\underline{h}(h,k,l)$ = vector in reciprocal space

T ≡ Fourier transform

T^{-1} ≡ inverse Fourier transform

$F(\underline{h})$ = vector amplitude of the radiation scattered by the crystal and received at the point $\underline{h}$ in reciprocal space

$$= V \int_{x,y,z=0}^{1} \rho(\underline{r}) \exp 2\pi i\, \underline{h}.\underline{r}\, dV \qquad (1)$$

where V = volume of the unit cell; $\rho(\underline{r})$ is the electron density at point $\underline{r}$ in the crystal, and since the crystal is periodic in three dimensions may be represented by a three dimensional Fourier series:

$$\rho(\underline{r}) = 1/V \sum_{h} \sum_{k=-\infty}^{+\infty} \sum_{l} F(\underline{h}) \exp -2\pi i\, \underline{h}.\underline{r} \qquad (2)$$

The structure factor $F(\underline{h})$ is also represented by the equation:

$$F(\underline{h}) = \sum_{j=1}^{N} f_j(\underline{h}) \exp 2\pi i\, \underline{h}.\underline{r}_j \qquad (3)$$

where N = number of atoms in the unit cell

$$f_j(\underline{h}) = V \int_{x,y,z=0}^{1} \rho(\underline{r}-\underline{r}_j) \exp 2\pi i\, \underline{h}.(\underline{r}-\underline{r}_j)\, dV$$

= scattering factor or form factor for the j^{th} atom at position $\underline{r}_j$ (fractional coordinates x_j, y_j, z_j)

$$F(\underline{h}) = \sum_{j=1}^{N} f_j \cos 2\pi\, \underline{h}.\underline{r}_j + i \sum_{j=1}^{N} f_j \sin 2\pi\, \underline{h}.\underline{r}_j$$

$$= A + iB$$

$$= |F(\underline{h})| \exp i\,\phi$$

Thus the structure factor $F(\underline{h})$ is seen to be a complex quantity with magnitude $|F(\underline{h})|$ and phase $\phi = \tan^{-1} B/A$. It is only possible to measure the intensity (=(Amplitude)^2) of the diffracted x-rays, and hence obtain a value for the structure factor magnitude $|F(\underline{h})|$ but not for its phase $\phi_{h,k,l}$. Without knowledge of the phases, equation (2) above cannot be used in determining a representation

of the molecular structure.

However by using a Fourier summation with the squared amplitudes as coefficients, this problem may be overcome since $|F(\underline{h})|^2$ for any reflection is directly proportional to the observed intensity. The relationship of the Patterson function (Patterson, 1934 and 1935), as this synthesis is called, to the electron density function of the crystal may be found by applying the Convolution Theorem.

$$T[F(\underline{h})F^*(\underline{h})] = V \int_0^1\int_0^1\int_0^1 \rho(\underline{r})\rho(\underline{r}-\underline{r}')dV = P(\underline{r}') = 1/V \sum_{h}^{+\infty}\sum_{k}^{+\infty}\sum_{l}^{+\infty} |F(\underline{h})|^2 \exp 2\pi i\, \underline{h}.\underline{r}'$$

Since $|F(\underline{h})| = |F(\overline{\underline{h}})|$ by Friedel's Law, the Patterson function may be represented by the series:

$$P(u,v,w) = 1/v \sum_{h}^{+\infty}\sum_{k}^{+\infty}\sum_{l} |F(\underline{h})|^2 \cos 2\pi(hu+kv+lw) \qquad (4)$$

(u,v,w are fractional coordinates)

Thus, a centrosymmetric set of interatomic vectors can be obtained from the measured intensities which has N(N-1)/2 unique vector peaks where N = number of atoms. The interpretation of this vector map is difficult if N is large and is much simplified if "heavy" atoms with high atomic number $\overline{Z}$ are present in the molecule. Since the size of each vector peak in the Patterson map is proportional to the product of the scattering factors for the two atoms concerned, the largest peaks can be identified and the positions of the heavy atoms in the crystal lattice found. This is the method used for the solution of the molecular structure of tetrachlorobispyridinesilicon (IV) ($SiCl_4$,2Py) and described in Chapter 4.

In the investigation of tetrafluorobispyridinesilicon IV (SiF_4,2Py)

discussed in Chapter 3 where apart from the Silicon atom, no one atom is much heavier than any other, use was made of the expected relative orientation of atoms and interatomic distances to interpret the Patterson vector set and position some of the atoms. The total scattering power of the atoms thus located was large enough for the investigation to proceed along the same lines as the "heavy atom method".

The structure factor for any reflection as given by equation (3) may be expanded in the form

$$F(\underline{h}) = \sum_{1}^{M_1} f_H \exp 2\pi i(hx_H+ky_H+lz_H) + \sum_{1}^{M_2} f_L \exp 2\pi i(hx_L+ky_L+lz_L)$$

$$= F_H + F_L$$

where F_H = contribution from the M_1 heavy atoms

F_L = contribution from the remaining $M_2 = N-M_1$ light atoms

F_H is the dominant term in the expression for $F(\underline{h})$ since $f_H > f_L$, and can be evaluated using the heavy atom coordinates $(x_H y_H z_H)$ found from the Patterson map. Thus the phase ϕ of $F(\underline{h})$ will be determined mainly by the phase contribution ϕ_H, from the heavy atoms, as shown vectorally in the Argand diagram:

$$\phi = \phi_H + \phi_L$$

$$\approx \phi_H$$

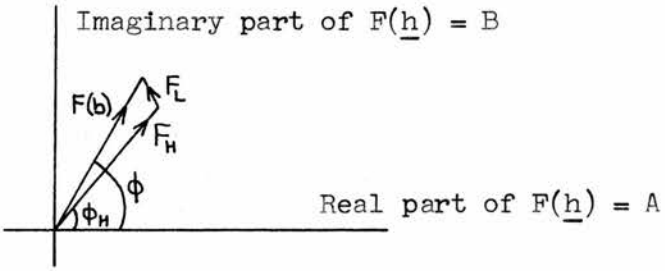

The calculated phases ϕ_H are almost equal to the true phases ϕ and are assigned to the experimentally obtained set of structure

amplitudes $|F_o(\underline{h})|$. Using the structure factors $|F_o(\underline{h})| \exp i \phi_H$ in equation (2), a Fourier synthesis of the electron density is computed, which will be sufficiently correct to indicate the positions of the remaining atoms within the unit cell. The final electron density distribution throughout the unit cell obtained from equation (2) is not a perfect image of the object due to termination effects in not summing the series from $-\infty$ to $+\infty$, and due to errors in estimation of structure amplitudes $|F_o|$ from both experimental measurement and physical factors.

1.2 The observed structure amplitude $|F_o(\underline{h})|$

The quantity actually measured in x-ray diffraction experiments, either by photographic or diffractometer techniques, gives the integrated intensity $I(\underline{h})$ of the diffracted beam for each reflection. This is related to the structure amplitude $|F_o(\underline{h})|$ by the following expression, which has its basis in the Thomson theory of the scattering of x-rays by electrons, with subsequent deductions by Bragg, James and Bosanquet (1921).

$$I(\underline{h}) = E(\underline{h})w/I_o = Q\,dV = \left(N^2\lambda^3 e^4/m^2c^4\right) \times L_p\, F_o(\underline{h})^2 dV \quad (5)$$

where $E(\underline{h})$ = total diffracted energy at $\underline{h}$

I_o = intensity of the incident x-ray beam

δv = volume of crystal bathed in x-rays

(assumed so small that absorption effects may be neglected)

w = angular velocity of the crystal, which must be rotated through the region of the Bragg reflection

because of the mosaic structure of the crystal.

N = number of unit cells per unit volume

The Polarisation factor $p = \frac{1}{2}(1+\cos^2 2\theta)$ is introduced since the original expression assumed plane polarised incident x-rays. In fact, the characteristic incident beam from the target is unpolarised with a consequent reduction in the diffracted intensity by the factor p, which is independent of the experimental geometry.

The Lorentz factor L is a measure of the relative time opportunity for the various crystal planes to reflect x-rays, and is therefore dependent on the experimental method.

For equi-inclination Weissenberg geometry, which was used for all data collection reported in this thesis, the Lorentz factor can be shown to be $1/\cos^2\mu\sin\Upsilon$ where the axis of rotation of the crystal makes angle $(\pi/2 - \mu)$ with the incident beam and Υ is the projection on the zero level of the angle 2θ between incident and reflected beams.

Thus, for one particular crystal using radiation of wavelength λ, equation (5) may be rewritten simply as:

$$|F_o(\underline{h})|^2 = \text{constant } x(Lp)^{-1}I(\underline{h}) \qquad (6)$$

A set of relative structure amplitudes may therefore be obtained for use in equation (4).

1.3 The atomic scattering factor

The scattering factor f_j used in calculating $F_c(\underline{h})$ from equation (3) is a measure of the efficiency of the j^{th} atom in scattering x-rays

and is defined such that the atom scatters f times as much as a single electron. It is a function of $\sin\theta/\lambda$ and as θ increases, f_j decreases because waves scattered by electrons in different parts of the atom interfere destructively. As $\theta \longrightarrow 0$, $f_j \longrightarrow Z_j$, the number of electrons in the atom or ion.

Estimates of atomic scattering factor curves f_{oj} have been calculated for most atoms using various atomic models (International Tables for X-Ray Crystallography, Vol. III, p. 201) but these all assume that the atom is at rest and that the electron density has a spherically symmetric distribution.

The form factor f_{oj} for the j^{th} atom at rest must be modified to take account of the thermal motion due to temperature. The effect of thermal vibrations is to reduce the structure factor $F_c(\underline{h})$ because two equivalent atoms will no longer scatter in phase, since displaced from their true positions. A more realistic scattering factor is:

$$f_j = f_{oj} \exp(-B \sin^2\theta/\lambda^2) \qquad (7)$$

The temperature factor $B = 8\pi^2 \overline{u_j^2}$ where $\overline{u_j^2}$ is the mean square atomic displacement (Debye, 1914 and Waller, 1927). B is not easily calculated theoretically and may be found for each atom by comparing $|F_o(\underline{h})|$ with $|F_c(\underline{h})|$ for successive refinements of a trial structure or obtained from an electron density map (Hamilton, 1955).

The scale and temperature factors may also be found by Wilson's Method (1942) or by taking a compromise between Wilson's plot and

another auxiliary curve. (Rogers, 1954). Rogers (1965) has considered isolating the origin peak of the Patterson, the source of Wilson's equation, and transforming it to minimise the effects of off-diagonal terms.

Although expression (7) is sufficiently accurate in the early stages of structure determination, it does assume isotropic thermal vibration, and during subsequent refinement must be replaced by a more realistic expression, assuming ellipsoidal anisotropic atomic motion (Cruickshank, 1956).

$$f_j = f_{oj} \exp -(B_{11}h^2 + B_{22}k^2 + B_{33}l^2 + B_{12}hk + B_{23}kl + B_{13}hl) \quad (8)$$

The anisotropic thermal motion is represented by an ellipsoid of vibration in real and reciprocal space. The six temperature factors B_{ij} for each atom define the principal axes and direction cosines of the ellipsoid.

This was the procedure adopted in the structure analyses described in Chapters 3 and 4.

1.4 Refinement

Once a structural model has been found by the methods already outlined it is necessary to improve the atomic coordinates and temperature parameters by a refinement procedure. This may be done by either Fourier or least squares techniques and since the latter method was used in this work only its relevant theory will be given. The advantages of least squares refinement over Fourier syntheses are that there are no series termination effects, and thus unobserved reflections can be safely excluded. Also, an

estimate of the accuracy of each $|F_o|_i$ can be included as a weighting factor w_i allotted to each reflection.

The method of least squares in x-ray crystallography consists of minimising the weighted sum of the squares of the discrepancy between the observed and calculated structure amplitudes, namely

$$R = \sum_{i=1}^{m} w_i(|F_o|_i - |F_c|_i)^2 \text{ (Hughes, 1941)}$$

$$= \sum_{i=1}^{m} w_i \Delta_i^2$$

where m = number of reflections included in the refinement.

R is a minimum when $\partial R/\partial u_s = 0$ i.e. $\sum_{i=1}^{m} w_i \Delta_i \partial\Delta_i/\partial u_s = 0$ (9)

u_s is one of n parameters to be adjusted.

The Δ_i are not linear in $u_s (s = 1 \rightarrow n)$ and equation (9) therefore represents a set of n simultaneous non-linear equations.

If however an approximate set of parameters u'_r is known the Δ_i may be expanded to the first order of a Taylor series

$$\Delta_i = g_i + \sum_{r=1}^{n} \left(\partial\Delta_i/\partial u_r\right) \delta_r \text{ where } \delta_r = u_r - u'_r$$

Substituting this into equation (9) one obtains

$$\sum_{i=1}^{m} \left[w_i \frac{\partial\Delta_i}{\partial u_s} \sum_{r=1}^{n} \frac{\partial\Delta_i}{\partial u_r} \delta_r \right] = - \sum_{i=1}^{m} w_i \Delta_i \frac{\partial\Delta_i}{\partial u_s} \quad (10)$$

These n equations (for $s = 1 \rightarrow n$) are the normal equations and are linear in the δ_s which may thus be determined.

The factor $\partial\Delta_i/\partial u_s = - \partial|F_c|_i/\partial u_s$ may be calculated for each of the n parameters (Cruikshank et al, 1961) and the trial values u'_s are substituted into equations (10). The following

procedure is used in programme 3 (Appendix A). Solution of the matrix is much simplified by making the following assumptions:

i) no interaction between the parameters of different atoms i.e. set terms of the type $(\partial|F_c| / \partial x_i).(\partial|F_c| / \partial x_j) = 0$

ii) no interaction between the coordinate parameters and temperature parameters for the same atom i.e. set terms of the type $(\partial|F_c| / \partial x_i).(\partial|F_c| / \partial B_i) = 0$

This is the block diagonal approximation (Cruikshank et al, 1961) and reduces the normal equations matrix to the following submatrices:

N 3x3 matrices for solution of positional parameters

N 6x6 matrices for solution of anisotropic B_{ij}'s

or 1x1 matrix for solution of isotropic temperature parameter B

N = number of atoms whose parameters are to be determined.

For solution of the shift in scale factor applied to $|F_o|$, a 2x2 matrix is used to take account of the interaction between the scale and overall isotropic temperature factor. This interaction is significant since a small decrease in scale has the same effect as a small increase in the overall B.

In programme A3 Schomaker's correction (1950) is applied to the shifts of the individual temperature factors for each atom. Thus if $\Delta B'$ is the overall isotropic temperature factor change calculated from a 1x1 matrix and $\Delta B''$ is the overall isotropic temperature factor change calculated from a 2x2 matrix (interaction with scale shift allowed for) then:

$$\Delta B_{\text{corrected}} = \Delta B_{\text{apparent}} + \Delta B'' - \Delta B'$$

$$\Delta B_{ij\ \text{corrected}} = \Delta B_{ij\ \text{apparent}} + (\Delta B'' - \Delta B')R_{ij}/\lambda^2$$

where the R_{ij}'s are defined as given in Appendix A3.

Use of the block diagonal approximation assumes that the atoms are resolved in Fourier space, and it neglects the effect of the thermal parameters of an atom with large vibration on the coordinates of its neighbours.

The parameter shifts δ_r calculated by least squares are generally too large and to prevent the solution oscillating a damping factor is applied to each δ_r, suggested values being given by Hodgson and Rollett (1963). The possible reasons for the necessity of this fudge factor have been discussed by Cruikshank (1961), Wegener (1961) and Sparks (1961).

An iterative procedure of least squares refinement is followed until $\sum_{i=1}^{m} w_i \Delta_i^2$ has been minimised. An indication of the agreement between the observed structure amplitudes $|F_o|$ and those calculated from the proposed atomic positional and thermal parameters, F_c, is the R factor $= \Sigma\left||F_o| - |F_c|\right| / \Sigma|F_o|$

1.5 Weighting Schemes

For successful use of the least squares method of refinement, sensible weights w_i must be chosen since a bad weighting scheme gives misleading conclusions. The observed structure amplitudes are subject to random and systematic errors due to the crystal itself, the geometry of the experiment and the intensity

measuring procedure.

In order to obtain the most accurate parameters with lowest standard deviation, the best choice is $w_i(\underline{h}) = 1/\sigma_i^2(\underline{h})$ where σ_i^2 = variance of $\Delta_i = (|F_o|_i - |F_c|_i)$. Two different schemes were used in the refinements (a) for photographic data (b) for the diffractometer data.

(a) Absolute values of w_i are unknown in advance and relative estimates are made, by approximating to a simple function of $|F_o|$. It is assumed that σ_i depends only on $|F_o|_i$ since the uncertainties are more strongly dependent on the random errors in $|F_o|$ than on any other factor. The scheme used must ensure that $\Sigma w\Delta^2$ is constant for any group of $|F_o|$'s and the one used was:

$$w = [\,1 + ((kF_o - F^{**})/F^*)^2]^{-1} \qquad (11)$$

where F^* was taken to be $8F_{min}$ and $F^{**}, 5F_{min}$. This is similar to that proposed by Cruikshank (1961) where $w = (a + |F_o| + c|F_o|^2)^{-1}$, $a \approx 2F_{min}$ and $c \approx 2/F_{max}$, and is effectively $w = 1/F_o^2$, which was the first scheme applied to structure analysis (Hughes, 1941).

(b) For diffractometer collected data with constant time spent on each integrated reflection, Grant et al (1968) have devised a suitable weighting scheme which takes into account not only counting statistical errors but other random errors as well.

Considering counting statistics alone, the least squares weight

$$w(\underline{h}) = \frac{4Lp}{K}\left(\frac{I-B}{I+B}\right) = \frac{1}{\sigma_1^2(\underline{h})}$$

where I = peak count and B = background count for $|F_o(\underline{h})|$.

However in diffractometer experiments other random errors are significant, for example due to the peak being off centre.

An improved weighting scheme which assumes that for a given crystal the peak shape near the centre is the same for all reflections, is:

$$\frac{1}{w(\underline{h})} = \frac{K}{4Lp}\left(\frac{I+B}{I-B}\right) + c^2 F_o^2(\underline{h}) \qquad (12)$$

$$= \sigma_1^2(\underline{h}) + \sigma_2^2(\underline{h}) = \sigma^2(\underline{h})$$

where c is a constant for a given crystal.

Once c has been determined an absolute numerical value of $w(\underline{h})$ may be assigned to each reflection.

By using the G-factor (Kitaigorodski, 1957) as a measure of goodness-of-fit, c^2 may be calculated relatively simply since

$$G^2 = \frac{\sum_h |\Delta(\underline{h})|^2}{\sum_h |F_o(\underline{h})|^2} = \frac{\sum \sigma^2(\underline{h})}{\sum |F_o(\underline{h})|^2}$$

by taking the estimate of $\sigma(\underline{h})$ as $\sigma(\Delta(\underline{h})) = \Delta(\underline{h})$ (Cruickshank, 1949). Substituting equation (12) into this gives:

$$c^2 = \frac{\sum_{i=1}^{m} (|F_o| - |F_c|)^2_i}{\sum_{i=1}^{m} |F_o|_i^2} - \frac{\sum_{i=1}^{m} \frac{K}{4Lp}\left(\frac{I+B}{I-B}\right)_i}{\sum_{i=1}^{m} |F_o|_i^2} \qquad (13)$$

$$= G^2(\text{theoretical}) - G^2(\text{counting statistics})$$

K is a scaling factor which must ensure that all the terms in equation (13) are on the same absolute scale.

G(theoretical) is an estimate of the total experimentally obtained discrepancy between all $|F_o|$ and F_c since it is directly

related to the correlation coefficient.

G(counting statistics) is a measure of the error due to counting statistics in the measured intensities, and thus c is equivalent to other errors incurred such as instrument inaccuracy, crystal quality and crystal missetting.

For both sets of linear diffractometer data, collected for SiF_4,2Py and $SiCl_4$,2Py, least squares refinement was continued as far as possible with the weighting scheme (a), and only then was c^2 calculated from equation (13) using the best set of F_c's available at that stage. Individual weights according to (12) were then applied to each $|F_o|$ and refinement continued until $\Sigma w \Delta^2$ was a minimum, and it will be seen in each case, close to its theoretical limit of (m-n) when on an absolute scale, where m=number of observations and n=number of parameters refined.

1.6 Accuracy of results

It can be shown (Cruikshank, 1965) that the estimated variance σ_s^2 of a parameter u_s, given by the variance of the shift δ_s, is:

$$\sigma_s^2 = (a^{-1})_{ss} \sum_{i=1}^{m} w_i \Delta_i^2/(m-n)$$

where $(a^{-1})_{ss}$ is a diagonal element of the inverted normal equations matrix (cf. equation (10))

For the diagonal approximation of the normal equations matrix, this equation is simply:

$$\sigma_s^2 = \frac{1}{\sum_{i=1}^{m} w_i \left(\frac{\delta |F_c|_i}{\delta u_s}\right)^2} \left(\frac{\sum_{i=1}^{m} w_i \Delta_i^2}{m-n}\right)$$

(Whittaker and Robinson, 1944; Cruikshank and Robertson, 1953).

These expressions are for weights $w_i = k/\sigma_i^2$ where the statistical expectation of $\Sigma w \Delta^2$ is k(m-n) (k being a constant), and assumes that a correct weighting scheme has been used.

The programme used for least squares refinement (A3) calculates the variances and covariances of the atomic positional parameters from the formula:

$$\sigma^2_{sr} = a^{-1}_{sr} A_s A_r \cos(sr) \sum_{i=1}^{m} w_i \Delta_i^2/(m-n) \ (\mathring{A}^2)$$

where A_s and A_r are cell edges and cos(sr) is the cosine of the angle between edges s and r. a^{-1}_{sr} is an element of the inverted submatrix in the block diagonal approximation of the normal equations matrix.

The errors in bond lengths and angles, which programme A3 also evaluates, are obtained from the following formulae, assuming independent atoms i.e. covariances σ^2_{sr} $(s \neq r)$ set equal to zero.

For the error in bond length AB between atoms A and B:

$\sigma^2(AB) = \sigma^2(A) + \sigma^2(B)$ where $\sigma(A)$ and $\sigma(B)$ are the standard deviations of atoms A and B in the direction AB.

For the error in bond angle β subtended by atoms A and C at atom B:

$$\sigma^2(\beta) = \frac{\sigma^2(A)}{AB^2} + \sigma^2(B)\left[\frac{1}{AB^2} - \frac{2\cos\beta}{AB \times BC} + \frac{1}{BC^2}\right] + \frac{\sigma^2(C)}{BC^2}$$

$$= \frac{\sigma^2(A)}{AB^2} + \frac{\sigma^2(B)AC^2}{AB^2BC^2} + \frac{\sigma^2(C)}{BC^2}$$

$\sigma(A)$ and $\sigma(C)$ are the standard deviations of atoms A and C in the ABC plane in directions perpendicular to AB and BC respectively.

σ(B) is the standard deviation of atom B in the direction of the centre of the circle through A, B, and C (Darlow, 1960).

2. EXPERIMENTAL

This chapter is mainly concerned with the Hilger and Watts linear diffractometer which was used to collect intensity data from single crystals of mercury dibenzyl (MDB), SiF_4,2Py and $SiCl_4$,2Py. These structures are discussed in detail in Chapters 5, 3 and 4 respectively.

Section 1 is a description of both the mechanical and electronic parts of the instrument. Section 2 describes the faults and errors which were encountered during the use of the instrument over a two year period and sections 3 and 4 discuss the techniques employed once the instrument was eventually operational. While the diffractometer was out of action, photographic methods were adopted for the measurement of diffracted x-ray intensities from SiF_4,2Py, and this procedure is outlined in the final sections.

2.1 The linear diffractometer (Arndt and Phillips, 1959,1961) is an instrument for"automatic"collection of single crystal diffracted intensities and is essentially a mechanical analogue of the Ewald sphere construction of the reciprocal lattice (Ewald, 1921). The condition for a family of planes [hkl] to diffract radiation of wavelength λ according to Bragg's law ($2d\sin\theta = n\lambda$) is equivalent to the requirement that the reciprocal lattice point P(hkl) lies on the surface of the Ewald sphere of reflection.

Figure 2.1.1

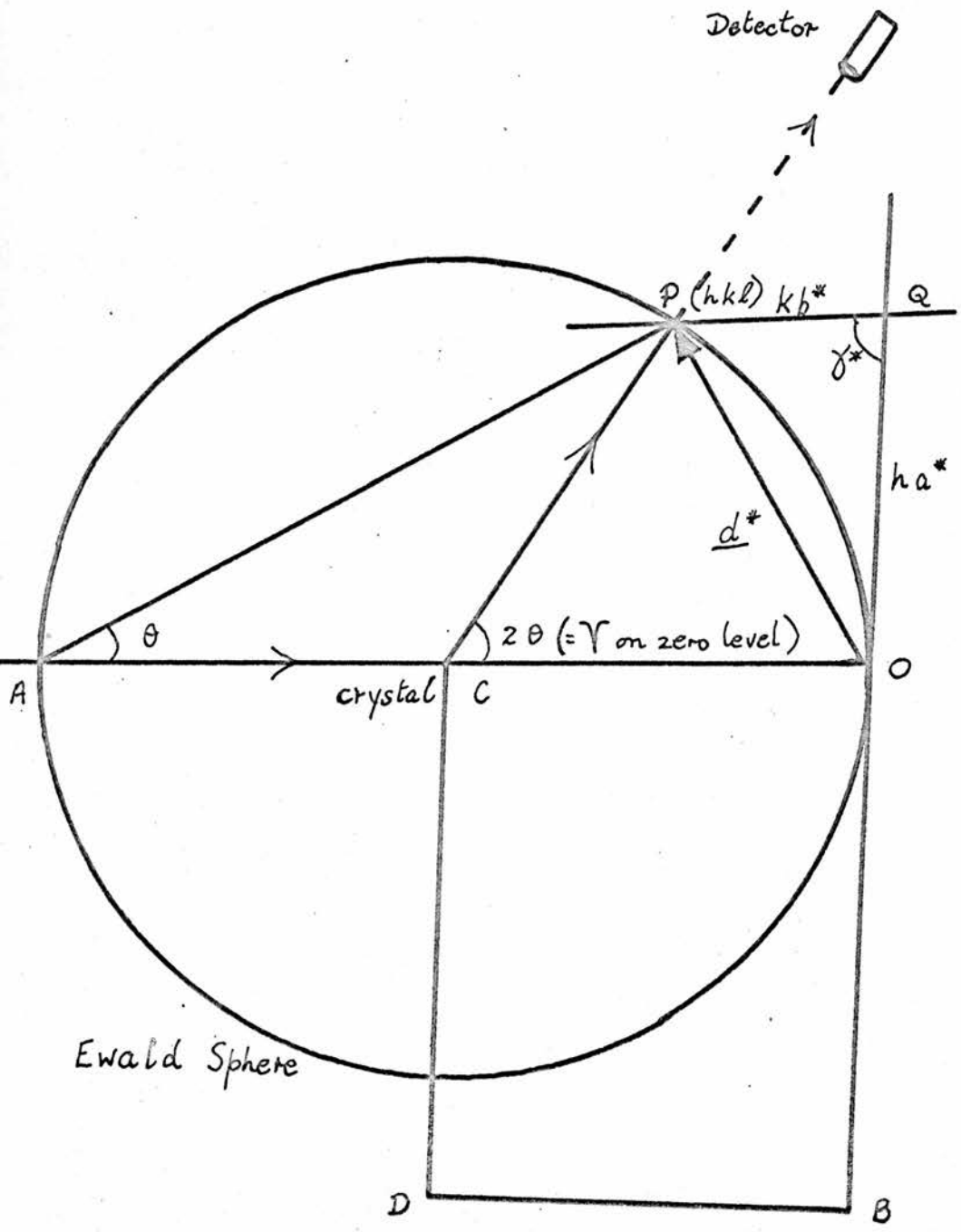
Detector
P (hkl)
kb*
Q
γ*
ha*
d*
θ
2θ (= γ on zero level)
A
crystal
C
O
Ewald Sphere
D
B

Figure 2.1.1 represents a horizontal section of the Ewald sphere, radius 1 reciprocal lattice unit (r.l.u.), and the two dimensional arrangement of the diffractometer when P(hkl) is in its reflecting position. AC and CP are the incident and reflected beams, C represents the crystal and O is the origin of the reciprocal lattice. OP is the reciprocal lattice vector $\underline{d}^*$ of the reflection P(hkl) $= h\underline{a}^*+k\underline{b}^*+l\underline{c}^*$, and of magnitude $\lambda/d(hkl)$. d(hkl) is the spacing of the [hkl] crystal planes, represented by AP, perpendicular to $\underline{d}^*$. The crystal is mounted with a real axis, say $\underline{c}$, along the goniometer axis ϕ and thus figure 2.1.1 is of the a*b* plane.

The diffractometer comprises three slides representing two reciprocal axes ($\underline{a}^*$ and $\underline{b}^*$) and a real axis ($\underline{c}$), to which the motions of crystal and detector are linked. A detector is placed on the bar CP, of fixed length ($\equiv 1$ r.l.u.), pivoted at C and pointing towards C to receive the diffracted beam. The reciprocal axes a* and b* are represented by the slides OQ and QP, pivoted at O and P, with OQ=ha* and QP=kb*(r.l.u.) for the reflection P. The crystal is pivoted at C, independently of the counter, and is linked by means of the parallelogram CDBO to the motion of the carriage Q along either slide OQ or QP. The crystal carrying arm CD bisects $A\hat{C}P$.

The carriage Q is moved in a linear fashion along either slide by driving the slides; the counter arm and crystal follow, rotating about the goniometer axis, and as successive reciprocal lattice points cut the

Figure 2.1.2

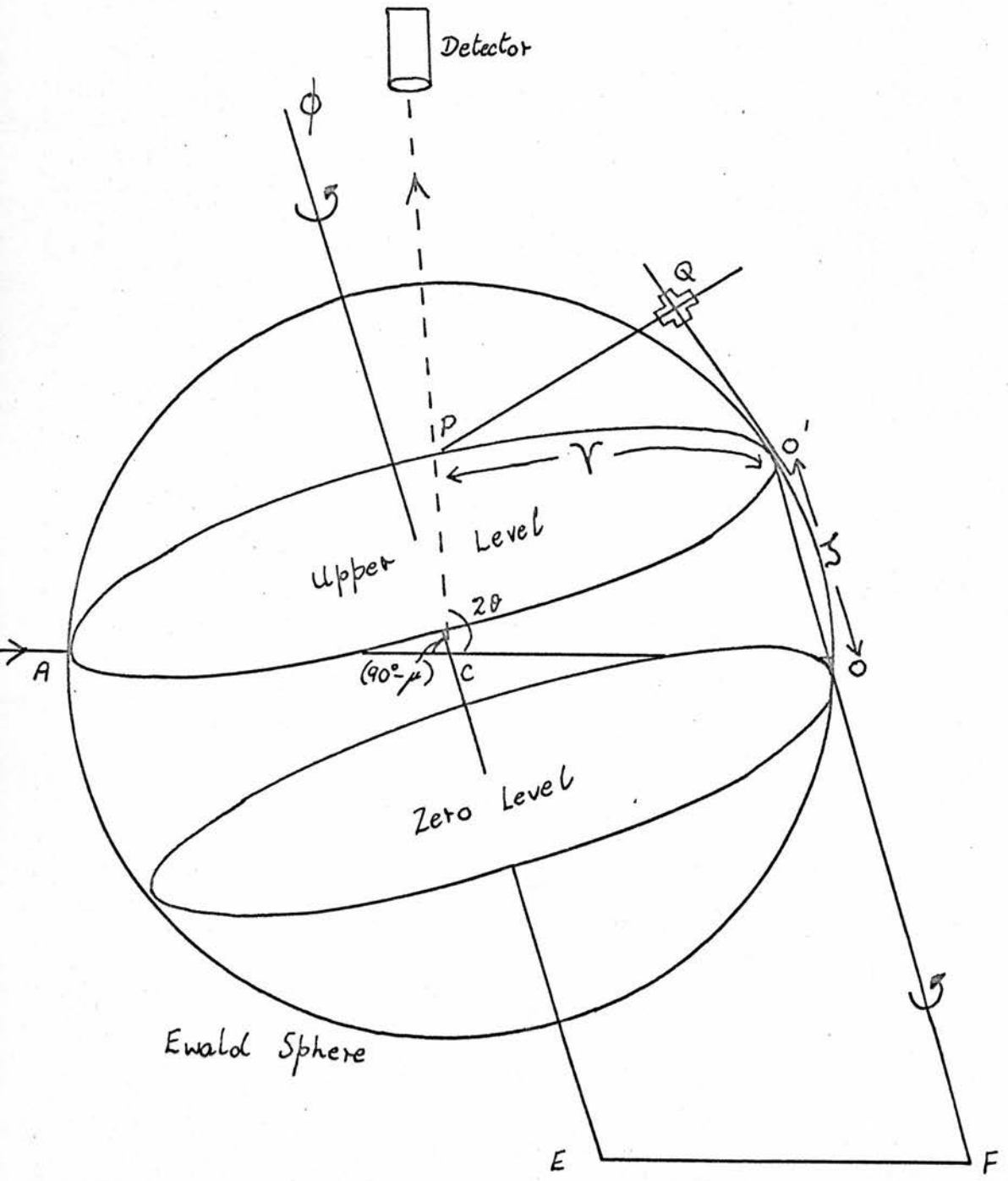
Detector
ϕ
Q
P
O'
γ
Upper Level
2θ
A
(90°-μ)
C
O
Zero Level
Ewald Sphere
E
F

surface of the Ewald sphere, the detector is always at the correct angle 2θ to the incident beam.

Figure 2.1.2 illustrates the extension of the principle to upper level data collection. Equi-inclination geometry is used since then the upper levels are similar to the zero level. A third slide OO', perpendicular to the plane of the other two, is kept parallel to the crystal axis c by means of a second parallelogram linkage CEFO, which also ensures equal rotation about CE and OO'. Since the x-ray beam is fixed, the whole system of figure 2.1.1 is tilted to give the correct height of level APO' as $\zeta = \frac{l\lambda}{c}$(r.l.u.) = OO'. The angle of tilt is independently set at $\mu = \sin^{-1} \zeta/2$ to put the counter in the correct orientation at angle $(90°-\mu)$ to the goniometer axis. Thus on each level, once ζ and μ have been set, only γ and ϕ, the angular positions of the counter and crystal respectively, are changed as P moves round the circle APO' by the usual method of linearly driving the slides O'Q and QP, and the counter moves round the cone of semiangle $(90°-\mu)$.

Once the reciprocal lattice of the crystal is correctly orientated with respect to the slide system, the normal measurement procedure for reflections is to track along successive reciprocal lattice rows on each level, keeping the stepping slide fixed on each row at the appropriate value of ha* or kb*, and moving in equal steps of b* or a* r.l.u. respectively along the other scanning slide. Once the counter arm reaches a preset γ limit switch on a

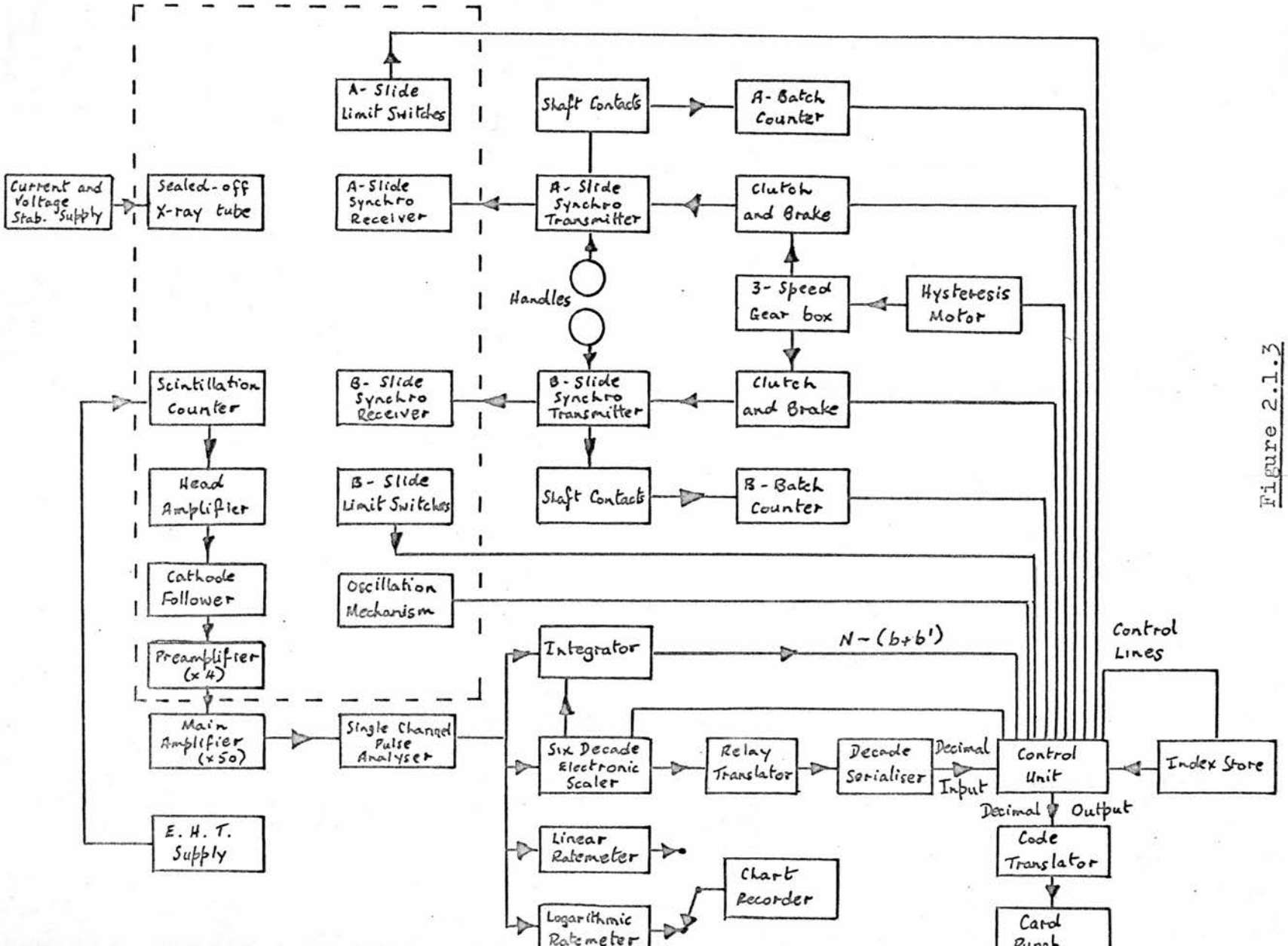
A- Slide Limit Switches
Shaft Contacts
A- Batch Counter
Current and Voltage Stab. Supply
Sealed-off X-ray tube
A- Slide Synchro Receiver
A- Slide Synchro Transmitter
Clutch and Brake
Handles
3- Speed Gear box
Hysteresis Motor
Scintillation Counter
B- Slide Synchro Receiver
B- Slide Synchro Transmitter
Clutch and Brake
Head Amplifier
B- Slide Limit Switches
Shaft Contacts
B- Batch Counter
Cathode Follower
Oscillation Mechanism
Preamplifier (x4)
Integrator
N - (b+b')
Control Lines
Main Amplifier (x50)
Single Channel Pulse Analyser
Six Decade Electronic Scaler
Relay Translator
Decade Serialiser
Decimal Input
Control Unit
Index Store
Decimal Output
E. H. T. Supply
Linear Ratemeter
Code Translator
Chart Recorder
Logarithmic Ratemeter
Card Punch

Figure 2.1.3

scan, the next intensity measurement is completed and the stepping slide moves one translation. Scanning continues as before and the process repeated automatically until the whole level is recorded in a zig zag fashion.

A stationary detector-moving crystal technique (Cochran, 1950) is used to measure the integrated intensity of each reflection. Since the constant speed linear motion of the carriage along the slides produces a very non-uniform rotation of the crystal, an independent constant-speed mechanism (Arndt, Faulkner and Phillips, 1960) is used to oscillate the crystal about the goniometer axis through the region of the Bragg reflection. This enables the usual equi-inclination Weissenberg Lorentz factor to be used.

During each measuring cycle an initial stationary background count b is taken for time t on one side of the reflection, after which time 2t is spent counting the integrated peak N as the crystal oscillates. Finally a second background b' is measured for time t on the other side, and the crystal then returns to its ofiginal position. The background corrected intensity of the reflection is thus N-(b+b').

In practice the two oscillation cycles are done on each reflection using a balanced filters unit (Ross, 1928) which sequentially introduces a β filter for the first cycle and an α filter for the second, between the crystal and detector (Zirconium and Strontium respectively for Molybdenum radiation). The filters'

Figure 2.1.4

The linear diffractometer

1. Telescope for crystal alignment
2. X-ray tube
3. Goniometer head
4. Scintillation counter
5. Balanced filters unit
6. } Horizontal slides
7. }
8. Vertical slide
9. Sliding carriage
10. Crystal oscillation mechanism and ϕ scale
11. μ scale for equi-inclination setting
12. IBM card punch
13. Head amplifier
14. Pre-amplifier

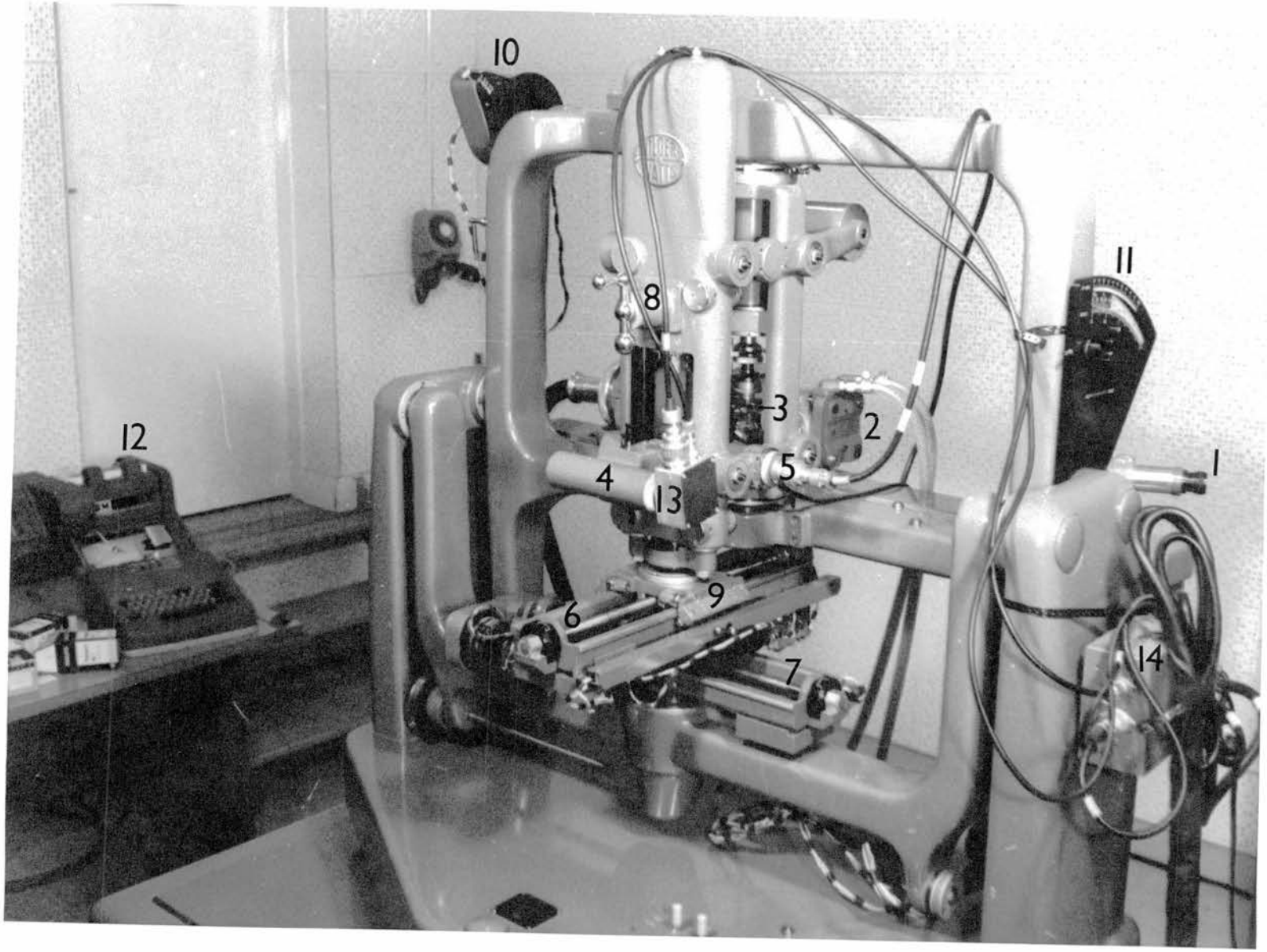
10
11
8
12
3
2
1
4
5
13
9
6
14
7

Figure 2.1.5

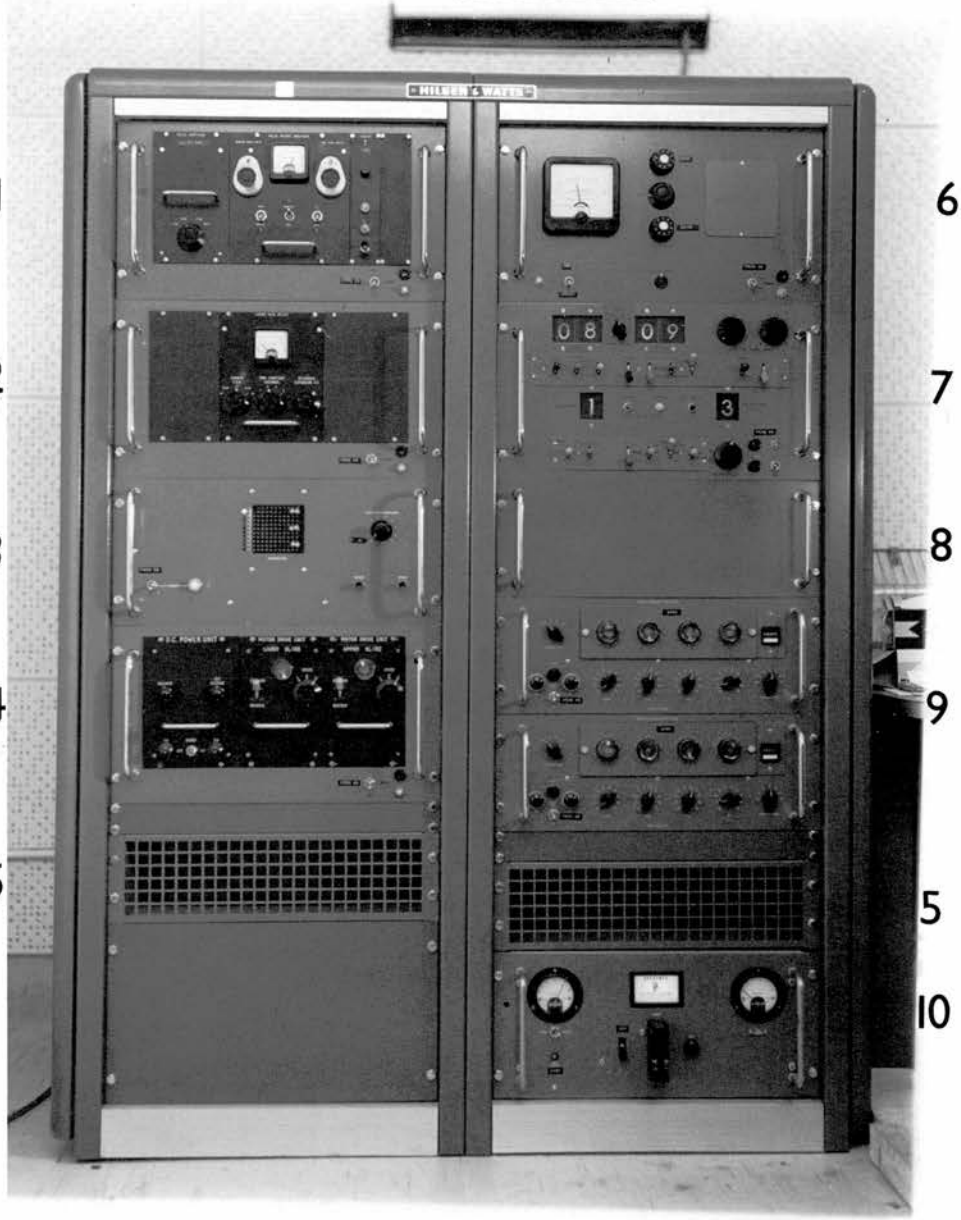

The electronic console

1. Pulse amplifier, pulse height analyser, N/4 scaler
2. Count rate meter
3. Racal programmed scaler
4. D.C. power and motor drive units
5. Blower for cooling batch counters
6. Scintillation counter E.H.T.
7. Control unit to programme data collection
8. Translator unit
9. Ericsson batch counters
10. Servomex voltage stabiliser

K absorption edges bracket the Kα line of the radiation used and thus the difference between the two background corrected integrated intensities gives the diffracted characteristic Kᾱ radiation.

The sequence of setting, measuring, printing and resetting operations are controlled by sequencing circuits which employ electromechanical devices such as relays, uniselectors and batch counters, and figure 2.1.3 illustrates the measuring and control system. Since Molybdenum radiation was used for all data collection, a scintillation counter was used as detector. The x-ray tube is supplied with smoothed d.c. power which gives x-ray intensity constant to $\frac{1}{2}\%$. An I.B.M. card punch was used to output the results; the indices h,k,l of the reflection are punched on one card, together with $b_1, N_1, b'_1, b_2, N_2, b'_2$, the recorded counts of the two oscillation cycles.

Figures 2.1.4 and 2.1.5 show the diffractometer slide system and electronic console.

2.2 Trials and tribulations

The following instrument faults were encountered when initially attempting to use the linear diffractometer for collection of intensity data:

1. The crystal oscillation mechanism was found to be in error in that the angle of crystal oscillation was not constant for all reflections, and did not equal the angle set. This fault was corrected.

2. The goniometer shaft was not long enough for a crystal, mounted on a normal length of fibre, to be centred in the x-ray beam. A new extended shaft cannot be used without a goniometer extension because of flexing.

3. It was eventually discovered that a misplaced machined stop, for the angle between the horizontal slides, gave rise to serious instrument damage every time this angle was changed from 90° to 60°, which inevitably occurred with the triclinic crystals studied. The centre of the instrument was irreversibly moved and a lengthy repair was necessary.

Before the cause of this damage was traced, it was thought that when certain combinations of slide settings and angle between the slides existed, a subsequent scan or step drive, in a direction towards the instrument centre, could cause sufficient strain to move the centre. A scale model of the horizontal slides and pantagraph system (c.f. figure 2.1.1) showed that this effect would be unlikely to cause the amount of movement required, other parts taking the majority of the stress and likely to break first.

4. The first intensity measurements made on the instrument were from a single crystal of mercury dibenzyl (MDB). The quality of zero level intensity data seemed good and a two dimensional Fourier map was satisfactory. The instrument was assumed to be operating equally well for upper levels but the resulting three

dimensional synthesis for MDB indicated that this was not so, and that upper level data was very unsatisfactory. This was confirmed by collecting data from α-glucose monohydrate (Ferrier, Killean and Young, 1962) and α-rhamnose monohydrate (Beevers and McGeachin, 1957) and comparing the diffractometer intensities with previously obtained photographic values. The agreement for upper levels was poor in both cases and indeed for α-glucose monohydrate the parameters of the model previously obtained moved to impossible positions on attempted refinement. It was obvious that the same effect would have been obtained with the α-rhamnose monohydrate data.

Careful analysis showed that upper level reflection peaks were displaced from their expected reciprocal lattice positions, and that this movement worsened as the level increased. A simple and quick test of the accuracy of the instrument was devised.

When one horizontal slide is reading zero and the other slide, representing $\underline{d}^*$ (see figure 2.1.1) is driven from +X to -X, then the angle of rotation of the crystal is 2θ where $X = 2\sin\theta$. Theoretical and experimental values of 2θ may be compared for $X = 0.1 \rightarrow 1$ r.l.u. at intervals of 0.1 r.l.u. for one slide and a similar test made on the other slide. The process was repeated on upper levels for $\zeta = 0 \rightarrow 1$ r.l.u. at intervals of 0.1 r.l.u. The discrepancy E between the two values of 2θ was plotted against X

Figure 2.2.1

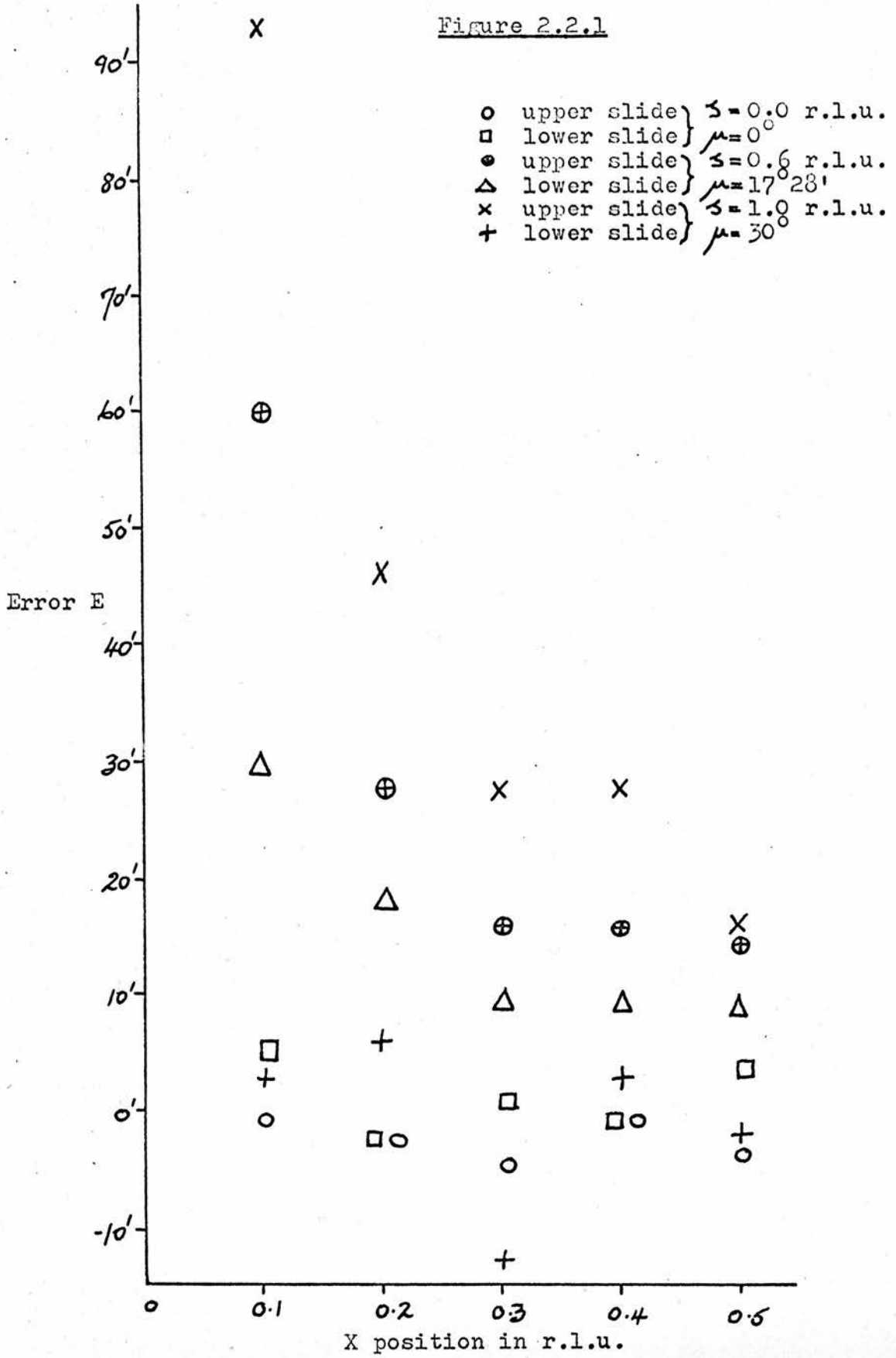
o upper slide } s = 0.0 r.l.u.
□ lower slide } μ = 0°
● upper slide } s = 0.6 r.l.u.
△ lower slide } μ = 17°28'
× upper slide } s = 1.0 r.l.u.
+ lower slide } μ = 30°
90'
80'
70'
60'
50'
40'
30'
20'
10'
0'
-10'
Error E
0
0.1
0.2
0.3
0.4
0.5
X position in r.l.u.

in each case, and figure 2.2.1 shows the results for ζ=0, 0.6 and 1 r.l.u.

It is seen that the inaccuracy in the crystal rotational position ϕ increases as the slide reading decreases, and also to a greater extent as ζ increases. The latter error was finally traced by experimenting to the equi-inclination angle μ scale. It was discovered that the ζ and μ scales on the instrument were not numerically linked, and when μ was set to $-\sin^{-1}\zeta/2$, for a particular level of height ζ, it did not in fact equal this equi-inclination angle.

The crystal setting angle ϕ is related to μ by the equation $\phi = 180° - \tau - \cos^{-1}((\xi^2 + \zeta^2 + 2\zeta\sin\mu)/2\xi\cos\mu)$. ξ and τ are the radial and angular coordinates of the reciprocal lattice point. Thus any inaccuracy in the equi-inclination setting μ causes an error in ϕ, and as ζ increases so does this error.

Once the μ scale supporting vernier screws were remachined by the manufacturer, the instrument test described above gave a $10'$ error in crystal position ϕ for both slides on all levels for $\xi > 0.1$ r.l.u. To minimise the effect of this remaining inaccuracy, the detector arm CP (see figure 2.1.1) was kept to one side of the instrument throughout intensity data collection from one crystal.

Arndt and Phillips (1961), Arndt (1963) and Binns (1964) have considered the setting precision of the linear diffractometer, and also show the inaccuracy due to backlash of the horizontal slides settings within 0.1 r.l.u. of their origin. Thus only

reflections with $\xi > 0.2$ r.l.u. were used for the crystal setting procedure outlined in the following section.

2.3 Crystal alignment on the linear diffractometer

The object of alignment is to set the crystal with two of its reciprocal lattice axes parallel to the two horizontal slides of the diffractometer. Depending on the crystal system the third reciprocal axis may or may not be parallel to the vertical slide. The best alignment procedure was found to be different for the two cases.

A. a reciprocal lattice axis coincides with the real axis along the goniometer axis ϕ, as for MDB, mentioned already in section 2.2 and discussed in more detail in Chapter 5.

B. the triclinic systems of SiF_4,2Py and $SiCl_4$,2Py (c.f. Chapters 3 and 4).

For both cases, the crystal is kept centred in the incident x-ray beam by means of the instrument telescope, and, when the peaks of reflections are studied, the crystal oscillation cycle is at the central position. A small collimator (1mm) is used.

A. Once the space group has been established by photographic methods, only approximate crystal setting and lattice parameter measurements need be made with cameras since these can be found more accurately on the diffractometer. For MDB $\underline{c}$ and $\underline{c}^*$ are coincident, and lie along the needle axis of the crystal. Using the diffractometer telescope, it can be approximately set by eye

parallel to the vertical slide. A strong 001 reflection is located and the goniometer arcs are adjusted until 360° rotation of the crystal gives constant peak count indicated on the chart recorder. The c* parameter is improved by varying the vertical slide reading, and its associated μ, until maximum constant count is obtained. The c* value and goniometer arc settings are checked and confirmed on other 00l reflections. Now $\underline{c}$ and $\underline{c}^*$ are parallel to, and reciprocal lattice planes perpendicular to the vertical slide and goniometer axis.

On the zero level with one slide at zero and the other (90° apart since $\gamma^*=90°$) at the expected ha* position of a strong h00 reflection, the crystal is rotated until this reflection is found and then clamped on the ϕ scale at the peak position. The Friedel reflection $\bar{h}00$ is also located by driving the slide to -ha*; and the parameter a* refined on both sides of the slide until both reflections are maximised and equal. A similar procedure is followed on the other slide to refine b* without unclamping the crystal, and the values checked against general zero and upper level reflections. Reflection peaks are now within 5-10' of the centre of the oscillation cycle for automatic collection of data. Corresponding Weissenberg photographs are a valuable aid for ease in finding suitable strong reflections.

B. For this category of crystal system a complete and accurate photographic study of the reciprocal lattice was found to be

essential prior to transferring the crystal to the diffractometer. This was achieved using Weissenberg and Precession cameras and the results are given in Chapters 3 and 4 for the two triclinic compounds studied. Since no reciprocal lattice axis coincides with a real axis, the goniometer arcs cannot be set by method A and the crystal is set with a real axis, say c, along the goniometer axis on a Weissenberg camera by the methods of Weisz and Cole (1948) and Davies (1950). Once correct setting was assured, the "sira" wax holding the crystal fibre or tube to the goniometer head was generously coated with shellac to prevent any crystal motion in the event of the wax becoming soft. After transfer to the diffractometer any desired reflection may be located, knowing the orientation of the three oblique reciprocal axes with respect to the goniometer head.

The angle between the horizontal slides is set at γ^* and the crystal clamped by eye so that the slides are approximately in the orientation of $\underline{a}^*$ and $\underline{b}^*$. With the slides reading ha^* and kb^* r.l.u. for a strong hk0 reflection, the crystal is slightly rotated and clamped at the peak position, which for both triclinic crystals, was within 2° of the initial visual setting. Since c^* is not perpendicular to the a^*b^* plane, the plane of the horizontal slides, the effective origin of upper levels is not coincident with the slides both reading zero, and the offsets of upper level origins along both slides must be found. With SiF_4,2Py

Figure 2.3.1

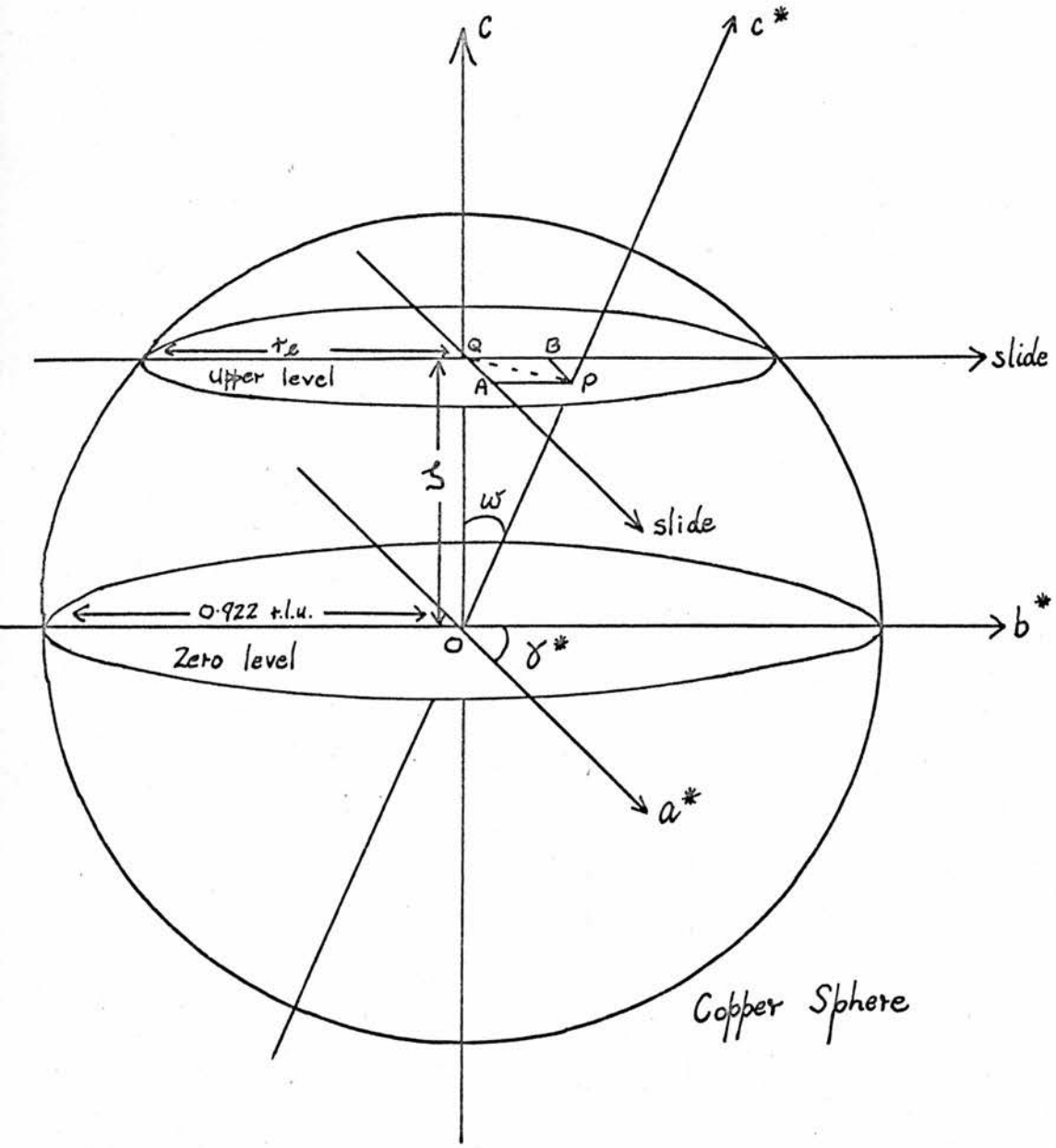
c
c*
Q
B
A
P
slide
Upper level
ζ
w
slide
0·922 r.l.u.
b*
Zero level
O
γ*
a*
Copper Sphere

and $SiCl_4$,2Py strong reflections on several upper levels were maximised by successively varying the slide readings, and the mean offset values used. This assumes that a* and b* values are sufficiently accurate so that their errors do not contribute to the offsets. In both cases the experimentally determined offsets were found to be insignificantly different from the values calculated as follows.

In figure 2.3.1, P represents the intersection of c* with an upper l-level, Q is the origin of the horizontal slides parallel to a* and b* and QA and QB are the displacements of P along the slides.

$$QA = \delta_{a^*} = \frac{QP\sin Q\hat{P}A}{\sin Q\hat{A}P} \quad \text{(Sine Rule in } \Delta QAP)$$

$$QP = OP\sin\omega = l(\lambda c^*)\sin\omega; \quad Q\hat{A}P = 180^\circ - \gamma^*$$

and it can be shown that $\cos Q\hat{P}A = \frac{\cos\alpha^*}{\sin\omega}$ where ω=angle between $\underline{c}$ and $\underline{c}^* = \cos^{-1}(1/cc^*)$.

Substituting into the above equation gives for the offset of P along the a* slide,

$$\delta_{a^*} = (\, l(\lambda c^*)/\sin\gamma^* \,) \sqrt{\sin^2\alpha^* - \cos^2\omega}$$

and similarly, $\delta_{b^*} = (l(\lambda c^*)/\sin\gamma^*) \sqrt{\sin^2\beta^* - \cos^2\omega}$

With both triclinic crystals refinement of the goniometer arcs setting and lattice parameters was attempted on the diffractometer but no significant improvement could be made on the photographic values due to the number of possible variables

which were difficult to isolate. There are five variables for zero level reflections: the two goniometer arcs, the horizontal slides and γ^*, plus a further three for upper level reflections: the vertical slide setting $l\lambda/c$ and the two offsets. Strong reflections were chosen and by varying in turn the goniometer arcs and slide settings, it was attempted to maximise the peak count.

The remaining setting problem for crystals of type B is to clamp the crystal in the best mean position for all reflections. The method adopted consisted of choosing four strong zero level reflections approximately 90° apart, and initially clamping the crystal at the peak position of one of them. The slides were driven to the other three reflections in turn and the position of arrival on the oscillation scale ϕ and the peak position noted in each case. It was then possible to clamp the crystal to a mean position such that the errors in peak missetting from the point of arrival on automatic scan were minimised and evenly distributed throughout the level. For both triclinic compounds the crystals used for data collection were set to within 10-15' for zero level reflections, using photographic values. The setting was checked on upper levels and again found to be the optimum, although the peak missetting did tend to increase slightly due to additional inaccuracies from the equi-inclination setting and offset values.

2.4 Setting the diffractometer for data collection.

Before data collection can commence the following variables must be selected:

2.4.1 Detector collimator and crystal oscillation angle.

A complete account of collimating and oscillation angle conditions which must be fulfilled to ensure proper measurement of integrated intensities is given by Furnas (1957).

The aim is to have maximum peak to background ratio (this decreases in proportion to the unnecessary background included in the integrated peak count) and backgrounds approximately equal. If the oscillation angle is too small then the background count on one side of the reflection may include part of the peak.

For each crystal studied, several reflections of varying intensities on various levels were selected to test combinations of collimator sizes and oscillation angles. The final values were chosen such that the above criteria were satisfied together with Friedel equivalent intensities being equal to within two or three standard deviations.

For upper level reflections, the crystal is not rotated about an axis perpendicular to the plane of reflection and the effective angular range of the reflections increases (Cox and Shaw, 1930; Tunnell, 1939). A further reason is the vertical divergence of the x-ray beam (Phillips, 1954) especially for reflections near the origin of the horizontal slides. Consequently the oscillation

angles for SiF_4,2Py and $SiCl_4$,2Py found most suitable for most of reciprocal space as described above, were too small for the highest levels and had to be increased.

2.4.2 Time spent at each reflection

There is a statistical uncertainty in the measurement of diffracted intensities because of the random nature of emission of x-ray photons. This can be reduced by prolonging the counting process at each reflection for some length of time, but against this must be weighed the amount of time available for data collection.

The total time spent counting may be altered in two ways. The time taken per oscillation cycle may be chosen as $\frac{1}{2}$ or 1 minute (2 motors available) and the number of oscillation cycles measured at each reflection selected.

It was found that the differences between integrated intensities obtained after counting for many oscillation cycles per reflection and those values after only two cycles, were less than the standard deviations $\sqrt{N}$ of the counts themselves. Thus there seemed little justification for spending any more time measuring each intensity than was necessary for two cycles using balanced filters i.e. 1 card per reflection.

Likewise, with time at a premium, the criterion used for choice of oscillation motor speed was the magnitude of the

diffracted intensities from each particular crystal. The largest peaks should give sufficiently high counts without overloading the scintillation counter.

2.4.3 Electronics

The scintillation counter E.H.T. is selected by maximising the peak count of a typical reflection with the pulse height analyser in the middle of its working range. A subsequent pulse height distribution curve gives the optimum low level and window width settings for the P.H.A. The x-ray generator voltage is set at least twice the excitation voltage of the target material, and the current chosen so that the counts obtained are within the desired range.

2.4.4 Collection of data

The maximum attainable Bragg angle θ on the linear diffractometer is 30° and thus only those reflections within a hemisphere of reciprocal space, of radius $2\sin\theta=1$ r.l.u. can be measured. However, although Mo radiation produced all diffracted intensities, the wavelength of copper Kα characteristic radiation is used for calculating the structure factors (see programme 3, appendix A).

For radiation of wavelength λ diffracted at the Bragg angle θ, $\sin\theta/\lambda$ is a constant for that particular reflection. When calculating structure factors with Cu$K\bar{\alpha}$ wavelength, maximum $\sin\theta$ required is unity and the corresponding $\sin\theta$ value for Mo$K\bar{\alpha}$ wavelength is $\lambda(\text{Mo}K\bar{\alpha}) \times 1/\lambda(\text{Cu}K\bar{\alpha})$. Thus only those reflections

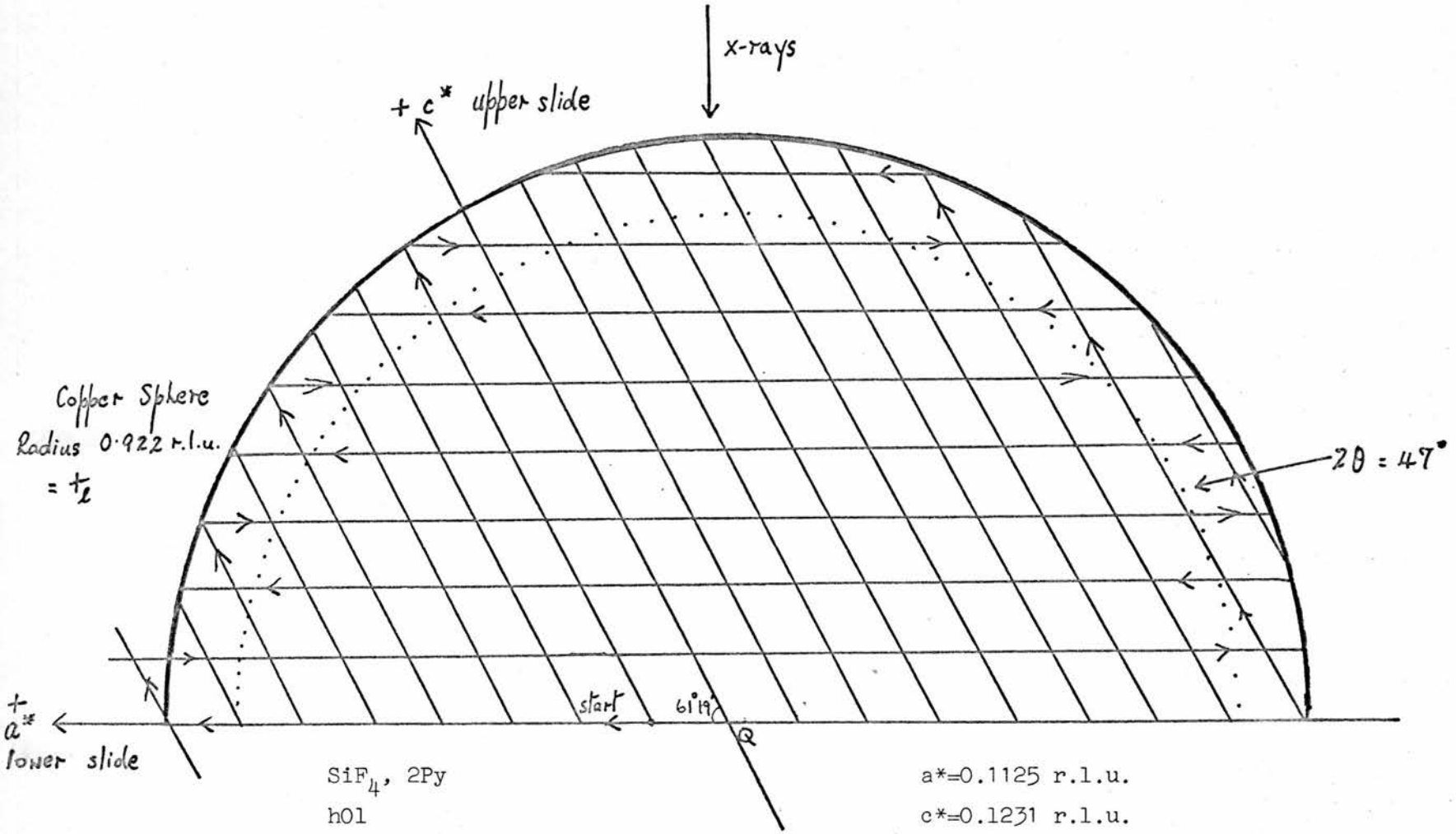

SiF_4, 2Py

h0l

a*=0.1125 r.l.u.

c*=0.1231 r.l.u.

Figure 2.4.1

Figure 2.4.2

SiF_4, 2Py h61

$\zeta = 0.6642$ r.l.u. $\mu = 19^\circ 24'$

offset of P along lower slide = PB = 0.0726 r.l.u.

offset of P along upper slide = QB = 0.2742 r.l.u.

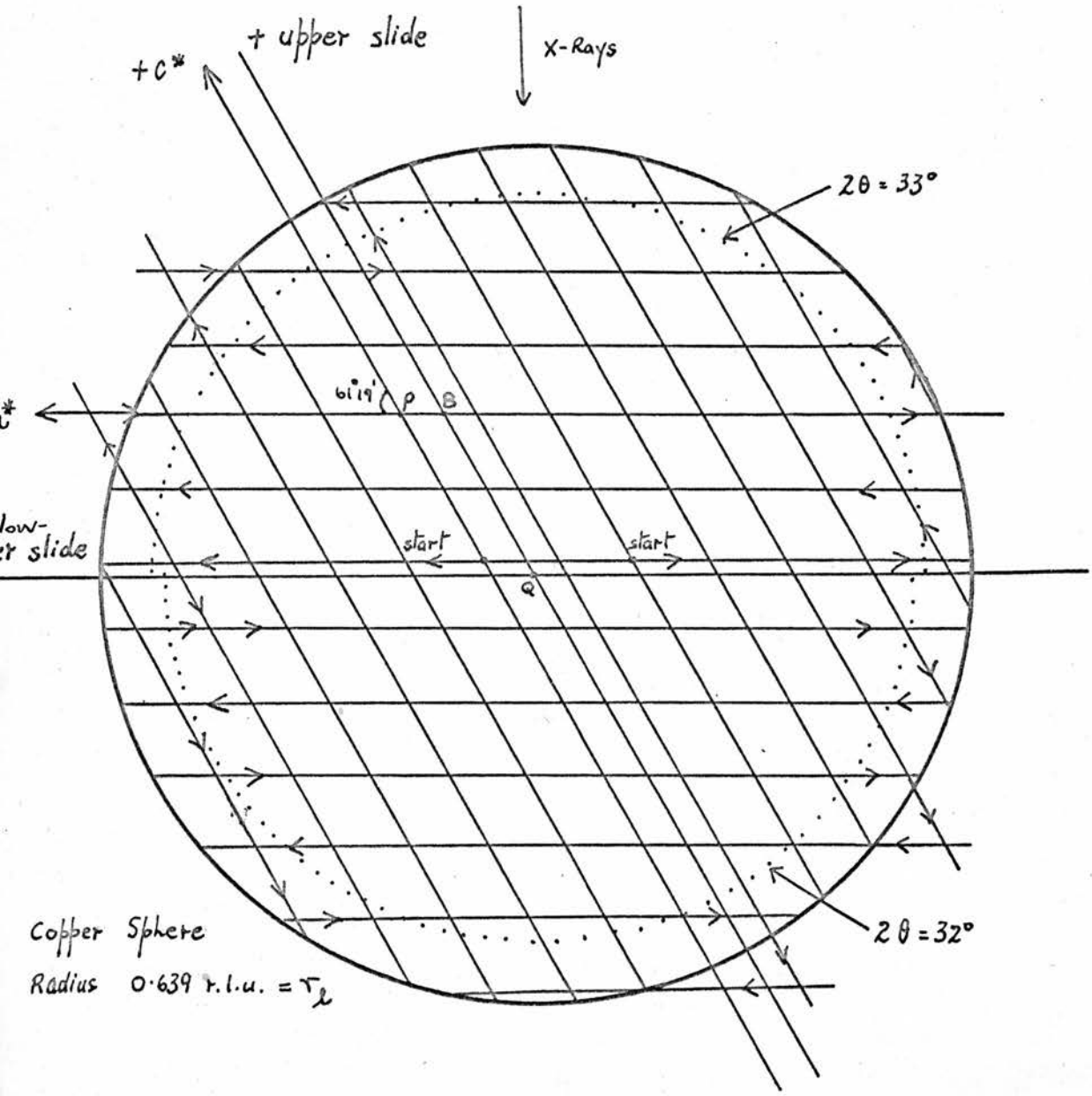

inside the "copper sphere" of radius 2 x $\lambda(MoK\bar{\alpha})/\lambda(CuK\bar{\alpha})$ = 0.9219 r.l.u. need be measured.

The radii r_1, of the circles of intersection of the copper sphere with each reciprocal lattice level of a crystal mounted on the diffractometer, may be calculated from the formula: $r_1 = \sqrt{(0.9219)^2 - \zeta^2}$ r.l.u. (see figure 2.3.1).

For the triclinic lattices of SiF_4,2Py and $SiCl_4$,2Py, every reciprocal level mesh was drawn on polar graph paper and the zero level only for M.D.B. since all levels are the same. The intersection of the goniometer axis with each level is at the centre Q, also the origin of the diffractometer horizontal slides. Examples of these are shown in figures 2.4.1 and 2.4.2, which are respectively the zero and sixth levels of SiF_4,2Py (mounted along b). The values of slide intervals, offsets etc. are taken from chapter 3, section 4.

The appropriate circle of radius r_1 is drawn on each diagram and the setting of the Υ limit switch (maximum 60°) chosen such that minimum time is spent measuring reflections outside the copper sphere. Reflections in both halves of each level, except the zero layer, were collected for the triclinic crystals in a zig-zag scan-step manner as shown and in a direction away from the origin of the slides Q. The layer plots are a further help in identifying those reflections in the inaccurate region of the instrument within 0.1 r.l.u. of Q, and those likely to cause

mechanical damage if driven to automatically.

As many reflections as possible are collected on automatic scan, and those near the origin of the horizontal slides are examined. If their backgrounds are very uneven they are centred and collected individually (cf. section 2.2).

Some chosen standard reflection is returned to after each level collected to check that the crystal has retained its correct alignment and has not deteriorated in the incident beam. This also provides a check on the stability of x-rays, detector and counting circuits.

2.5 Photographic method of recording integrated intensities

An integrating Nonius Weissenberg camera (Wiebenga, 1947; Wiebenga and Smits, 1950) was used to record the diffracted intensities of SiF_4,2Py.

For each equi-inclination Weissenberg level the following values must be set:

a) equi-inclination angle $\mu=\sin^{-1}(\zeta/2)=\sin^{-1}[\sin\tan^{-1}(2y/D_F)]/2$

ζ = height of level in r.l.u. obtainable from a rotation photograph.

y = rotation film layer line height in mm.

D_F= diameter of film cassette = 57.29mm.

b) shift of layer line screens from the zero level position = S.tanμ where S = effective radius of the layer line screens (mean of internal and external values) = 24.25mm. The narrowest possible screen gap of 3mm was used, to reduce

the background.

The integrating mechanism on the camera performs two movements at the end of every usual Weissenberg film translation by means of turning through 1 notch a pinwheel with 14 notches.

1. a small horizontal translation parallel to the goniometer axis.

2. a small vertical rotation about the goniometer axis.

After one complete rotation of the notched pinwheel the film has traversed 14 times, 14 small displacements have been made in both directions and the rotational position of the film cassette returns to its original position. The horizontal displacement may be continued up to 30 times more, when the cassette begins to translate in the opposite direction for a further 14x30 small translations until back at its original position. For one rotation of the pinwheel, the rotational displacement = total vertical displacement b, and the translation movement = one horizontal step a, and up to 30 or multiples of 30 translation steps may be taken per exposure.

The total displacements must exceed the dimensions of the spots to be measured, the size of the excess determining the size of the integrated intensity plateau. Thus initial trial integration settings were chosen by measuring the average spot size, x and y m.m. horizontally and vertically respectively, and choosing total film displacements of 0.3 m.m. in excess of those

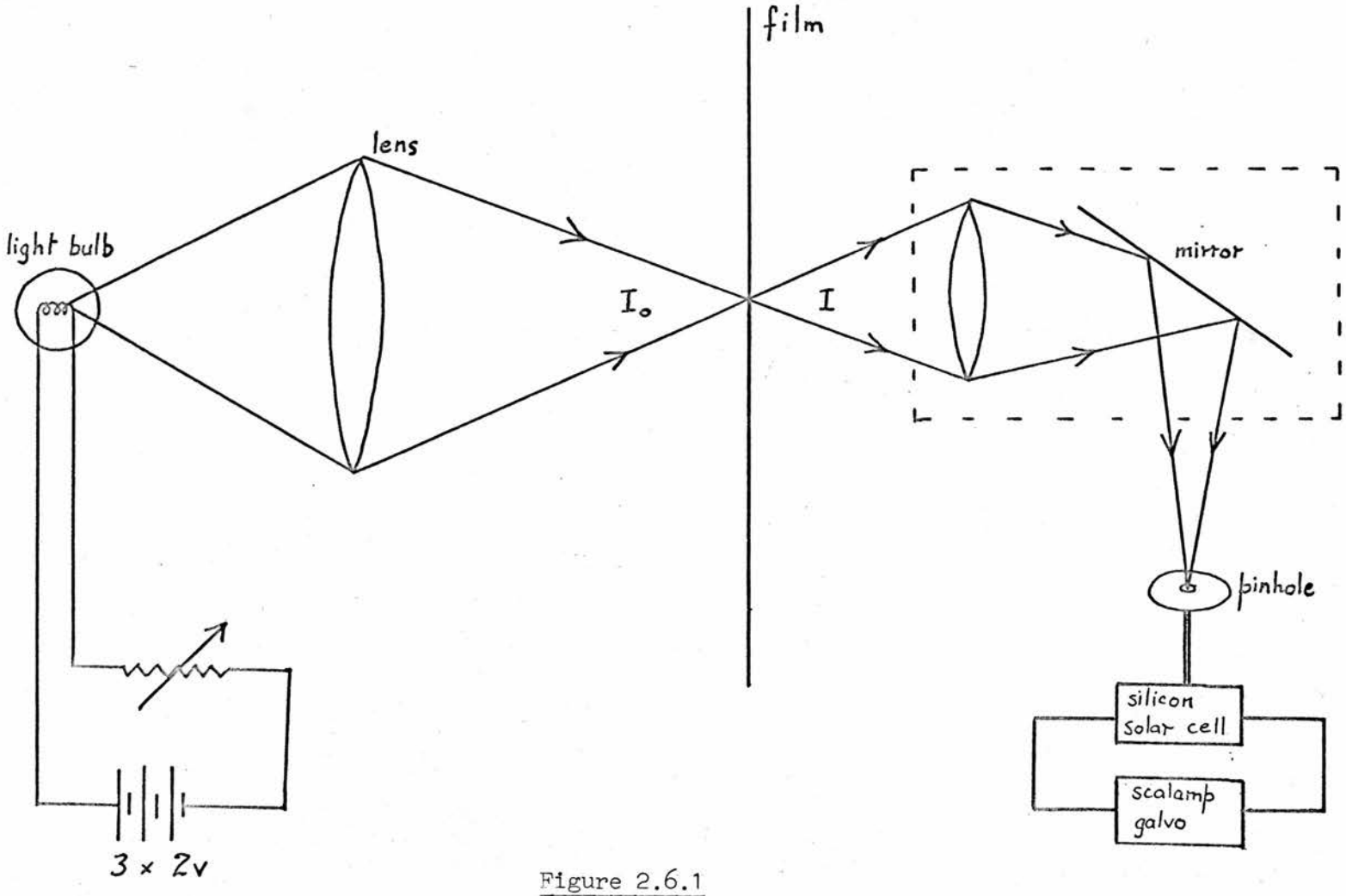
film
lens
light bulb
I_o
I
mirror
pinhole
silicon
solar cell
scalamp
galvo
3 × 2v

Figure 2.6.1

values, giving plateau sizes of approximately $(0.3)^2 mm^2$. The total vertical displacement b=(y+0.3)mm and the translation step a=(x+0.3)/n mm are set on two scales on the camera. n=number of translation steps in one direction made during the exposure (maximum of 30). These settings must be chosen such that a large plateau region is obtained consistent with no spot splitting, which occurs if the integration steps are too large. This was especially critical for the crystal of SiF_4,2Py since there were powdery fragments surrounding it in the tube.

2.6 Measurement of photographic integrated intensities

For a reflection recorded on film as described in 2.5 the integrated intensity I($\underline{h}$) of x-rays striking the film is the effective intensity of the reflection in the plateau region. This is linearly proportional to the effective film blackening or optical density D of the plateau and is measured with a Nonius microdensitometer, represented schematically by figure 2.6.1.

The density D at any point is defined by $\log_{10}(I_o/I_1)$, where I_o is the intensity of light incident on the film, and I_1 is the transmitted intensity received by a solar cell and causing a deflection on the galvanometer.

The effective optical density D of the plateau

= density of plateau - density of background

= $\log_{10}(I_o/I_P) - \log_{10}(I_o/I_B)$

= $\log_{10}(I_B/I_P)$

= $\log_{10}(B/P)$

I_B and I_P are the light intensities transmitted by the background and plateau regions respectively of the film and are linearly proportional to the deflections B and P on the galvanometer. Thus, for any reflection, the integrated intensity $I(\underline{h})$ is proportional to $\log_{10}(B/P)$, and for constant I_o for one film, a set of relative intensities recorded on the film is obtained.

At density values beyond a certain value, the relationship with x-ray intensity ceases to be linear, smaller increments of blackening occurring with larger exposure, and thus for all films, only those spots with B/P ratio of less than 12,corresponding to a maximum density of 1.079,were measured on the densitometer. By comparing sets of Friedel equivalent reflections, very light reflections with $B/P < 1.1$ were found to have such a high measurement inaccuracy as warranted their exclusion too. Thus the range of integrated intensities on one film measurable on the microdensitometer is $0.041 \rightarrow 1.079$.

The film to be measured is inserted in a holder which can be moved by hand vertically or horizontally. A dummy film, indexed by scratching the Weissenberg festoons on it, is fixed above and once aligned with the integrated film, a pointer indicates on the dummy the spot being measured below.

The light intensity I_o illuminating the film was chosen for each film by varying the rheostat such that on the lightest portion of the film the galvanometer deflection was a maximum but not

off scale.

With a focussed light spot and the smallest available detector pinhole (0.8m.m.) the graining of the films caused such oscillatory galvanometer deflections that the sensitivity of the system had to be reduced. Testing was done on several films to find the conditions for best peak resolution without excessive oscillations, and also for best agreement between Friedel equivalent reflections. A 1m.m. pinhole was eventually used and the light beam unfocussed by moving the light bulb further away from the film (this assumes a one to one correspondence between the light passing through the film and the pinhole).

The peak plateau region of each reflection was located by slowly moving the film until minimum galvanometer deflection P was recorded. The film was then moved vertically to either side to obtain background galvanometer readings B_1 and B_2 with mean B. White radiation streaks if present are therefore included in the background.

3. THE CRYSTAL AND MOLECULAR STRUCTURE OF TETRAFLUOROBISPYRIDINESILICON (IV)

3.1 Introduction

Long wavelength infrared spectroscopy is now widely used to investigate the structure of coordination compounds, and it is important that in some selected cases other physical techniques should be used to confirm the spectroscopic conclusions. No adducts of silicon tetrahalides, of the type $Si(Halogen)_4$, 2(Ligand), have been examined in detail by single crystal x-ray techniques although the infrared spectra have been reported and interpreted usually in terms of six coordinate cis or trans geometrical isomers. The infrared spectrum of $SiF_4,2(NC_5H_5)$ has been interpreted in terms of a trans octahedral stereochemistry (Beattie and Webster, 1965; Campbell - Ferguson and Ebsworth, 1967) on the basis of one i.r. absorption line in the Si-F stretching region.

3.2 Description of crystals

The crystals were supplied by Dr. M. Webster and had been prepared by heating the solid compound $SiF_4,2Py$ with excess pyridine in sealed tubes and allowing the tubes to cool slowly. Using a dry-box the better crystals were transferred to lithium borate glass capillary tubes and well sealed as these crystals must be kept moisture free.

Preliminary small oscillation x-ray photographs were taken to determine which of the incapsulated crystals were suitable for single crystal x-ray diffraction study. This was difficult to decide on the basis of a microscope examination only, as generally they were of poor quality, being fairly large and fragmented.

Only one single crystal was found in the first sample and it was used to determine the space group and unit cell dimensions before it was unfortunately knocked off the goniometer. A second sample of crystals again produced only one suitable crystal, 1.3mm long and 0.6mm x 0.5mm cross-section and this was used for the structure determination, both by photographic and diffractometer methods. This second crystal was lying in the Lindemann tube in approximately the same orientation as the initial crystal.

3.3 Unit cell dimensions

Rotation and equi-inclination Weissenberg photographs were taken using a Unicam camera for initial approximate measurements of the cell parameters, and indicated that no cell angles were equal to 90°. Since it was impossible to remount the crystal in its tube in a different orientation on the goniometer head, it was transferred to a Buerger precession camera on which all necessary photographs for a complete study of reciprocal space could be taken, and with greater accuracy than on the Unicam camera.

Using copper radiation, a prominent reciprocal axis a* was aligned parallel to the goniometer axis by the method of Fisher (1952 and 1953)

and an A-faced reciprocal cell with all sides and angles unequal was located. From it a suitable triclinic primitive (P) cell was found (a^*_P along the dial axis) and its lattice parameters were determined. Since not all real angles were $\geqslant 90°$, a Delaunay reduction was performed (Delaunay, 1933) to find the reduced (R) primitive cell.

The vector transformations obtained were:

$$\underline{a}_R = -\underline{b}_P - \underline{c}_P \; ; \qquad \underline{b}_R = \underline{a}_P \; ; \qquad \underline{c}_R = \underline{c}_P$$

$$\underline{a}^*_R = -\underline{b}^*_P \; ; \qquad \underline{b}^*_R = \underline{a}^*_P \; ; \qquad \underline{c}^*_R = \underline{c}^*_P - \underline{b}^*_P$$

It was therefore possible by making appropriate changes to the goniometer arcs and dial readings on the camera, to locate the reduced triclinic cell itself (b^*_R along the goniometer axis) and measure its lattice parameters directly.

The following factors were considered in obtaining accurate reduced cell parameters:

(i) The crystal setting with b* along the dial axis was checked for the four dial positions with hk0 and 0kl parallel to the film cassette.

(ii) The horizontal and vertical separations of pinhole marks were measured on undeveloped and normally developed film. Negligible difference was found and thus no correction was made for film shrinkage.

(iii) The crystal to film distance F, on the Buerger precession camera, was calibrated as described in Appendix B and gave F=59.74mm.

The final reduced triclinic cell parameters are:

a = 7.234Å	b = 6.420Å	c = 6.987Å($\pm$0.008)
α = 109°43'	β = 114°35'	γ = 95°42'($\pm$10')

Volume V = 266.71± 0.06Å^3

Measured density = 1.16 ± 0.04gm/cc

Calculated density with 1 molecule per unit cell = 1.63gm/cc

The space group is P1 or P$\bar{1}$ if the molecule has a centre of symmetry.

Linear absorption coefficient μ for Mo$K\bar{\alpha}$ = 2.6cm^{-1}

For collection of intensity data, the crystal was realigned with the b axis of the reduced cell along the goniometer axis, and reflections on equi-inclination Weissenberg photographs were indexed with respect to the reduced cell. This is especially tricky for a triclinic cell since the direction of displacement of upper level reflections relative to the zero level is important, and if this shift is small, careful study must be made to ensure thatthe axes are correctly orientated consistent with maintaining a right handed set and all reciprocal angles acute.

The results from a study of the compound SiF_4,2Py using the linear diffractometer for measurement of diffracted intensities are given in section A (3.4-3.7), and the photographic results in section B (3.8-3.11).

Photographic work was well under way by the time diffractometer data were collected, but due to the much longer time taken for photographic measurements, the linear data were used for the Patterson and initial Fourier syntheses from which the structure was essentially solved. Comparisons between the two final structural models, obtained after refinement using both sets of data, are given at the end of the chapter in section 3.12.

Section A Linear Diffractometer Data

3.4 Measurement of intensities

The same crystal used for the photographic recording of integrated intensities was afterwards transferred to the linear diffractometer, once it was operating satisfactorily, and set up for data collection as described in Chapter 2 (2.3 and 2.4).

The following values were selected:

1.5mm detector collimator 2°45' oscillation angle

2 oscillation cycles 1 minute oscillation motor

P.H.A. : low level = 20 volts, window width = 40 volts.

Generator : 40kV 16mA

Scanning (lower) slide interval = a^* = 0.1125 r.l.u.

Stepping (upper) slide interval = c^* = 0.1231 r.l.u.

Angle between slides = β^* = 61°19'

Spacing on vertical slide between equi-inclination k levels = λ/b = 0.1107 r.l.u.

As discussed in section 2.3, the displacements of upper level origins relative to the horizontal slides were found experimentally, and the values used for collection of data from the k^{th} level were:

Offset along the upper c^* slide = +0.0457 x k r.l.u.

Offset along the lower a^* slide = +0.0121 x k r.l.u.

These experimental values compare favourably with those calculated later as described in 2.3, and equal to 0.0452 and 0.0127 r.l.u.

respectively. Missetting of a reflection by 0.0006 r.l.u. is not significant since an integrated count is taken.

Intensity data were collected by the method described in section 2.4.4 from levels k=0→7 using Mo radiation (see figures 2.4.1 and 2.4.2 of the zero and sixth levels.) At the 5th level it was noticed that the background counts on either side of the peaks had become very unequal, even for reflections >0.1 r.l.u. from the slides' origin. It was discovered that, when the crystal oscillation mechanism was in its "CENTRE" position, it was 10' away from the true centre of the oscillation range. This instrument error was subsequently corrected for future data collection but no doubt contributed to the unequal backgrounds found with this crystal. Intensity profiles of reflections on the highest levels were very uneven due to the quality of the crystal and very elongated. Consequently, according to the discussion in section 2.4.1, the oscillation angle was increased, for the remainder of data collection from h51-h71, to a maximum of 5°35'. This was sufficiently large to encompass the error in peak missetting, which for h51-h71 was as much as 30' for some reflections for the reasons given in 2.3. Using some reflections on h51-h71 for testing, the net integrated intensity on automatic scan with this increased oscillation angle was always within two standard deviations of the value obtained when the peak was centred by hand. Background counts were now approximately equal again, and to compensate for the subsequent decrease in total count,

the generator current was increased to 20mA.

Scaling between the two sets of intensity data collected under different conditions was accomplished using those ten largest h51 reflections common to both and with $\sin\theta/\lambda > 0.2$ r.l.u.

3.5 Data processing and Patterson and Fourier syntheses.

The data cards from the linear diffractometer were processed using programmes 1 and 2 as described in Appendix A to give a set of $|F_o|^2$ and $|F_o|$ values. The multiplying factor for the h51-h71 intensity estimates to put them on the same scale as the h01-h41 data was 1.427, applied in programme 2 as part of the scale factor. The "R" factor for the h51 reflections used for scaling = $\Sigma|\Delta(\underline{h})|/\Sigma I(\underline{h})$= 0.048 where $I(\underline{h})$= intensity estimate with 2 3/4° oscillation angle and $\Delta(\underline{h})$=$I(\underline{h})$ - 1.427 x (intensity with maximum oscillation angle). Hence the scaling process will cause only a 2.4% error in $|F_o|$ values. No correction for absorption was made since the effect is small with Mo radiation, and considering the irregular shape of the crystal and its enclosure in a tube, difficult to evaluate significantly.

A Patterson synthesis was calculated with programme A4 using 1285 $|F_o|^2$ values. 31 sections were computed for z/c = 0-1, and on each section x/a = 0-$\frac{1}{2}$ and y/b = 0-1, all at intervals of 1/30. Since the Si-F bond length in $[SiF_6]^{2-}$ ion is 1.71Å, this is probably the order of magnitude of the bond in the SiF_4,2Py molecule, and thus a vector sphere of radius 1.71Å, centred at the origin of the Patterson vector set, was considered. To confirm the existence of possible peaks on

Figure 3.5.1

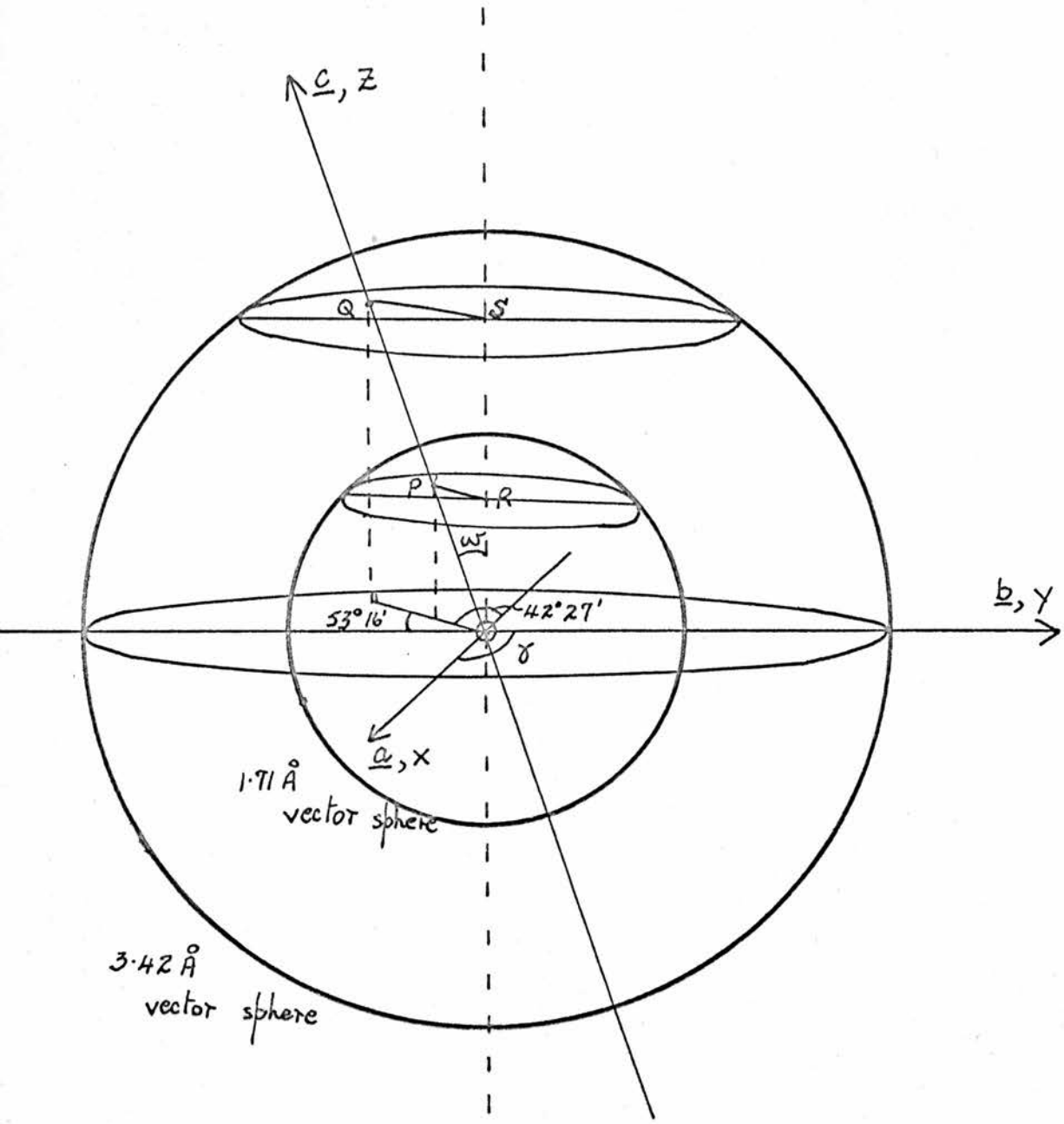
c, Z
Q
S
P
R
53° 16'
42° 27'
γ
b, Y
a, X
1·71 Å
vector sphere
3·42 Å
vector sphere

the sphere's surface due to Si-F vectors, vectors of length 3.42Å were also located.

In figure 3.5.1, O is the origin of vector space and centre of both spheres. The decreasing radii of the circles of intersection of the spheres with the computed Z sections are calculated from simple geometry. The direction of displacement of the intersections P and Q of the Z axis with successive sections makes angles 42°27' and 53°16' with the -X and -Y axes respectively when projected on to the XY plane as shown. $PR=OP \sin\omega = Z\sin\cos^{-1}(1/cc^*)$. Thus for each Z section whose origin is P or Q, the position of R or S, the centre of the appropriate circle, may be found.

The computed values of P(u,v,w) at mesh points near the vector spheres were plotted on polar graph paper, and remembering that the Patterson function is centrosymmetric and utilising all equivalent parts of the vector set, pictures of both hemispheres for vectors ~1.7 and 3.4Å were obtained.

Three regions with high P(u,v,w) values were located on the smaller hemisphere and the coordinates of their peak positions determined. The lengths of these interatomic vectors and the angles between them were calculated to be 1.95, 1.49, 1.52Å and 88.5°, 93.4°, 90.5°, which is quite satisfactory.

Corresponding peaks in the same orientation appeared on the larger hemisphere confirming that the above three vectors, together

with those related by the centre of symmetry, are the four Si-F and two Si-N bonds in the molecule. No attempt was made to distinguish between them because of the approximate equality of the sizes of the F and N atoms (Z=9 and 7 respectively).

The triclinic vector set is difficult to interpret and it was decided not to look further for interatomic vectors involving the carbon atoms but to feed the $|F_o|$ values obtained already and the coordinates found above into a structure factor calculation, according to equation (3), section 1.1, using programme A3.

The silicon atom was placed at the origin of the unit cell, which for space group P1 may be chosen anywhere. The six vector peaks therefore give directly the atomic coordinates of 4 fluorine and 2 nitrogen atoms and were allocated according to a cis-configuration in order to bias away from the expected trans-configuration of the molecule (see section 3.1).

The first calculation of structure factors F_c was performed with no refinement to obtain a correct scale factor $\Sigma|F_c|/\Sigma|F_o|$ to be applied to the $|F_o|$ values in the second cycle, again with no refinement on the atomic parameters. According to the theory given in section 1.1 the calculated phases assigned to the $|F_o|$'s will not be exactly correct since no carbon atoms have been included. However the Si,4F and 2N atoms ($\Sigma Z^2=618 \propto \Sigma f^2$) form the majority of the scattering power of the molecule (ΣZ^2 for the remaining 10 carbon and 10 hydrogen atoms= 370) and later inclusion of the other atoms will not greatly alter

Figure 3.5.4

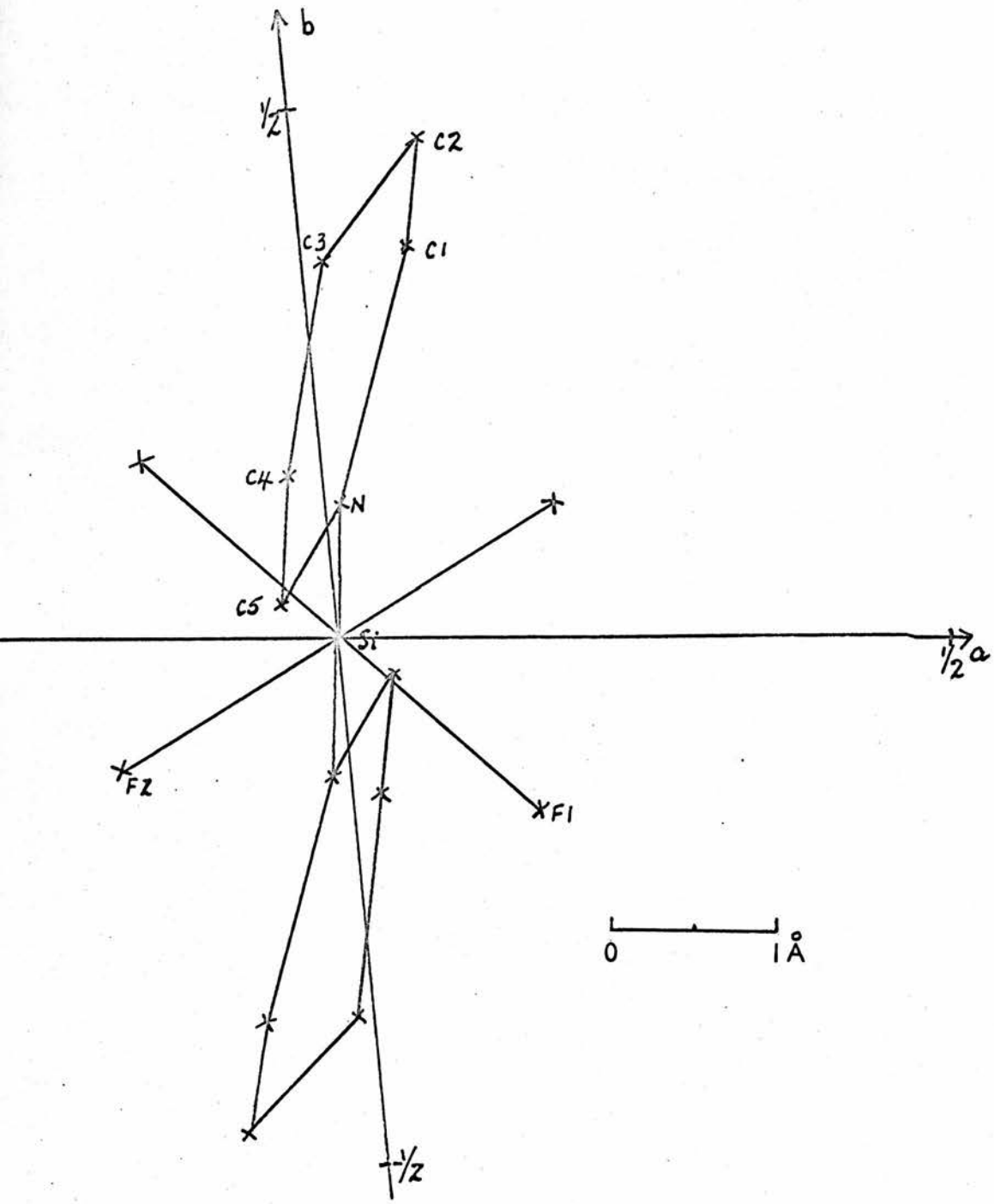

the phases of reflections with large $|F_o|$ and F_c values. 138 such reflections from the second cycle output of programme A3 were used to compute a Fourier synthesis throughout the unit cell using programme A4 and as described in section 1.1 (equation (2)).

Seventeen regions of high electron density were found in the three dimensional Fourier map corresponding to all the atoms except hydrogens in the SiF_4,2Py molecule. The coordinates of the centres of the peaks are shown in figure 3.5.4 projected on to the ab plane (the displacement of increasing Z section origins was calculated earlier-see figure 3.5.1). The molecule has a trans configuration and the pyridine ring geometry is sensible.

3.6 Structure refinement

A structure factor calculation, computed using the seventeen atomic positions gave an R value (see section 1.4) of 0.27 (once the scale factor for the $|F_o|$ values had been determined as before). Assuming space group P1, a few cycles of least squares refinement of the scale factor, atomic coordinates and isotropic temperature factors (see section 1.4) reduced this to a minimum of 0.214. For all reflections, the real part A of F_c was very much greater than B (see section 1.1) and the departure of the structure from $P\bar{1}$ was less than the standard deviations of the atomic coordinates. Refinement was thus continued with space group $P\bar{1}$, the Si atom being placed at the centre of symmetry (0,0,0). The Si formfactor values were halved (see Appendix A3) and the positions of only 2 fluorine,

Table 3.6.1

k-level	1st Scale factor S_1	2nd Scale factor S_2
0	0.958	0.9821
1	0.951	0.9991
2	0.979	0.9908
3	0.941	0.9882
4	1.021	0.9324
5	0.937	0.9691
6	0.958	0.9142
7	0.891	0.9494

1 nitrogen and 5 carbon atoms given in the directives for programme A3 since the asymmetric unit of the unit cell contains only half the molecule. Further refinement reduced R to 0.20 when the latest isotropic B values, given below, were converted to anisotropic B_{ij}'s by programme A3. R fell instantly to 0.168.

ATOM	Si	F1	F2	N	C1	C2	C3	C4	C5
B	2.657	3.915	3.786	2.726	3.171	3.808	4.297	3.948	3.373

During subsequent cycles, the following operations were executed:

(i) Because of inaccuracies in instrument and crystal setting, a separate scale factor $S_1 = \sum|F_c| / \sum|F_o|$ was found for each k level of intensity data collected, using the largest values and programme A6. They are given in table 3.6.1 and were applied to the $|F_o|$ values.

(ii) The positions of the five hydrogen atoms in the pyridine ring were calculated as described in Appendix C using the latest coordinates of the other atoms. At this stage R=0.149 and the parameter shifts were reduced to the 4th decimal place. The H atomic coordinates are given in the final table of coordinates 3.7.1. It was not felt necessary to recalculate them since subsequent molecular geometry was sufficiently good (see section 3.7). Each H atom was given the last isotropic B value of its corresponding carbon atom (see above), since the thermal motion will be similar, and no least squares refinement was attempted on the hydrogen parameters.

(iii) Reflections outside the copper sphere (section 2.4.4) were removed and also those with net intensity estimate I less than 20 counts, since they have large counting statistics errors.

(iv) k level scale factors S_2 were calculated for the second time using all the latest $|F_c|$ and $|F_o|$ values for each level and are listed in table 3.6.1.

Successive cycles of least squares refinement on the 79 parameters were performed with the remaining 959 intensities until minimum $\Sigma w \Delta^2$ was reached and R=0.0887. A card output of this best cycle to date was taken.

So far the weighting scheme given by equation (11), section 1.5 had been used (F_{min}=0.44) but now the more realistic scheme (equation (12), section 1.5) for diffractometer data was applied by means of programmes 7-11 (see Appendix A).

The scale factor K/4 applied to each level of data during the processing of (I+B)/(I-B) (from A7) must be carefully evaluated so that K is the correct factor to put the (I+B)/(I-B) values on to the same absolute scale as the latest values of $|F_o|^2$ and $|F_c|^2$. For SiF_4,2Py, therefore, K is the product of four terms: (the original scale factor for processing each k level of diffractometer intensities) x (level scale S_1)^2 x (level scale S_2)^2 (see table 3.6.1) x (latest structure factor scale in A3)^2.

Substituting the results of three summations by A8 and A9 into equation (13), section 1.5, gave c^2=0.010836, c=0.1041,

Figure 3.6.1

A composite map of electron density in SiF_4,2Py viewed along a (from sections nearest centres of Si peaks).

C1-C5: first contour at 2e/Å^3, then at 1e/Å^3 intervals.

N,F1,F2: first contour at 2e/Å^3, then at 2e/Å^3 intervals.

Si: first contour at 5e/Å^3, then at 5e/Å^3 intervals.

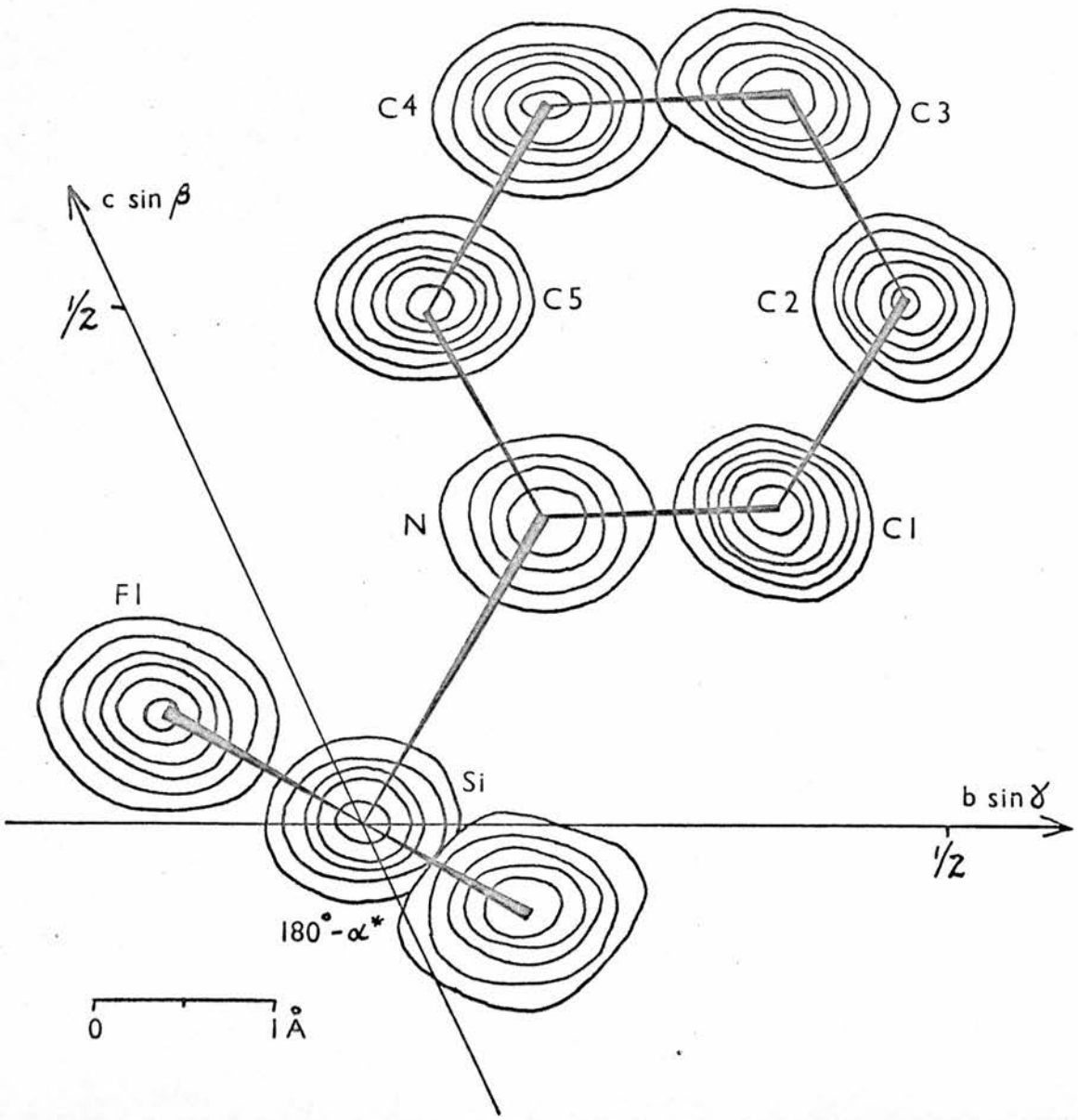

G(counting statistics) = 0.0329 and G=0.1092. These values indicate that, as expected, the error in intensity measurement by the linear diffractometer due to counting statistics is much smaller than other errors, and hence the decision to record only two oscillation cycles at each reflection is justified (see section 2.4.2).

The factor $D = 0.99/\sqrt{w_{max}}$, which is used to obtain a scaled set of $\sqrt{w}$ values in the correct format for use in programme A3, was 0.1371. The resulting output from A11 becomes the new input for further cycles of SFLS calculations. The first cycle with this weighting scheme gave a significantly smaller $\Sigma w \Delta^2$.

After three more cycles, a card output was taken and programme A12 used to find those reflections with a difference Δ between the observed and calculated structure amplitudes greater than 3 or 4 standard deviations $\sigma(=1/\sqrt{w})$. As many as 34 reflections had $\Delta > 3\sigma$ (on an absolute scale), probably because of the crystal quality, its surrounding tube and the inexact setting of the triclinic crystal on the diffractometer. 17 reflections with $\Delta > 4\sigma$ were probably subject to non-random errors in intensity measurement and were given zero weight. Four of these reflections were in the inaccurate region of the instrument, near the origin of the horizontal slides (see section 2.2), and another reflection $(\bar{6},0,2)$ proved to be a Renninger reflection, discussed in section 3.10. No obvious cause of the large inaccuracy in the other 12 intensities could be detected.

Structure refinement continued until, after five further cycles, $\sum w\Delta^2$ was minimised and R=0.0758. $\sum w\Delta^2$ computed by A3 is on the basis of the scaled $\sqrt{w}$ values, and hence absolute $\sum w\Delta^2$ = (scaled $\sum w\Delta^2)/D^2$. Account must also be taken of any change in the SFLS scale factor between the calculation of absolute $\sqrt{w}$ values and this final cycle.

The final F_o and F_c values, $(F_o)_L$ and $(F_c)_L$, are listed in table A at the end of the thesis. $\sum_{1}^{m} w\Delta^2 = 901.186$ on an absolute scale and since (m-n) = 959-79 = 880, $\sum w\Delta^2/(m-n) = 1.024$, which is close to its theoretical limit of unity (see section 1.5).

A Fourier synthesis was computed from the experimental $|F_o|$ values with the phases (+1 or -1) calculated from the final structural model. See figure 3.6.1.

3.7 Discussion

The final fractional coordinates and their standard deviations for the atoms in the asymmetric unit are given in table 3.7.1 and anisotropic temperature factors in table 3.7.2. A perspective view of the structure along the b axis is shown in figure 3.7.1, drawn by the computing department programme PAMOLE.

Programme A5 was used to compute interatomic bond lengths and angles and these are listed in tables 3.7.3 and 3.7.4 together with their standard deviations obtained from the final SFLS calculation. No standard deviations are available for those values involving hydrogen atoms since they were not included in least squares refinement.

Table 3.7.1

Atom	x/a	σ(x/a)	y/b	σ(y/b)	z/c	σ(z/c)
Si	0.0000	0.0000	0.0000	0.0000	0.0000	0.0000
F1	0.1723	0.0004	-0.1314	0.0004	0.1081	0.0004
F2	-0.1529	0.0004	-0.1005	0.0004	0.0893	0.0004
N	0.1437	0.0005	0.2735	0.0005	0.2929	0.0006
C1	0.2070	0.0007	0.4813	0.0007	0.3030	0.0008
C2	0.3090	0.0007	0.6743	0.0007	0.5078	0.0009
C3	0.3457	0.0007	0.6601	0.0008	0.7104	0.0008
C4	0.2776	0.0007	0.4420	0.0008	0.6981	0.0008
C5	0.1813	0.0007	0.2533	0.0008	0.4917	0.0007
H1	0.1765		0.4861		0.1500	
H2	0.3555		0.8313		0.5059	
H3	0.4174		0.7991		0.8658	
H4	0.3076		0.4286		0.8462	
H5	0.1325		0.0954		0.4800	

Table 3.7.2

Anisotropic temperature factors x 10^4

Atom	B_{11}	B_{22}	B_{33}	B_{23}	B_{13}	B_{12}
Si	167	243	193	165	169	52
F1	263	314	270	184	159	213
F2	260	342	292	165	341	-43
N	167	257	244	196	224	63
C1	217	265	282	209	255	158
C2	226	279	359	209	261	170
C3	207	346	283	46	178	101
C4	223	406	258	174	247	79
C5	217	363	253	268	237	77

FIGURE 3.7.1

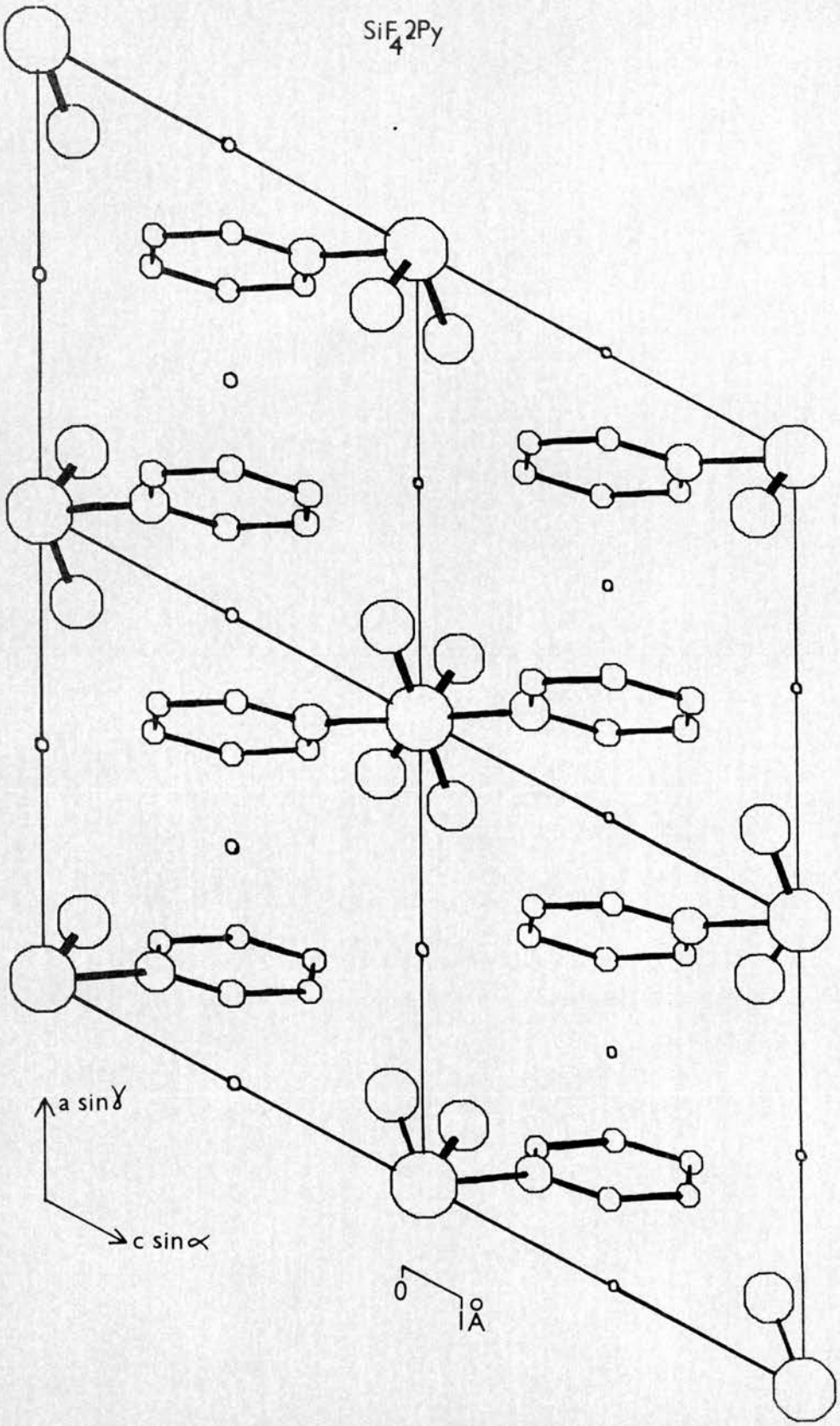

Table 3.7.3

Intramolecular bond lengths

Bond	Length (Å)	σ(Å)
Si-F1	1.640	0.003
Si-F2	1.653	0.003
Si-N	1.948	0.005
N-C1	1.335	0.006
C1-C2	1.368	0.011
C2-C3	1.365	0.009
C3-C4	1.399	0.008
C4-C5	1.360	0.011
C5-N	1.354	0.007
C1-H1	1.010	
C2-H2	1.037	
C3-H3	1.015	
C4-H4	1.001	
C5-H5	1.004	

Table 3.7.4

Intramolecular bond angles (°)		σ(°)
F1-Si-F2	90.2	0.1
F1-Si-N	90.4	0.2
F2-Si-N	90.0	0.2
Si-N-C1	121.6	0.4
Si-N-C5	119.5	0.4
C1-N-C5	119.0	0.6
N-C1-C2	122.1	0.5
C1-C2-C3	120.3	0.5
C2-C3-C4	117.2	0.7
C3-C4-C5	120.7	0.5
C4-C5-N	120.8	0.5
N-C1-H1	115.6	
C2-C1-H1	122.3	
C1-C2-H2	118.9	
C3-C2-H2	120.7	
C2-C3-H3	123.1	
C4-C3-H3	119.7	
C3-C4-H4	118.0	
C5-C4-H4	121.3	
C4-C5-H5	121.7	
N-C5-H5	117.6	

A5 gave the shortest intermolecular distances (< 3.2Å) as (in Å):

F1-H1	F1-H2	F1-H3	F2-H3	H1-H4	H2-H5	C2-H5	C5-H2
2.571	2.643	2.890	2.720	2.599	2.453	3.132	3.113

Due to steric hindrance of the hydrogen atoms with the fluorine atoms of adjacent molecules, the plane of the pyridine ring does not bisect the angle F1-Si-F2. By dropping perpendiculars from C4 and C5 on to the line joining F1 and F2, and applying simple geometry, it was calculated that atoms C4 and C5 are rotated about the Si-N-C3 axis towards F2 by 9.4°. The angle Si-N-C3 is 180° and there are no unduly short intermolecular distances.

The best plane through the five carbon atoms was calculated as described in Appendix D. It is given by $lx'+my'+nz' = p$ with respect to orthogonal axes (x', y', z') chosen according to Appendix C. l=+0.93799, m=-0.32126, n=+0.13024 and p=+0.02138Å. The perpendicular distances of the atoms from this plane are (in Å):

Si	N	C1	C2	C3	C4	C5
-0.021	-0.007	-0.008	+0.008	+0.000	-0.008	+0.008
F1	F2	H1	H2	H3	H4	H5
+1.296	-1.011	-0.009	+0.012	-0.012	+0.013	+0.010

The deviations of Si and N are not significant and thus the Py-Si-Py part of the molecule is planar. The pyridine plane is confirmed to lie nearer F2 than F1.

The Si-F1-F2 plane, $l'x' + m'y' + n'z' = 0$, was also calculated

Figure 3.7.2

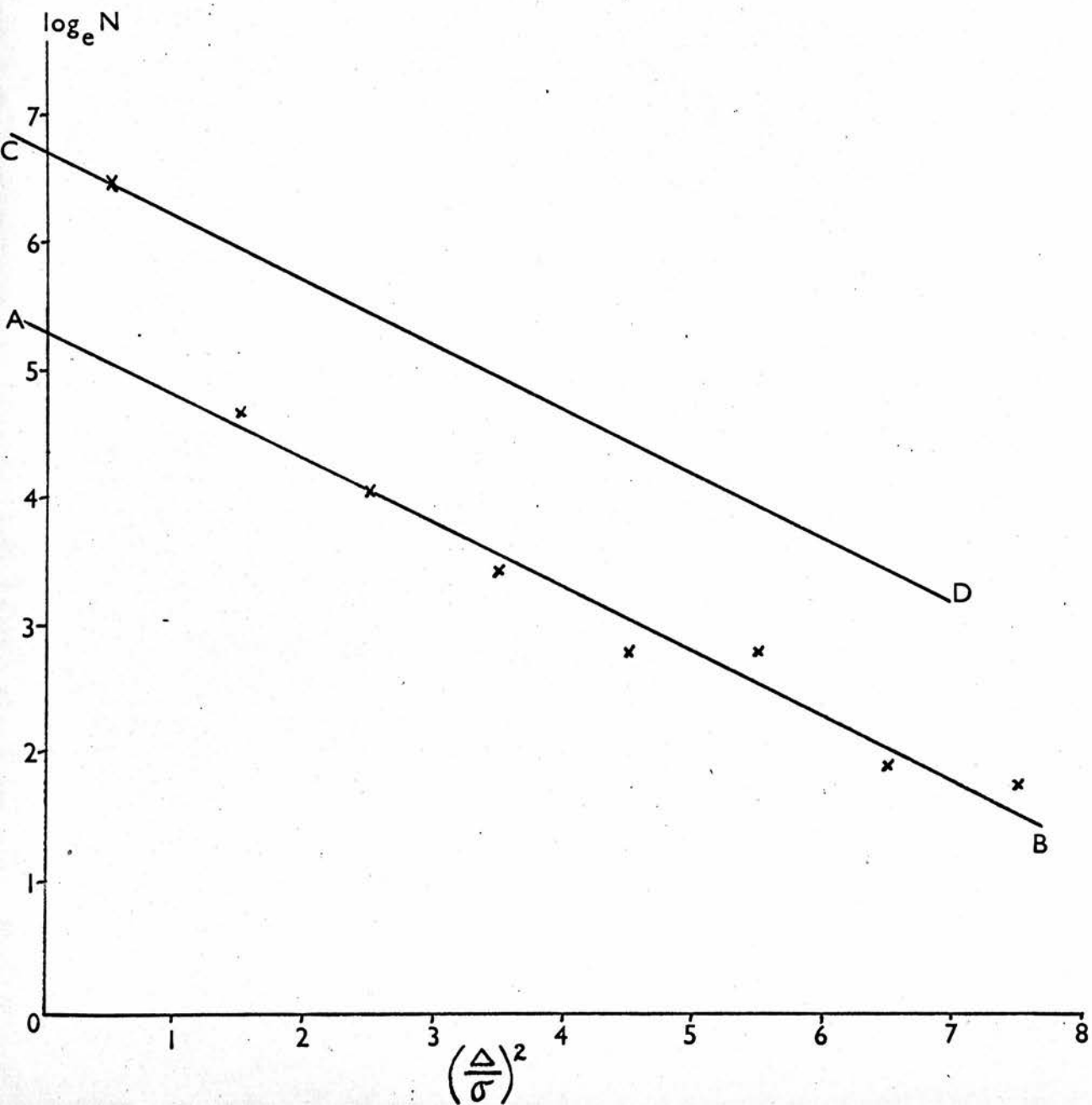

and the angle between the two planes, given by $\cos^{-1}(ll'+mm'+nn')$, found to be 89°15'. $l' = +0.06058$, $m' = +0.48878$, $n' = +0.87030$.

With respect to the oblique axes of the reduced triclinic cell, the pyridine ring plane is : $\frac{x}{a} + \frac{y}{b} + \frac{z}{c} = 1$; where $a = +0.02215$Å, $b = -0.06655$Å and $c = -0.10291$Å are the intercepts on the axes (see Appendix D).

If the weights assigned to the diffractometer intensities according to equation (12), section 1.5 and as described in section 3.6 are absolute, then the distribution of Δ/σ values ($=\sqrt{w}\Delta$) should obey a Gaussian curve: $N = \frac{1}{\sigma\sqrt{2\pi}} \exp -\frac{1}{2}\left(\frac{\Delta}{\sigma}\right)^2$.

In order to check this, programmes A13 and A14 were used to plot $\log_e N$ v. $w\Delta^2$ where N is the number of reflections with $w\Delta^2$ values in each of the 16 intervals from 0-16 (the 17 reflections with $\sqrt{w}.|\Delta| > 4$ having been removed). The resulting graph is shown in figure 3.7.2. Points with $(\Delta/\sigma)^2 > 8$ have been omitted because of the small number of reflections in each of these intervals. The best least squares straight line AB through all points except the first was evaluated by the computer library programme CLPOLF. Its slope = -0.50= -B and intercept on $\log_e N$ axis=5.33=$\log_e A$, where $N=Ae^{-B(\Delta/\sigma)^2}$. B equals the theoretical value of $\frac{1}{2}$. The deviation of the first point with $(\Delta/\sigma)^2 = 0 \rightarrow 1$, from this normal distribution could be because reflections, too small to be recorded by the linear diffractometer and with $(\Delta/\sigma)^2 > 1$, have been omitted. If included, N might increase for all points except the first one,

keeping them linear with slope = $-\frac{1}{2}$, to give the normal distribution represented by the line CD, with intercept = $\log_e A = 6.75$.

Section B Photographic Data

3.8 Measurement of intensities

The linear diffractometer not yet being operational due to the faults discussed in section 2.2, integrated intensities were recorded on equi-inclination integrated Weissenberg photographs for $k=0 \rightarrow \bar{7}$ as described in section 2.5 Test photographs were taken of sections of various k levels with different integration settings a and b (see section 2.5) and different exposure times. The range of x-ray intensities diffracted by SiF_4,2Py was very large and as seen in section 2.6, only a certain range of spot density can be measured on the microdensitometer. Thus the film pack technique (DeLange, Robertson and Woodward, 1939; and Robertson, 1943) was employed with two films per exposure: an "industrial G" film (nearer the x-rays) and a less sensitive, smaller grained B film (Iball, 1954). The following exposures per level were found to be the optimum using MoK$\bar{\alpha}$ radiation:

1. Films G_1 and B_1. Each spot traversed 4 x 30 times (~53 hours) with vertical displacement b=0.6mm and translation step a=1.5/30 = 0.05mm. 40kV 20mA.
2. Films G_2 and B_2. Each spot traversed 15 times (~7 hours) with b=0.6mm and a=1.5/15 = 0.1mm. 40kV.
   10mA for h0l - h$\bar{3}$l 20mA for h$\bar{4}$l - h$\bar{5}$l

Table 3.8.1

Level	No. of films	$S_1=G_1/B_1$	$S_2=B_1/G_2$	$S_3=G_2/B_2$	No. of different reflections
h01	4	3.278	3.974	3.980	96
$h\bar{1}1$	4	3.945	3.530	3.420	150
$h\bar{2}1$	4	3.576	3.782	3.936	157
$h\bar{3}1$	4	3.598	4.294	4.171	151
$h\bar{4}1$	4	2.335	2.852	4.668	109
$h\bar{5}1$	3	3.737	2.069		92
$h\bar{6}1$	2	3.961			84
$h\bar{7}1$	2	3.743			45

The shorter exposure B_2 film must contain the strongest reflections, light enough for accurate densitometer measurement, and the longer exposure G_1 film, as many measurable weak reflections as possible.

All the films for one level were processed together in complete darkness by agitating in fresh developer. It is essential that each film on one level contains a sufficient number of measurable reflections common to the next strongest and weakest films so that the scale factors between the films on each level may be calculated. The factors to scale all films per level up to the G_1 film are given in table 3.8.1. The vast majority of a total of 1535 reflections were measured by Mrs. J. Page, as described in section 2.6. Of these about half were used for inter-film scaling, 884 unique intensity estimates remaining, as listed in table 3.8.1.

The accuracy in intensity measurement was found by comparing Friedel equivalent intensities on both halves of three h0l films. The mean ratios of such intensities were 1.06, 1.07, 1.09. The mean intensity reduction between the G and B films in a pack is 3.72 (from the 13 values in table 3.8.1) and its standard deviation of 0.52 implies 14% accuracy.

3.9 Data processing

Precession photographs had been taken for scaling the intensity estimates between k levels but were not used since the diffractometer data were now available. By comparing the largest photographic

intensities from each level with the equivalent diffractometer values, a scale factor was found for each level to put all the photographic data on the same scale as the diffractometer intensities. Programme A2 was used to apply these scale factors and Lp corrections and obtain $|F_o|$ values.

By this time a set of atomic coordinates for the molecule had been obtained from the solution of the Patterson vector set and subsequent Fourier map described in section 3.5.

3.10 Structure refinement

The latest $P\bar{1}$ atomic coordinates and anisotropic temperature factors from the present stage of refinement of the structural model from the diffractometer data (section 3.6) were used for an SFLS calculation by programme A3 together with the photographic $|F_o|$ values. The calculated hydrogen parameters (section 3.6 and table 3.7.1) were also given but not included in least squares calculations. The first calculation gave R = 0.230 and before refinement on the 79 parameters, those reflections outside the copper sphere ($\sin\theta > 0.461$) were removed.

During refinement, each pair of $|F_o|$ and $|F_c|$ values was examined, and those reflections with a large discrepancy between them and between the diffractometer $|F_o|$ value were traced back to the film measurement stage. Some errors were found and corrected: namely, reflections misindexed, specks of dust on the film measured instead

of the actual spot which often was invisible, mispunched intensities on cards and some reflections included twice.

A scale factor $\Sigma|F_c|/\Sigma|F_o|$ was calculated for and applied to each k level (see section 3.6).

Level	h0l	h$\bar{1}$l	h$\bar{2}$l	h$\bar{3}$l	h$\bar{4}$l	h$\bar{5}$l	h$\bar{6}$l	h$\bar{7}$l
Scale	0.9505	0.9891	0.9938	0.9352	1.1466	0.9232	0.8674	0.7677

When structure refinement had progressed to the stage where R = 0.126, it was decided to check the space group by moving the atoms away from their centrosymmetric configuration (m = 771, n = 79) and proceeding with refinement using space group P1 (m = 771, n = 154). After several cycles R and $\sum w\Delta^2$ reached minimum values, R at 0.134. Since $\sum w\Delta^2/(m-n)$ had increased to 1.32 x its value when P$\bar{1}$ was assumed and the molecular geometry was not so sensible, the centrosymmetric nature of the molecule was confirmed.

Weighting scheme (a) (equation (11), section 2.5) was used throughout, being the most suitable for the photographic data (F_{min} = 0.84).

The ($\bar{6}$, 0, 2) reflection, having extremely poor agreement between F_o and F_c, was omitted from the refinement procedure which was continued with the other 770 reflections until minimum $\sum w\Delta^2$ and R = 0.0960 were obtained. With ($\bar{6}$, 0, 2) included, final R = 0.0975, which was thought to be satisfactory in view of the quality of the crystal, its incapsulation and the errors involved in

Table 3.11.1

Atom	x/a	σ(x/a)	y/b	σ(y/b)	z/c	σ(z/c)
Si	0.0000	0.0000	0.0000	0.0000	0.0000	0.0000
F1	0.1721	0.0008	-0.1309	0.0010	0.1090	0.0008
F2	-0.1511	0.0008	-0.0984	0.0010	0.0894	0.0009
N	0.1422	0.0010	0.2706	0.0013	0.2910	0.0011
C1	0.2054	0.0013	0.4781	0.0017	0.3026	0.0015
C2	0.3100	0.0014	0.6750	0.0018	0.5067	0.0016
C3	0.3482	0.0014	0.6608	0.0020	0.7111	0.0016
C4	0.2804	0.0014	0.4432	0.0020	0.6988	0.0015
C5	0.1809	0.0013	0.2525	0.0017	0.4898	0.0014

Table 3.11.2

Anisotropic temperature factors x 10^4

Atom	B_{11}	B_{22}	B_{33}	B_{23}	B_{13}	B_{12}
S1	112	325	155	145	142	34
F1	179	404	218	165	85	188
F2	201	390	241	140	257	-40
N	124	322	195	152	128	96
C1	160	309	205	95	155	108
C2	184	335	284	170	181	63
C3	165	442	250	88	208	134
C4	200	489	152	109	169	47
C5	158	371	173	123	135	63

the photographic measurement of intensities.

The $(\bar{6}, 0, 2)$ reflection ($F_o \gg F_c$) is probably a Renninger reflection (Renninger, 1937) caused by double diffraction from the $[2, 0, \bar{1}]$ and $[\bar{4}, 0, \bar{1}]$ crystal planes. Using the polar plot of h0l level (figure 2.4.1) the Ewald sphere of reflection was found to pass through the reciprocal lattice points $(2,0,\bar{1})$ and $(\bar{4},0,1)$ simultaneously. The $(2,0,\bar{1})$ and $(\bar{4},0,1)$ reflections are very large and fairly large respectively, as seen in Table A where the final F_o and F_c values, $(F_o)_P$ and $(F_c)_P$, are listed. For the photographic data, the listed indices of reflections are the Friedel equivalents of those measured ($k = 0\text{-}\bar{7}$) since diffractometer intensities were measured for $k = 0\text{-}7$.

3.11 Molecular geometry

The final atomic coordinates of the refined structural model obtained from photographic intensities are given in table 3.11.1 together with their standard deviations. Hydrogen coordinates are not listed since they have been given already in table 3.7.1. Anisotropic B_{ij}'s are tabulated in table 3.11.2, and intramolecular bond lengths and angles and their standard deviations in tables 3.11.3 and 3.11.4.

A scan of interatomic bond lengths and angles by programme A5 showed that, as obtained before for the structural model from diffractometer intensities, the angle Si-N-C3 is 180° and the shortest intermolecular distances are equal to those given in

Table 3.11.3

Intramolecular bond lengths

Bond	Length (Å)	σ(Å)
Si-F1	1.639	
Si-F2	1.637	
Si-N	1.932	0.012
N-C1	1.329	0.013
C1-C2	1.379	0.012
C2-C3	1.375	0.015
C3-C4	1.395	0.017
C4-C5	1.376	0.012
C5-N	1.347	0.012
C1-H1	1.019	
C2-H2	1.027	
C3-H3	1.011	
C4-H4	1.005	
C5-H5	1.004	

Table 3.11.4

Intramolecular bond angles (°)		σ(°)
F1-Si-F2	90.1	
F1-Si-N	90.2	
F2-Si-N	89.5	
Si-N-C1	121.8	0.8
Si-N-C5	120.2	0.8
C1-N-C5	118.0	0.7
N-C1-C2	123.6	0.9
C1-C2-C3	119.2	1.0
C2-C3-C4	117.1	0.8
C3-C4-C5	120.8	1.0
C4-C5-N	121.2	0.9
N-C1-H1	116.3	
C2-C1-H1	120.0	
C1-C2-H2	120.5	
C3-C2-H2	120.3	
C2-C3-H3	123.4	
C4-C3-H3	119.4	
C3-C4-H4	118.5	
C5-C4-H4	120.8	
C4-C5-H5	121.1	
N-C5-H5	117.7	

section 3.7. Again, the pyridine ring is rotated, by 9.1°, towards F2 to ease the steric repulsion between hydrogens and fluorines of adjacent molecules.

The least squares best fit plane (see Appendix D) through C1-C5 was calculated to be:

$-0.93866x' + 0.32269y' - 0.12158z' = 0.00135$ with respect to orthogonal axes x', y', z' (see Appendix C). Atomic deviations from this plane are (in Å) :

Si	N	C1	C2	C3	C4	C5
-0.001	+0.002	+0.008	-0.009	+0.002	+0.006	-0.007
F1	F2	H1	H2	H3	H4	H5
-1.311	+0.985	-0.003	-0.004	+0.037	+0.007	-0.009

Thus, it is again apparent that Si and N lie on the plane, which is nearer F2 than F1. The Si-F1-F2 plane was also calculated with respect to x', y' and z': $0.06250x' + 0.49309y' + 0.86773z' = 0$. The angle between it and the plane of the pyridine ring is 90°17'.

In terms of the reduced triclinic cell axes, the pyridine ring plane is:

$$-\frac{x}{0.00140} \qquad \frac{y}{0.00419} \qquad \frac{z}{0.00630} = 1$$

3.12 Conclusion

Structural models have been found for SiF_4,2Py from intensities measured by diffractometer and photographic techniques. Comparison

of both sets of results, given in tables 3.7.1 - 3.7.4 and 3.11.1 - 3.11.4, indicates no significant differences in atomic parameters and molecular geometry.

The values of l,m and n for the best fit pyridine plane, $lx' + my' + nz' = p$, calculated for both models (sections 3.7 and 3.11) differ in the third decimal place. The angle between the planes is 30' and their separation, given by $p_1 + p_2$ since they are fractionally on opposite sides of the origin (Si atom), is 0.023Å. The angle between both Si-F1-F2 planes is 17' and their l,m and n values also differ in only the third decimal place.

The final R factor for the linear diffractometer data, 0.0758, is lower than that for the photographic observations (0.0975) and the standard deviations of the diffractometer model are smaller (cf. tables 3.7 and 3.11). This is a consequence of the greater precision of the counter data and the larger number of reflections measured (m = 959 and 771 respectively).

Thiourea has also been used for a comparison of counter and photographic observations (Truter, 1967) and gave similar results.

The centrosymmetric trans configuration of SiF_4,2Py in the solid state confirms the conclusions obtained from infrared spectroscopy and is similar to that claimed for tetrachlorobispyridinegermanium (IV) (Hulme, Leigh and Beattie, 1960). Their crystallographic deductions are based on one two dimensional Patterson map using 32 structure factors, the space group being

postulated mainly on this basis.

The molecules of SiF_4,2Py are arranged in the lattice with the pyridine rings stacked one above the other, almost normal to a of the reduced triclinic cell. Hence the separation of adjacent pyridines is $\approx \frac{1}{2}a = 3.62$Å.

4. THE CRYSTAL AND MOLECULAR STRUCTURE OF TETRACHLORCBISPYRIDINESILICON (IV)

4.1 Introduction

The infrared spectrum of solid $SiCl_4,2(NC_5H_5)$ has been interpreted as the basis of a cis geometrical isomer from both the number and position of Si-Cl stretching vibrations (Beattie et al, 1964). A single crystal x-ray examination of the compound was briefly reported in the same paper (Hulme, personal communication). Statistical tests (Howells, Phillips and Rogers, 1950) gave inconclusive results, but a trans configuration was excluded and a cis isomer postulated.

The i.r. spectrum of $SiCl_4$,2Py in the solid state has also been reported by Campbell-Ferguson and Ebsworth (1967) and agrees with the earlier work, although they suggest the prescence of polymeric cations. More recent Raman spectroscopy measurements have led to a revised and more cautious view on the stereochemistry of the Si $(Halogen)_4$, 2 Pyridine systems. A single crystal x-ray examination of $SiCl_4$,2Py was undertaken, to establish its structure unambiguously.

4.2 Description of crystals

The crystals of $SiCl_4$,2Py had been prepared by the same method used for SiF_4,2Py but were of poorer quality and were sealed in pyrex tubes. The crystals were supplied by Dr. M. Webster.

Triclinic cell parameters were established using the best crystal in an initial sample, and considerable time was spent trying to set this crystal on the linear diffractometer as described in section 2.3 for collection of intensity data. The crystal was fragmented and powdery, and the intensity profiles of reflections, seen on the chart recorder by tracking through the oscillation scale, were of the forms:

The profile of any one reflection did not remain the same when different portions of the rather long crystal were centred in the x-ray beam. Intensity profiles worsened as ζ increased and Friedel equivalent intensities on the zero layer were very unequal.

It was impossible to set the crystal either such that the main intensity peak was isolated and set for all reflections at the centre of the oscillation range, or such that the whole profile of all reflections was included in even the maximum oscillation range.

Thus the linear diffractometer could not be used for measurement of intensities from this fragmented triclinic crystal. Intensity estimates could have been obtained from integrated photographs, but by this time a second sample of crystals was available. The best single crystal it produced [0.7mm by (0.6 x 0.4) mm^2] had an

additional small fragment enclosed with it in the pyrex tube, and this was seen from photographs to produce additional spots. These however were generally well separated from the main reflections, and hence this crystal was used for an x-ray diffraction study.

4.3 Unit cell dimensions

Preliminary rotation and equi-inclination Weissenberg photographs were taken with a Nonius camera using Mo radiation and indicated that the crystal was triclinic. The most prominent unit cell was chosen, c along the goniometer axis, and values of c, a*, b* and γ^* were obtained. By considering the Weissenberg geometry and the displacement of upper level reflections, the cell axes were labelled such that a right-handed system was maintained with real angles obtuse and reciprocal cell angles acute. Absences noted were: $h + k = 2n + 1$; $k + l = 2n + 1$, $h + l = 2n + 1$. This cell is therefore centred on all faces.

For further information the crystal was transferred to a Nonius precession camera and c* was aligned along the dial axis. Zero, first and second layer photographs with a and b perpendicular to the film cassette were taken. The chosen unit cell was confirmed to be an F cell and its parameters accurately determined, giving:

$a_F = 13.071$Å	$b_F = 12.540$Å	$c_F = 8.247$Å
$\alpha_F = 95°8'$	$\beta_F = 99°7'$	$\gamma_F = 104°40'$

Volume = 1279.26Å^3 Measured density = (1.71 ± 0.02)gm/cm^3

Calculated density = 1.70 gm/cm^3 for 4 molecules in the F cell.

Only a primitive cell may be reduced by the method of Delaunay (1933) and suitable parameters were found from the following vector transformations:

$$\underline{a}_P = \tfrac{1}{2}\underline{b}_F + \tfrac{1}{2}\underline{c}_F \; ; \; \underline{b}_P = \tfrac{1}{2}\underline{a}_F + \tfrac{1}{2}\underline{c}_F \; ; \; \underline{c}_P = \tfrac{1}{2}\underline{a}_F + \tfrac{1}{2}\underline{b}_F$$

This P cell had all real angles acute and a Delaunay reduction was performed. Four steps were necessary to give six negative scalar products $\underline{a}.\underline{b}$, $\underline{b}.\underline{c}$, $\underline{c}.\underline{a}$, $\underline{a}.\underline{d}$, $\underline{b}.\underline{d}$ and $\underline{c}.\underline{d}$, where $\underline{d} = -(\underline{a} + \underline{b} + \underline{c})$, and hence all angles obtuse. The three shortest vectors obtained for the reduced cell were:

$$\underline{a} = \underline{a}_P = \tfrac{1}{2}\underline{b}_F + \tfrac{1}{2}\underline{c}_F$$

$$\underline{b} = \underline{b}_P - \underline{c}_P = -\tfrac{1}{2}\underline{b}_F + \tfrac{1}{2}\underline{c}_F$$

$$\underline{c} = -\underline{b}_P = -\tfrac{1}{2}\underline{a}_F - \tfrac{1}{2}\underline{c}_F$$

giving reduced triclinic cell parameters:

a = 7.189Å b = 7.806Å c = 7.152Å

α = 117°9' β = 90°3' γ = 113°27'

Volume = 319.36Å^3

Calculated density for 1 molecule in the reduced cell is 1.71gm/cm^3.

The space group is P1 or P$\bar{1}$.

Linear absorption coefficient $\mu = 9.9\text{cm}^{-1}$ for Mo$K\bar{\alpha}$ radiation.

If a zero scalar product occurs, which means one 90° angle, then the Delaunay reduction is ambiguous, since by "changing the sign" of the zero term, another tri - obtuse cell

may be obtained, perhaps with shorter axes (Patterson and Love, 1957). Consequently since β above is effectively 90°, the alternative reduced cell was determined, but found to have one longer axis. Hence the reduced cell with the three shortest non-coplanar translations is as given above.

The orientation of the crystal in the pyrex tube was such that it was impossible to align any of the reduced cell axes along the goniometer axis, without causing awkward absorption effects due to very different path lengths through the pyrex for different reflections.

Consequently, since c_F lay approximately along the length of the tube, the necessary goniometer arcs' movements were calculated and c_F was accurately realigned along the goniometer axis for measurement of diffracted intensities on the linear diffractometer. Reflections were initially indexed and collected with respect to the F cell, but converted to reduced cell indices for subsequent calculations.

Throughout the measurement and calculation of lattice parameters, reference was made to Hulme's published parameters for $SiCl_4$,2Py (Beattie et al, 1964) but no similarity or relationship between them and the values reported in this thesis could be detected.

A rough check of the published values was made, using only what information was available; namely the lattice parameters of

the triclinic body centred I cell which was used for intensity data collection, and the "reduced" cell values, supposedly related to the I cell by the matrix given as:

$$\begin{bmatrix} \underline{a} \\ \underline{b} \\ \underline{c} \end{bmatrix} = \begin{bmatrix} 1 & 0 & 0 \\ \frac{1}{2} & \frac{1}{2} & \frac{1}{2} \\ \frac{1}{2} & \frac{1}{2} & -\frac{1}{2} \end{bmatrix} \begin{bmatrix} \underline{a}_I \\ \underline{b}_I \\ \underline{c}_I \end{bmatrix}$$

If this matrix is applied to the I cell then one obtains the published primitive cell axes, but angles which are all acute and equal to 180° minus the published values. A Delaunay reduction on this cell gives a reduced cell unlike both Hulme's and the one determined above. Due to this inconsistency and the conclusion that the given I cell must also be incorrect, no confidence can be placed in these earlier crystallographic deductions about $SiCl_4$,2Py.

4.4 Measurement of intensities

The crystal was set on the linear diffractometer as described in section 2.3 and intensity data were collected for $l_F = 0 \rightarrow \overline{10}$ using Mo radiation (see section 2.4).

$1\frac{1}{2}$ mm collimator 2°45' oscillation angle

2 oscillation cycles $\frac{1}{2}$ minute oscillation motor

P.H.A. : E.H.T. = 1045 volts, low level = 30 volts,

window = 38 volts.

Generator : 40kV 16mA

Experimentally determined offsets for upper level l_F:

- 0.0146 x l_F r.l.u. along the lower a^*_F slide

- 0.0086 x l_F r.l.u. along the upper b^*_F slide

Calculated offsets : - 0.0143 r.l.u. and - 0.0081 r.l.u. respectively.

For levels with even l_F, only reflections with both h_F and k_F even are present, and for odd l_F, $h_F = 2n + 1$ and $k_F = 2n + 1$. Hence, to avoid counting systematically absent reflections, the intervals on each level were set as:

scanning (upper) slide interval = $2b^*_F$ = 0.1183 r.l.u.

stepping (lower) slide interval = $2a^*_F$ = 0.1144 r.l.u.

Angle between slides = γ^*_F = 74°13'

Since the indices recorded on cards by the linear (h_L,k_L,l_L) increase by 1 after each interval, the resulting intensities will not be correctly indexed with respect to the F cell. For $l_F = 2n$, $h_F = 2h_L$ and $k_F = 2k_L$. For $l_F = 2n + 1$, the $(1,1,l_F)$ reflection was labelled $(0,0,l_F)$ with respect to the diffractometer and thus $h_F = 2h_L + 1$ and $k_F = 2k_L + 1$.

Several reflections with very uneven backgrounds were examined with reference to the Weissenberg photographs, and found to consist of the main peak, set to within 20', plus a small adjacent peak due to the extra fragment of crystal present in the tube (see 4.2). These reflections were corrected.

For the highest levels, $l_F = \bar{9}$ and $\bar{10}$, the oscillation angle was increased to 5°20' for the reasons given in sections 2.4.1

Figure 4.5.1

(A) TRANS

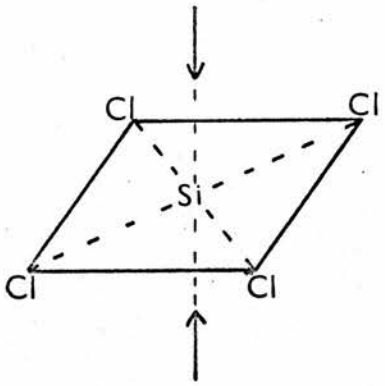

vector space

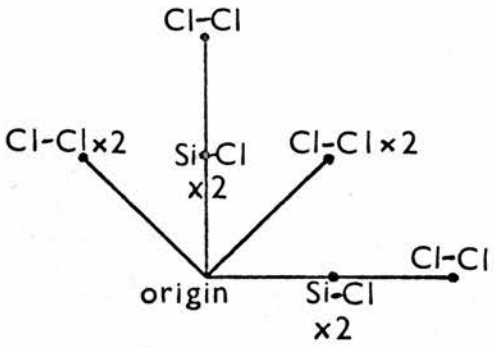

(B) CIS

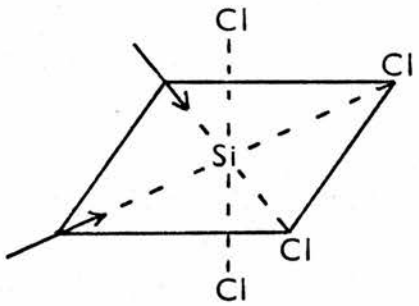

vector space

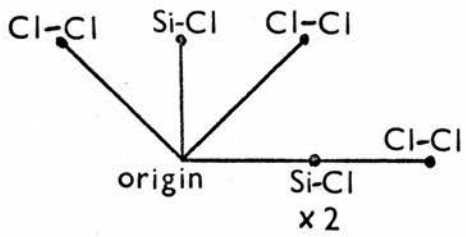

plus 4 more vectors out of the plane.

and 3.4. 56 reflections on hk$\bar{8}$ were recollected and used for scaling between the two sets of data.

4.5 Data processing and Patterson and Fourier syntheses

The diffractometer data cards were first reindexed for the F cell by programme A15, and then processed by A1 and A2. The additional multiplying factor for data with $l_F = \bar{9}$ and $\overline{10}$, to put them on the same scale as the rest, was 1.694. No absorption corrections were made. The F cell indices of the set of $|F_o|$ and $|F_o|^2$ values were changed to those of the reduced primitive cell (see section 4.3) by programme A16. Reflections outside the copper sphere, and those with zero $|F_o|$, were removed, prior to computing a Patterson synthesis with the remaining 1360 $|F_o|^2$ values. The same intervals were taken as for SiF_4,2Py in section 3.5.

The first problem was to determine from the Patterson map if possible, whether the one molecule in the reduced cell was cis or trans. The interatomic vectors involving chlorine atoms will give much larger peaks than other vectors, since $Z_{Cl} = 17$. (Unlike SiF_4,2Py, where a Fourier synthesis was necessary before its trans nature was established). The vector sets, for the silicon and four chlorine atoms in both cases, are illustrated in figure 4.5.1. There are 10 interatomic vectors but in the trans case (A), only 6 are unique. They are planar as shown and 4 have double weight. For a cis configuration (B), there are 9

unique vectors, 5 in a plane and only 1 of double weight.

The expected relative sizes of these vector peaks are given by:

$Si - Cl \approx Z_{Cl} \times Z_{Si} = 238 \times 2 = 476$

$Cl - Cl \approx Z_{Cl}^2 = 289 \times 2 = 578$

Hence the largest peak expected is (Cl-Cl) x 2 or (Si-Cl) x 2 for either vector set (A) or (B) respectively.

Since six large peaks were found in the computed vector map, and the largest was 3.2Å from the origin, a trans configuration was indicated. It was discovered that, of these six peaks, two of equal height, had coordinates which were almost half those of another two equally sized peaks. The peak height of the former was 1.66 times that of the latter, and since the expected ratio (Si - Cl) x 2 / (Cl - Cl) is 1.65, these vectors were undoubtedly pairs of Si - Cl (double weight) and Cl - Cl vectors respectively.

The six vectors were finally and unambiguously allocated according to case (A), figure 4.5.1 and thus the trans configuration of the molecule was confirmed. Mean ratio of peak heights (Cl - Cl) x 2 / (Si - Cl) x 2 = 1.3; expect 1.2. The difference between the coordinates of every pair of vector peaks was calculated, and found to equal the coordinates of another vector, or the difference between another two vectors i.e. all vector coordinates obtained from the Patterson map tied in with vector set (A) to within 2/240 $^{th's}$ of the reduced cell edges.

The lengths of both Si - Cl vectors were calculated to be 2.14 and 2.18 Å and the angle between them 91°44'.

Placing the silicon atom at the origin of the reduced unit cell, the coordinates of the Si - Cl vectors position the two chlorine atoms directly (plus another 2 chlorines related by the centre of symmetry) and a structure factor calculation was computed using these coordinates and the set of $|F_o|$'s with reduced cell indices.

After one cycle to obtain a sensible scale for the $|F_o|$'s, another was computed (no least squares refinement) whose output was used for a Fourier synthesis with x/a, y/b, z/c from $0 \rightarrow \frac{1}{2}, 1, 1$ respectively at intervals of 1/30. The R factor for the largest $|F_o|$ and F_c values was 0.26. The electron density map will be centrosymmetric because the chlorines were put in with centrosymmetric coordinates, and therefore all B_c's = 0.

As discussed in section 1.1, not all the phases calculated from the contributions of the heavy atoms located from the Patterson map will be correct. For the centrosymmetric case, this means that not all reflections will have the same sign for F as was calculated for F_H. Considering the function $(\sum f_H^2 / \sum f_L^2)^{\frac{1}{2}} \approx (\sum Z_H^2 / \sum Z_L^2)^{\frac{1}{2}} = 1.70$ for this case, about 88% of the $|F_o|$ terms in the computed electron density function will have had their signs correctly determined (Sim, 1961).

A pyridine ring was identified from the Fourier; nine regions

Figure 4.5.2

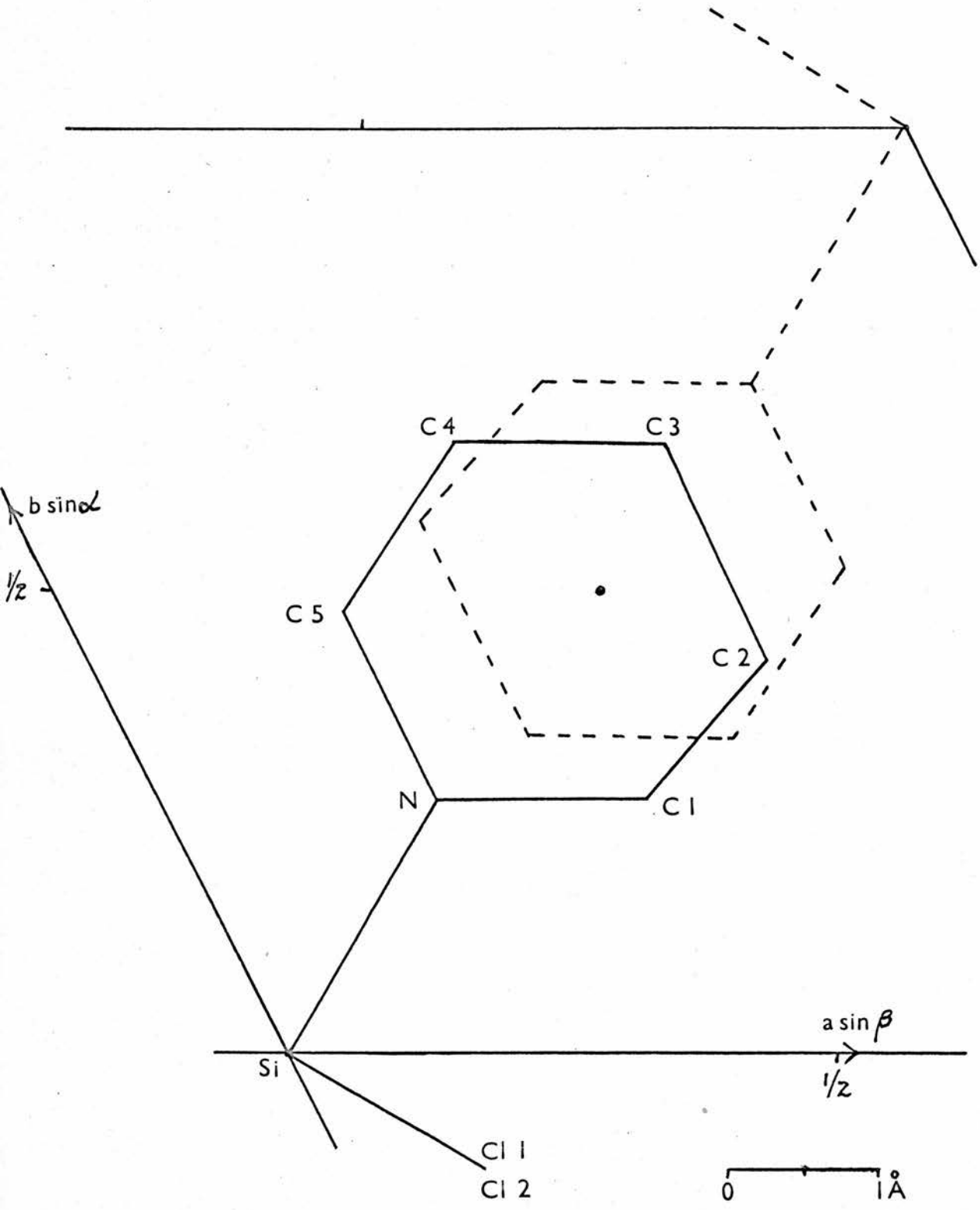

of high electron density appeared, whose centres are shown plotted in figure 4.5.2, looking vertically down the c axis of the reduced triclinic cell. The projection of a onto this plane perpendicular to c is a sinβ, and of b, b sinα. The angle between them = 180° - γ*.

4.6 Structure refinement

Once the $|F_o|$ scale had been adjusted, the first meaningful R factor was 0.245 for a structure factor calculation using the reduced cell coordinates for Si, Cl1, Cl2, N and C1 - C5 obtained from the Fourier. The space group was initially chosen as $P\bar{1}$. If the structure is not centrosymmetric, it will not refine and its molecular geometry will be poor with large standard deviations. The Si atom was given an isotropic temperature factor of 2 and the remaining atoms B = 4, being approximately the corresponding values for SiF_4,2Py (see section 3.6).

After a few cycles of least squares refinement of the 34 parameters, R had slightly increased, and although the scale shift was very small, $\Sigma|F_o| \gg \Sigma|F_c|$. The B shifts for Cl1 and Cl2 were large and negative and since they are the largest scatterers, it was concluded their thermal parameters were too high, causing the calculated F's to be too small. It is also seen from equation (7), section 1.3, that this effect should increase with sinθ, and this was observed.

Hence the chlorine isotropic temperature factors were decreased to 2, and four further cycles were sufficient to reduce all coordinate

and B shifts to the 3rd and 2nd decimal places respectively. At this stage R = 0.146 and the B values were :

Si	C11	C12	N	C1	C2	C3	C4	C5
1.768	2.431	2.391	1.987	3.087	3.102	2.341	2.750	2.301

Before converting these to anisotropic B_{ij}'s, hydrogen coordinates with respect to the reduced cell were calculated as described in Appendix C for inclusion without refinement in subsequent structure factor calculations. They are listed in the final table of coordinates, 4.7.1. Each H atom was given the last isotropic B value of its corresponding carbon atom (see above). If estimates of the hydrogen positions are not included at this stage, then the ellipsoid of thermal vibration of each carbon will be falsely elongated in the direction towards its bonded H atom, to account for the hydrogen's unincluded contribution to F_c.

Reflections with net intensity estimate I less than 20 counts were removed and refinement of the 79 parameters was continued until after eight cycles R was a minimum at 0.119. A card output was taken and its reduced cell indices were changed to F cell indices by programme A17 in order to find a scale factor for each equi-inclination l_F level of data collected. The card output from A17 was sorted into l_F levels, and for each level, $\sum|F_c|$ and $\sum|F_o|$ were computed by A6. The scale factors $\sum|F_c| / \sum|F_o|$ are:

l_F=0	$\bar{1}$	$\bar{2}$	$\bar{3}$	$\bar{4}$	$\bar{5}$	$\bar{6}$	$\bar{7}$	$\bar{8}$	$\bar{9}$	$\bar{10}$
0.959	1.179	0.933	0.894	0.916	0.934	0.971	0.961	1.070	1.010	1.213

A simple SPS programme applied the appropriate scale to each of the $|F_o|$ values (F cell indices). The indices were converted back to reduced cell values by A16 for further SFLS calculations.

Before layer scaling, nine reflections, all with $h + k = l_F = \bar{1}$, had poor agreement between F_o and F_c, but these discrepancies disappeared afterwards. The $(\bar{1}, \bar{1}, 0)$ reflection also had a large Δ, which was not improved by the scaling procedure. This reflection has indices $(2, 0, \bar{2})$ with respect to the F cell and, although was very close to the origin of the diffractometer slides, had not been centred and measured by hand. Hence it was excluded from the calculation of l_F scale factors and from further structure refinement.

After scaling, R fell to 0.0933 and further cycles, with 1245 reflections, reduced $\sum w \Delta^2$ and R to minimum values (R = 0.0872). A more realistic R value with $(\bar{1}, \bar{1}, 0)$ included was 0.0887.

At no time during refinement was it felt necessary to depart from space group $P\bar{1}$, since the molecular geometry was very satisfactory and the R value above is the same as was obtained for centrosymmetric SiF_4,2Py at the same stage (see section 3.6). The deviation of the pyridine rings from a centrosymmetric configuration is less than the standard deviations of the atomic coordinates, and hence too small to be detected. The limiting values of the standard

Figure 4.6.1

A composite map of electron density in $SiCl_4$,2Py, viewed along c (from sections nearest centres of peaks).

Contours at intervals of $2e/Å^3$ for N, Cl-C5 beginning at $2e/Å^3$.

Contours at intervals of $10e/Å^3$ for Si and chlorines, beginning at $10e/Å^3$.

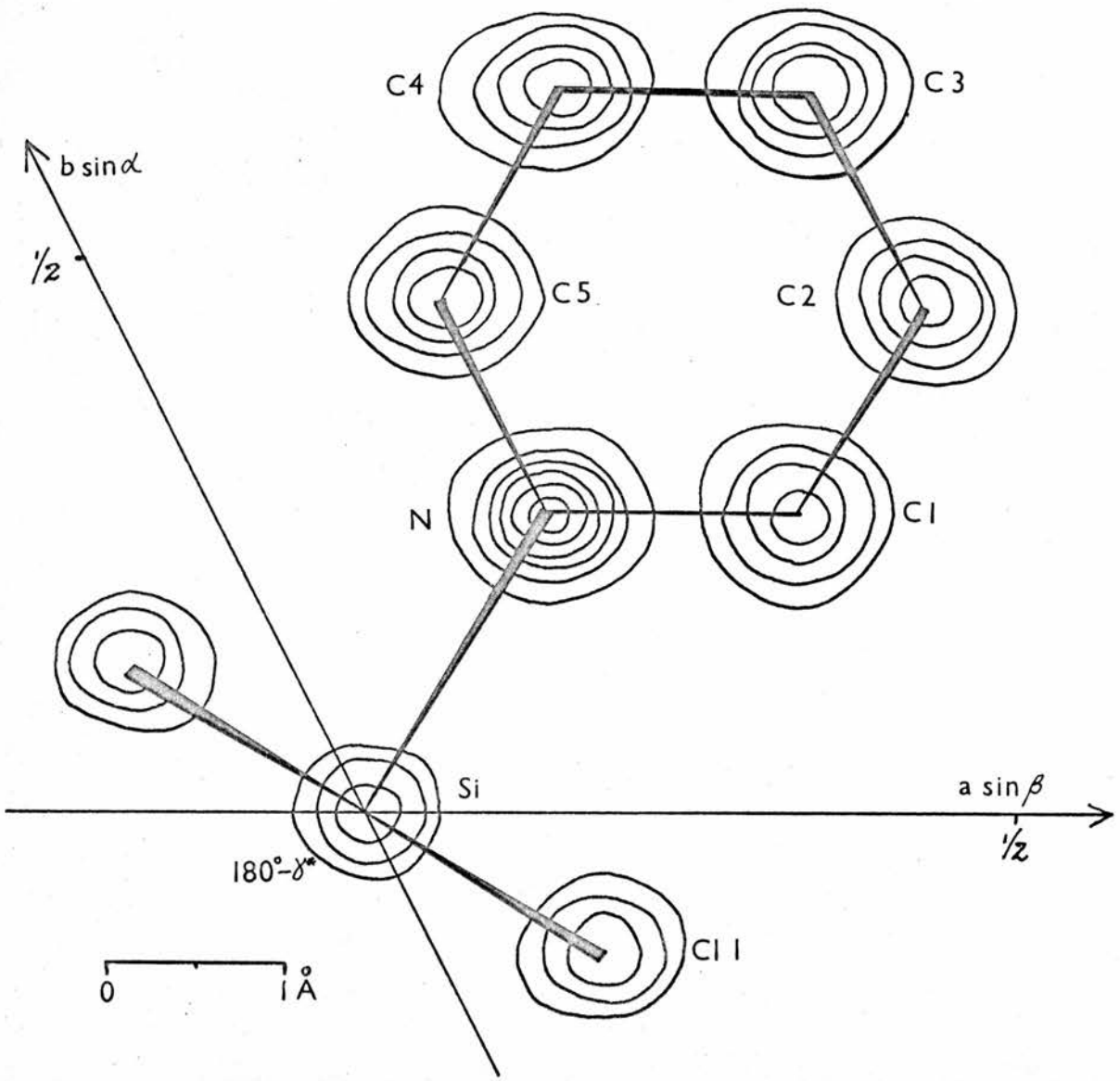

deviations are determined by the quality of intensity data, which in turn is dependent on the crystal quality, setting precision of the crystal, diffractometer and counting statistics errors.

So far weighting scheme (a) (section 1.5) had been used (F_{min} = 1.18), but now scheme (b) was applied, according to the procedure described for SiF_4,2Py in section 3.6 and in programmes A7-A11. The (I + B)/(I - B) were processed with respect to the F cell used for data collection. c^2 was calculated = 0.013574 - 0.000977 = 0.012597. Hence c = 0.1122, G = 0.1165 and G(counting statistics) = 0.0313, confirming again that counting statistics errors are very small.

(K/4Lp)(I + B)/(I - B) values were reindexed from the F cell to reduced cell by A16 before using A10 to compute absolute $\sqrt{w}$ for each reflection. A11 applied a scaled $\sqrt{w}$ to each $|F_o|$ data card for further SFLS calculations (reduced cell indices). D = 0.29013 (see A11 and section 3.6).

The first cycle gave a very much reduced $\sum w\Delta^2$ and four cycles later, the card output was used to find reflections with $\Delta > 3\sigma$ or 4σ (A12) : 28 and 10 in number respectively. Two of the latter 10 reflections had been measured near the slides' intersection (one was ($\bar{1}$, $\bar{1}$, 0)). Another six had $l_F = \bar{1}$ (μ = 2°28') and since this level had a large scaling factor, it suggests that the diffract meter equi-inclination setting is very sensitive at such small μ. With SiF_4,2Py this effect did not appear; its smallest μ =

Table 4.7.1

Atom	x/a	σ(x/a)	y/b	σ(y/b)	z/c	σ(z/c)
Si	0.0000	0.0000	0.0000	0.0000	0.0000	0.0000
Cl1	0.1271	0.0002	-0.1282	0.0002	0.1539	0.0002
Cl2	0.1270	0.0002	-0.1283	0.0002	-0.2826	0.0002
N	0.2580	0.0006	0.2716	0.0007	0.1369	0.0008
C1	0.4464	0.0008	0.2713	0.0009	0.1370	0.0011
C2	0.6282	0.0008	0.4566	0.0010	0.2280	0.0012
C3	0.6220	0.0008	0.6509	0.0009	0.3250	0.0010
C4	0.4302	0.0009	0.6515	0.0008	0.3256	0.0010
C5	0.2532	0.0008	0.4646	0.0008	0.2330	0.0010
H1	0.4526		0.1283		0.0676	
H2	0.7668		0.4475		0.2180	
H3	0.7537		0.7901		0.3949	
H4	0.4234		0.7929		0.3897	
H5	0.1167		0.4749		0.2403	

Table 4.7.2

Anisotropic temperature factors x 10^4

Atom	B_{11}	B_{22}	B_{33}	B_{23}	B_{13}	B_{12}
Si	95	106	132	121	47	91
Cl1	146	142	187	189	21	123
Cl2	145	148	160	136	119	133
N	105	105	164	128	25	76
C1	135	117	235	133	92	75
C2	105	176	245	206	74	80
C3	124	141	194	167	55	71
C4	191	113	204	160	77	112
C5	130	126	203	184	86	92

FIGURE 4.7.1

$SiCl_4 2Py$

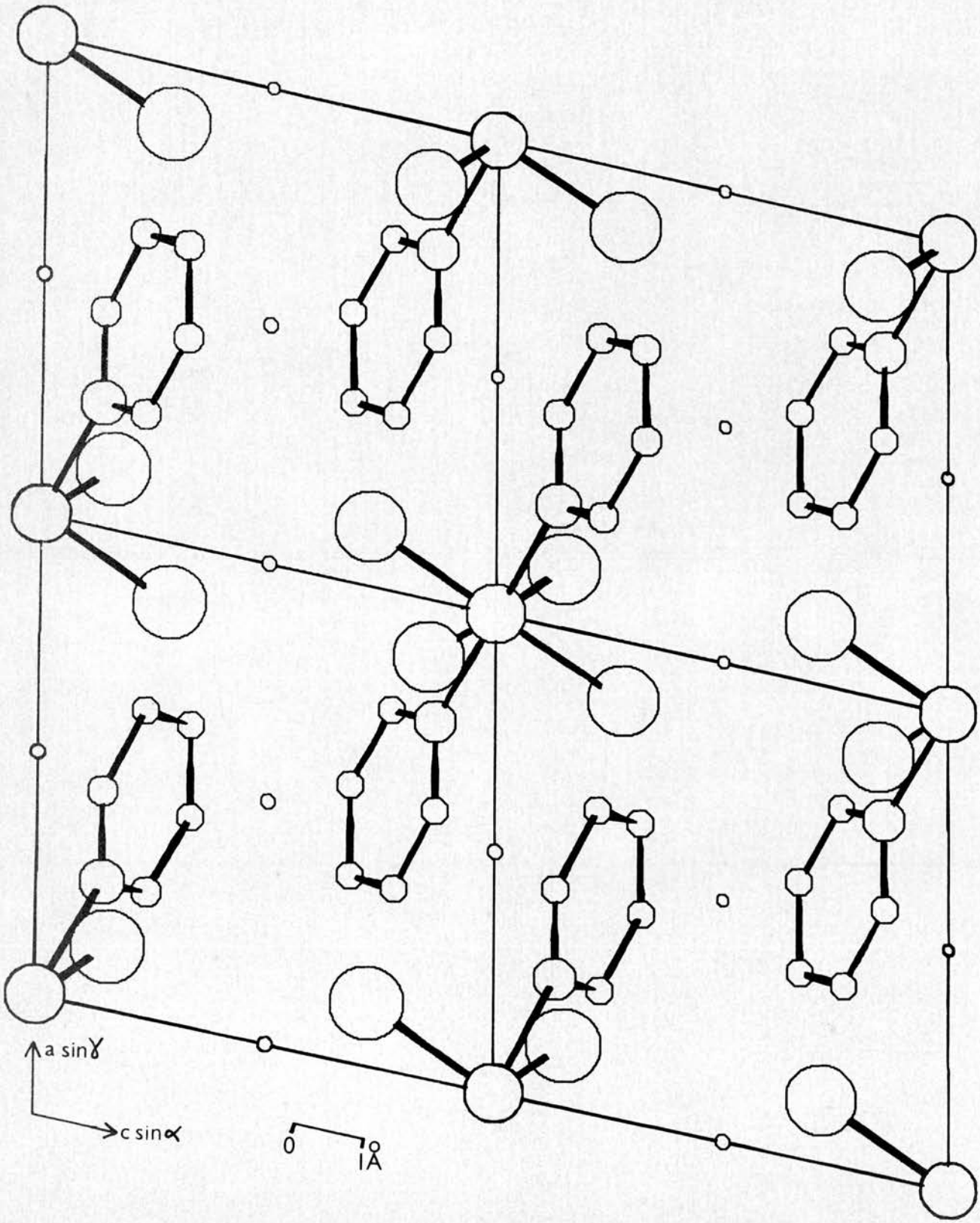

3°10' for k = 1. The remaining two reflections with $\Delta > 4/\sqrt{w}$ were on the 8th and 9th l_F levels, where the instrument and crystal setting inaccuracies are more significant (cf. sections 2.2 and 2.3).

When these 10 reflections were given zero weight, $\sum w\Delta^2$ dropped by 16% and after six more cycles reached its minimum value of 1286 on an absolute scale. R = 0.0878, m-n = 1246-79 = 1167 and $\sum w\Delta^2/(m-n) = 1.102$.

Table B at the end of the thesis lists the $|F_o|$'s with the phases obtained from this final calculation of structure factors, and the resulting electron density map is shown in figure 4.6.1.

4.7 Molecular geometry

The atomic coordinates of the final model are given in table 4.7.1 as fractions of the reduced cell edges, together with their standard deviations. Final anisotropic B_{ij}'s are listed in table 4.7.2 and bond lengths and angles and their standard deviations in 4.7.3 and 4.7.4. A perspective view of the structure along the b axis is shown in figure 4.7.1, drawn by PAMOLE.

A molecular scan by A5 gave the angle Si-N-C3 as 180° and the shortest intermolecular distances (< 3.5 Å) as (in Å):

Cl1-H3	Cl1-H4	Cl1-H5	Cl2-H3	Cl2-H4	Cl2-H5	C5-H2	C2-H5	H2-H5
3.199	3.122	3.398	3.196	3.185	3.379	3.446	3.457	2.437

Intermolecular distances are generally larger than those of SiF_4,2Py, and the looser packing of $SiCl_4$,2Py enables the pyridine

Table 4.7.3

Bond	Length (Å)	σ(Å)
Si-Cl1	2.186	0.001
Si-Cl2	2.192	0.002
Si-N	1.966	0.007
N-C1	1.355	0.007
C1-C2	1.363	0.015
C2-C3	1.370	0.013
C3-C4	1.381	0.009
C4-C5	1.351	0.014
C5-N	1.356	0.010
C1-H1	1.014	
C2-H2	1.027	
C3-H3	1.006	
C4-H4	1.006	
C5-H5	1.015	

Table 4.7.4

Intramolecular bond angles (°)		σ(°)
Cl1-Si-Cl2	91.0	0.1
Cl1-Si-N	90.0	0.1
Cl2-Si-N	90.5	0.2
Si-N-C1	120.9	0.6
Si-N-C5	121.2	0.4
C1-N-C5	118.0	0.8
N-C1-C2	122.4	0.8
C1-C2-C3	119.3	0.6
C2-C3-C4	118.4	0.9
C3-C4-C5	120.6	0.7
C4-C5-N	121.3	0.6
N-C1-H1	118.9	
C2-C1-H1	118.8	
C1-C2-H2	119.3	
C3-C2-H2	121.4	
C2-C3-H3	121.0	
C4-C3-H3	120.6	
C3-C4-H4	119.2	
C5-C4-H4	120.1	
C4-C5-H5	117.2	
N-C5-H5	121.5	

ring to lie in a position equidistant from Cl1 and Cl2, unlike SiF_4,2Py (see section 3.7). By dropping perpendiculars from C1 and C2 onto the line Cl1-Cl2, it was calculated that the pyridine ring bisects the angle Cl1-Si-Cl2 to within 20'.

The best plane $lx' + my' + nz' = p$ through C1-C5 was found as described in Appendix D with respect to orthogonal axes x', y', z' chosen according to Appendix C. l = -0.19482, m = -0.45491, n = +0.86897 and p = +0.02137Å. Atomic deviations from this plane are (in Å):

Si	N	C1	C2	C3	C4	C5
-0.021	-0.003	+0.002	-0.003	+0.001	+0.001	-0.001
Cl1	Cl2	H1	H2	H3	H4	H5
+1.536	-1.584	+0.014	-0.039	+0.009	-0.043	+0.013

Thus, as with SiF_4,2Py the structure is planar, and it is confirmed that the perpendicular distances of Cl1 and Cl2 from the pyridine plane are insignificantly different.

The plane Si-Cl1-Cl2 was calculated :

$$-0.77127x' - 0.47381y' - 0.42503z' = 0$$

The angle between it and the best fit pyridine plane given above is 90°12'. The pyridine plane has the following intercept equation with respect to the reduced triclinic cell.

$$\frac{x}{9.41569} - \frac{y}{0.04698} + \frac{z}{0.02137} = 1$$

Figure 4.7.2

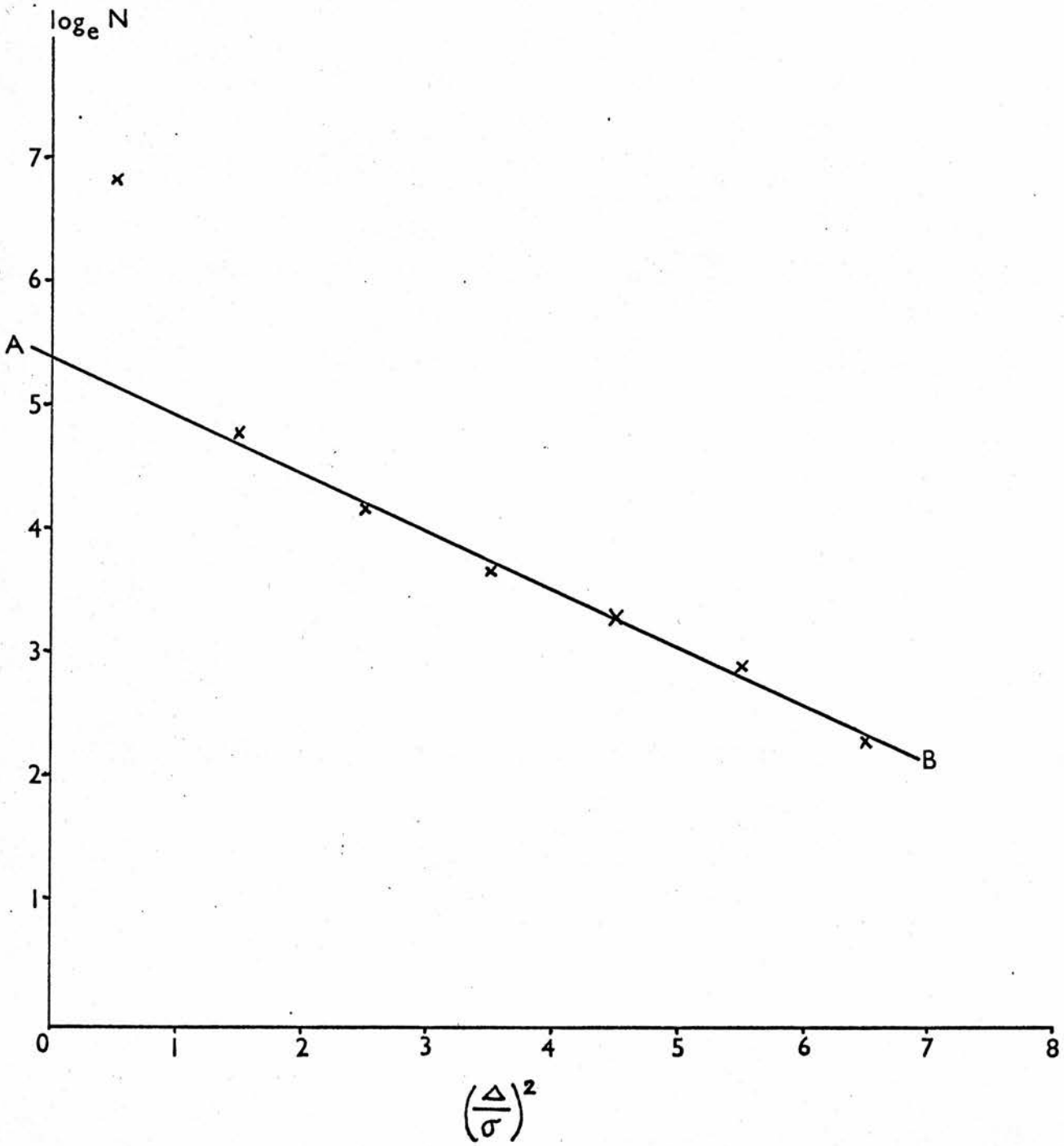

The pyridine rings are layered, almost perpendicular to c of the reduced cell, with separation $\approx \frac{1}{2}c = 3.58\text{Å}$; since $\beta = 90°$, the pyridine planes are also approximately parallel to a (cf. large intercept on a, 9.416Å, of the best fit pyridine plane given above.)

The absoluteness of the weights applied to the $|F_o|$ values was checked as described in section 3.7 for SiF_4,2Py, and gave the results shown in figure 4.7.2. Best least squares straight line AB has intercept $\log_e A = 5.39$ and slope $= -B = -0.47$, which is almost the theoretical value of $\frac{1}{2}$ for a normal distribution. The first point deviates from this Gaussian curve as in figure 3.7.2 for SiF_4,2Py, and probably for the same reason given in section 3.7.

4.8 Conclusions

A comparison of the final structural models for SiF_4,2Py and $SiCl_4$,2Py indicates that the pyridine ring geometry is the same, within the listed standard deviations (cf. tables 3.7.3, 3.7.4 and 4.7.3, 4.7.4). Mean Si-F and Si-Cl bonds are 1.65 and 2.19Å. Standard deviations of equivalent atomic coordinates, bond lengths and angles are larger for the chloride complex, as are $\sum w\Delta^2/(m-n)$ and R. Both compounds are layered in the crystal lattice, with approximately equal separation between the pyridine rings (~3.6Å). $SiCl_4$,2Py temperature factors are lower (cf. tables 3.7.2 and 4.7.2) and hence Fourier peaks are higher (cf. figures 3.6.1 and 4.6.1) due to less thermal vibration.

The molecular orientation in the reduced triclinic cell is not identical for both compounds, and a comparison of the reduced cells' parameters (a of SiF_4,2Py ≡ c of $SiCl_4$,2Py) confirms that they are not isomorphous. Another pair of primitive triclinic cells may exist, in which both molecules have identical orientations, and if these were identified from appropriate vector transformations, then a comparison could be made between them to test for isomorphism. It was decided however that this problem was not of sufficient importance to pursue further.

The structure of $SiCl_4$, 2Py has been shown to be molecular with a centrosymmetric trans configuration. This result contradicts the stereochemistry assigned from infrared vibrational analysis.

The infrared spectra of addition compounds of the type MH_4L_2 where M is silicon, germanium or tin, H = halogen and L is a monodentate ligand, have been interpreted using a simplified model in which the coupling between M-H and pyridine vibrations was neglected. For a trans adduct only one fundamental M-H stretching vibration of perturbed planar MH_4 was predicted. By considering the MH_4 residue of a cis isomer distorted as shown due to the addition of the ligands, and using group theory arguments, a closely spaced triplet of i.r. absorptions was predicted with a weaker vibration at lower frequency (all M-H stretching vibrations).

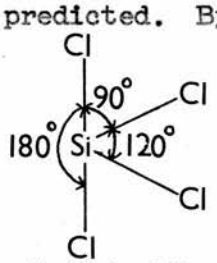

The infrared spectrum of $SiCl_4$,2Py followed this pattern and also was similar to the spectra of bidentate ligand adducts of silicon tetrachloride, which can exist only in a cis configuration. The necessary distortion of a trans isomer to produce the observed $SiCl_4$,2Py absorption bands was considered to be too great.

Crystal-field effects, causing separation of degenerate peaks, are one of the possible reasons for misinterpretation of absorption spectra, listed by Beattie et al (1963). However this cannot be the case with $SiCl_4$,2Py since it was shown in section 4.7 that the pyridine rings are completely symmetric with respect to the chlorines. The packing symmetry of the fluoride adduct is lowered however due to repulsion between intermolecular close contacts (see sections 3.7 and 3.11), but this has not caused any resolution of the Si-F stretching band.

The crystallographic results reported in this thesis clearly show that the assumption that the MH_4 unit can be treated separately when interpreting i.r. spectra is not generally valid. In view of these results, recent force constant calculations (Beattie, Gilson and Ozin, 1968) using the whole $SiCl_4$,2Py molecule have indicated how the i.r. spectrum with three strong lines in the M-H stretching region can arise for a trans isomer.

Further pyridine adducts of tetrahalides of Group IV metals, whose stereochemistry has been deduced from their solid state spectra on the basis of the simple model discussed above are:

GeF_4,2Py	trans	(Ozin, 1967)
SnF_4,2Py	cis	(Muetterties, 1960)
$GeCl_4$,2Py	trans	(Hulme et al, 1960; Beattie et al, 1963)
$SnCl_4$,2Py	trans	(Beattie et al, 1963)
	cis	(Clark and Wilkins, 1966)
$SiBr_4$,2Py	cis	(Beattie et al, 1964)
$SnBr_4$,2Py	cis	(Clark and Wilkins, 1966)

The cis assignments obviously require revision.

Preliminary x-ray investigations of $SnCl_4$,2Py and $SnBr_4$,2Py have subsequently been carried out in this laboratory and confirm (Clark and Wilkins, 1966) that they are isomorphous in monoclinic space group C2/m. A two dimensional Fourier synthesis indicated a trans configuration for the chloride complex and hence also for the bromide. Miss M. Milne, Chemistry Department, University of Southampton is analysing the i.r. vibrations of $SnBr_4$,2Py in more detail utilising the whole molecule, and has calculated that the observed complex spectrum is consistent with a trans stereochemistry.

None of the octahedral complexes MH_4L_2 so far studied in any detail by x-ray diffraction techniques has been a cis isomer, and further x-ray investigations would be desirable to confirm that the whole series is trans.

5. AN X-RAY DIFFRACTION STUDY OF MERCURY DIBENZYL

5.1 Introduction

The structural chemistry of mercury compounds has been recently reviewed (Grdenić, 1965) and it is apparent that there is a lack of structural data for the di-alkyl and di-aryl derivatives, although recent data presented at the 7th International Congress of Crystallography has improved the situation (Pakhomov, 1966).

Several mercury dialkyl and diaryl compounds were available and mercury dibenzyl, $(C_6H_5.CH_2)_2Hg$, was selected for structural investigation since some additional data concerning bond energies had been determined kinetically for this compound (Calvert, 1958). From the unusually low mercury-carbon bond dissociation energy it was anticipated that these bonds should be especially long.

5.2 Description of crystals

Pure mercury dibenzyl had been made by D. Calvert using the method of Hein and Wagler (1925) and was recrystallised from spectroscopic grade iso-octane under vacuum conditions. Colourless needle crystals of approximately rectangular cross-section were obtained. On prolonged exposure to x-rays it became apparent that the crystal was decomposing, a black deposit of free mercury being observed in those parts of the crystal exposed to the beam. A similar decomposition was also detected on exposure of the crystal to visible light.

5.3 Unit cell dimensions and space group

Rotation, Weissenberg and precession photographs indicated that the structure was tetragonal with a = 12.91 ± 0.02Å and c = 7.08 ± 0.03Å, along the needle axis of the crystal. Measured density = 2.19 ± 0.03 gm/cm^3. Calculated density = 2.155 ± 0.015 gm/cm^3 for four molecules in the unit cell.

The following conditions limiting possible reflections were noted: hk0 : h + k = 2n; 00l : l = 2n. This suggested $P4_2/n$ as the space group with eight symmetrically related positions in the unit cell. Therefore one half of the molecule is the asymmetric unit and the mercury atoms must be at special positions. It was observed that those lines with l = 2n were very much stronger than those with l = 2n + 1. Applied to space group $P4_2/n$, this special condition gives the equivalent mercury positions as ± (3/4,1/4,z; 3/4,1/4,1/2 + z) when the unit cell origin is at the centre of symmetry.

Further strong reflections due to diffraction by the Hg atoms were : h + k + l/2 = 2n for l even, which implies near body-centring of the Hg atoms in terms of c = 3.54Å, with equivalent positions (x,y,z) and (x + 1/2, y + 1/2, z + 1/4) in the unit cell. Combining the two sets of equivalent positions gives the following mercury atomic coordinates, where the z coordinate may only be a close approximation : ± (3/4,1/4,3/8; 3/4,1/4,7/8).

5.4 Absorption

The linear absorption coefficient $\mu = \rho \sum p_i (\mu/\rho)_i$

where ρ = density of crystal

p_i = fractional weight of element i in the unit cell

$(\mu/\rho)_i$ = mass absorption coefficient of atom i for the radiation used.

Therefore for MDB, $\mu = \rho [p_{Hg}(\mu/\rho)_{Hg} + p_C(\mu/\rho)_C + p_H(\mu/\rho)_H]$

$= 133.5 \text{ cm}^{-1}$ for MoK$\bar{\alpha}$ radiation.

Thus the mercury atoms in crystals of MDB absorb x-rays to a great extent and in order that comparatively simple absorption corrections could be applied, initial attempts were made to grind crystal surfaces to a cylindrical or spherical form using a modified version of Bond's method (1951) but these were unsuccessful.

To minimise absorption effects, very small crystals with cross-section as square as possible were selected for alignment on the linear diffractometer as described in section 2.3 (case A) with c along the goniometer axis. However, several initial crystals had to be abandoned because very variable peak counts for 00l reflections were obtained when the crystal was rotated through 360° (see section 2.3). Since the best available crystal still gave significant fluctuations, corrections for x-ray absorption were necessary and were applied to diffracted intensities using a

programme written by Dr. A.J. Cole of the Computing Laboratory.

The view along the needle axis (c) of the crystal was determined as

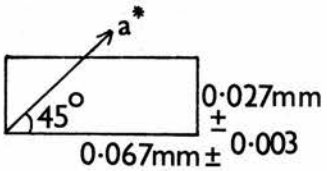

For each reflection recorded by the diffractometer, the positions of the crystal and detector, ϕ and Υ, with respect to the incident x-ray beam (see figure 2.1.2 and section 2.1) are found from the formulae:

$$\Upsilon = 2\sin^{-1}[(h^2 + k^2)^{\frac{1}{2}}a^*/2\cos\mu]$$

$$\phi = \Upsilon/2 + 90° - \tan^{-1}(k/h)$$

for a* initially parallel to the incident beam (Buerger, 1960). Assuming a rectangular crystal of infinite length the absorption programme calculated the path length r of x-rays through the crystal for each diffraction maximum, and evaluated the corrected intensity $Ie^{\mu r}$.

5.5 Two dimensional analysis

MDB was the first compound studied, using the linear diffractometer, and the very considerable instrumental difficulties discussed in section 2.2 had not in some cases been discovered and in others resolved. Several attempts were made to measure accurately the intensities of diffracted MoKα radiation in one quadrant of the copper sphere as described in section 2.4. a* = b* = 0.0551 r.l.u. c* = 0.1004 r.l.u. From preliminary experiments, a low generator current was chosen and data were collected quickly in order to minimise radiation damage to the crystal. Zero level intensities

Figure 5.5.1

Projection of electron density in MDB,

for two of the four molecules in the unit cell.

Contours at equal but arbitrary intervals.

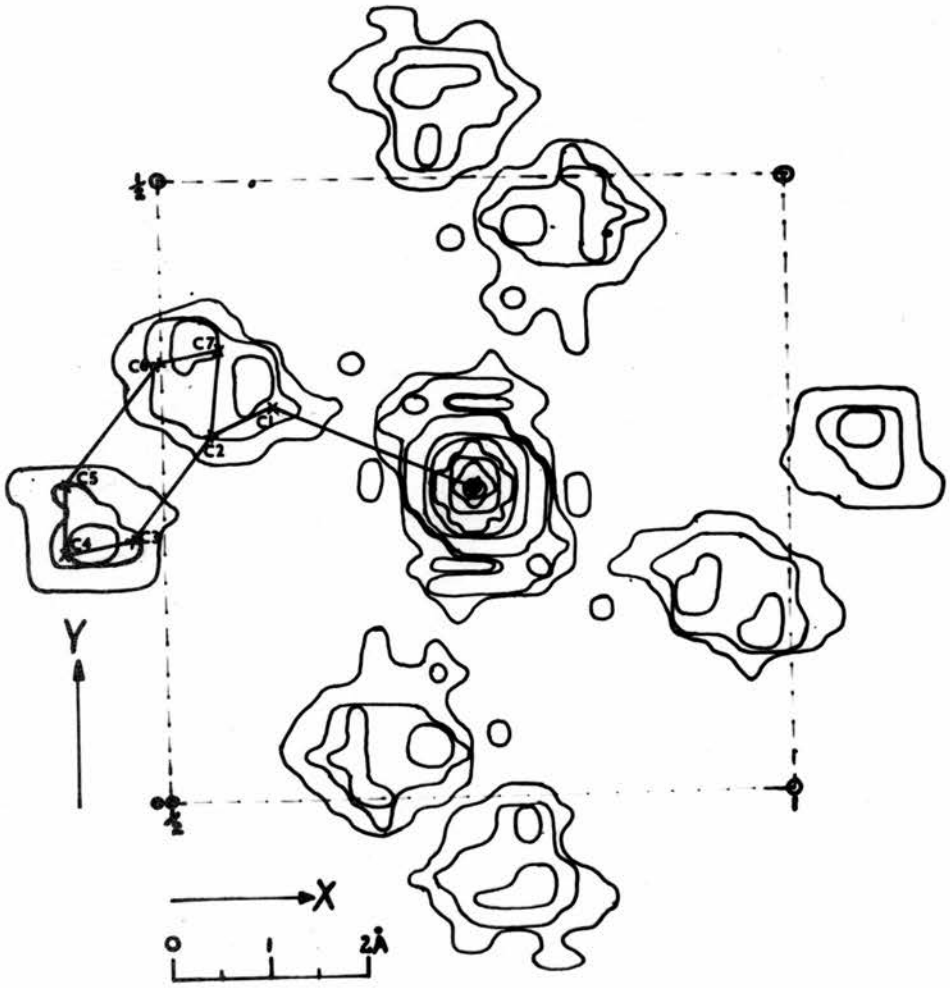

were satisfactory and gave the results reported in this section. X-ray form-factors for mercury have been calculated recently from relativistic Hartree-Fock atomic fields (Doyle and Turner, 1967).

hk0 data were processed as usual and structure factor calculations were computed using the mercury x and y coordinates determined from space group considerations alone. Several cycles of refinement of the scale and isotropic temperature factor reduced R to 0.146, when a two dimensional Fourier synthesis was computed with the $|F_o|$ values and calculated phases (0 or π). This is shown in figure 5.5.1. Using a model of the molecule, only one possible molecular orientation was found which fitted the projection of electron density and is shown on figure 5.5.1. The four molecules in the unit cell appeared to pack with two Hg atoms on each four-fold screw axis, $\frac{1}{2}$ cell apart, and the attached benzyl groups stacked one above the other, all having the same orientation but each successively rotated through 90°.

x and y coordinates were determined for the 7 carbon atoms in the asymmetric unit and all atoms were assigned isotropic B values. Four SFLS cycles to refine the 23 parameters reduced coordinate shifts to the 4th decimal place and R to a minimum at 0.084. The final fractional x and y coordinates and B's are given in table 5.5.1. Another two dimensional electron density map was computed with the last F_o values but the resolution of the benzyl group was no better than in figure 5.5.1 This lack of

Table 5.5.1

Atom	x/a	y/b	B	z/c
Hg	0.7500	0.2500	4.47	0.36
C1	0.5882	0.3177	5.74	0.36
C2	0.5391	0.2969	3.81	0.51
C3	0.4741	0.2135	3.74	0.54
C4	0.4186	0.2014	3.39	0.69
C5	0.4209	0.2596	4.64	0.87
C6	0.4976	0.3516	5.12	0.86
C7	0.5457	0.3663	4.07	0.67

improvement, in spite of including the carbons, was a result of the excessive heaviness of the mercury (Z = 80). Most of the magnitudes and phases of the overall structure factors were equal to those calculated from the mercury position alone, and the contributions of the lighter carbons to the F_c's were as small as the experimental error involved in the measurement of intensities. The Hg-Cl bond length was estimated as 2.26Å. No further refinement could be achieved using only zero level intensity data.

5.6 Three dimensional analysis

An investigation of the three dimensional structure of MDB was undertaken with intensities from levels $l = 0 \rightarrow 6$, prior to discovery of instrument fault (4) (section 2.2). Since considerable time was spent attempting to analyse the data, which were subsequently found to be erroneous for $l > 0$, a brief summary of the methods employed is given.

The first problem considered was to determine if the Hg atom of the asymmetric unit was situated exactly at $z = 3/8$ i.e. was the condition for diffraction by mercury atoms, $h + k + l/2 = 2n$ for l even, exact or only a close approximation. The $l = 2n + 1$ diffraction maxima were receiving no contribution from the Hg atoms from symmetry considerations (see section 5.3). Using different parts of the observed data for SFLS calculations and including only the Hg, R was reduced to a minimum in each case given below.

Data	Hg position	R
h + k + 1/2 = 2n, for l = 2n	0.75, 0.25, 0.375	0.110
all l = 2n	0.75, 0.25, 0.3546	0.103
h + k + 1/2 = 2n, for l = 2n	0.75, 0.25, 0.3546	0.093
h + k + 1/2 = 2n + 1, for l = 2n + 1	0.75, 0.25, 0.3546	0.161

It was therefore concluded that Hg z-coordinate was not exactly 3/8. This was borne out by the observation from photographs that the intensity difference between h + k + 1/2 = 2n and 2n + 1 reflections (for l even) decreased with increasing sinθ. Calculations, with the structure factor equation for $P4_2/n$ and Hg not at z = 3/8, showed that as l increased, the mercury contribution to h + k + 1/2 = 2n + 1 reflections increased, and to h + k + 1/2 = 2n reflections decreased.

A three dimensional difference Fourier synthesis was computed with $(F_o - F_c)$ for all l = 2n reflections, where F_c was calculated from the Hg position given above. A difference Fourier eliminated the diffraction ripple in a Fourier synthesis surrounding the heavy Hg atomic peak due to series termination. This could have affected the positions of the light atoms and especially those nearest the heavy atom.

All 7 carbons were located; the x and y coordinates obtained were equal within 0.01 to those values found from the electron density projection and given in table 5.5.1. The z coordinates obtained are given in table 5.5.1. Using 653 reflections with

intensity estimates $\geqslant 100$ counts from all levels $l = 0\text{-}6$ least squares refinement of the atomic positions and B values was attempted. R was reduced to 0.09 but the geometry of the benzene ring was poor with large standard deviations (~ 0.1 Å for bond lengths and $\sim 6°$ for bond angles), This situation could not be improved because of the poor quality data and the dominance of the structure by the mercury. Additional difficulties were due to the Hg occupying a special position, and the $l = 2n + 1$ intensities being so weak with a high measurement inaccuracy. The R factor with the carbons included was insignificantly different from the value obtained using only Hg. Any Fourier synthesis would tend to show only the Hg atom clearly; carbon atoms would be seen with difficulty and their positions would always be inaccurate.

Photographic techniques using a Nonius integrating precession camera were adopted for more accurate determination of intensities, and initial films were measured. However photographic measurements were terminated in view of the results deduced from the space group considerations outlined in the following section.

5.7 Space group considerations

On the basis of space group $P4_2/n$, $l = 2n$ reflections are receiving contributions from all atoms in the molecule and intensities with l odd from only the benzyl groups. Hence the expected ratio of intensities is $\sum_{\frac{1}{2}Hg,C1\text{-}C7} Z^2 / \sum_{C1\text{-}C7} Z^2 = 7.3/1$.

But the ratio observed was ~30/1 and possible reasons for this anomaly were considered. Pseudo-symmetry within the asymmetric unit could result in carbon contributions to l = 2n + 1 levels very nearly cancelling, causing those intensities to be very small. The benzene ring of the asymmetric unit is situated with its centre at approximately (1/2,1/4,1/2), or equivalently (0,1/4,1/2) (see table 5.5.1 and figure 5.5.1), which are pseudo-special positions.

For space group $P4_2/n$ with origin at $\bar{1}$ there are four expressions for A (Vol. I, International Tables for X-ray Crystallography) for the following four combinations of indices:

(i)	(ii)	(iii)	(iv)
h + k = 2n	h + k = 2n	h + k = 2n+1	h + k = 2n+1
k + l = 2n	k + l = 2n+1	k + l = 2n	k + l = 2n+1

The plane of the benzene ring is approximately parallel to c with a mirror plane through its centre almost parallel to the ab plane. Expressions (iii) and (iv) for A contain the factor $\sin 2\pi lz$, and hence with a mirror plane at z = 0 or 1/2, vanish for l odd and even, considering carbons C2-C7. An inversion centre was assumed for the benzene ring at (0,1/4,1/2); trigonometrical manipulation of the structure factor equations for cases (i) and (ii) in conjunction with possible combinations of h, k and l, gave the result that expression (i) equalled zero for l = 2n + 1, but did not vanish for l = 2n, and vice versa for expression (ii). Thus considering the atomic positions of C2-C7 of the benzyl group

their contribution to F for $P4_2/n$ would be small for all l values except where h, k, l = 2n and h, k = 2n, l = 2n + 1. These calculations therefore showed no reason why l odd levels were so much weaker than l even levels.

It was concluded that the unit cell has c = 3.54Å and contains two molecules, with stacking faults causing the appearance of very weak intermediate l layer lines and pseudo-tetragonal symmetry. Since tetragonal symmetry can no longer be obeyed, the space group must be monoclinic with c the unique axis, $\gamma = 90°$ and systematic absences on hk0, h + k = 2n + 1. New axes (subscript m for monoclinic) were chosen as shown, looking down c.

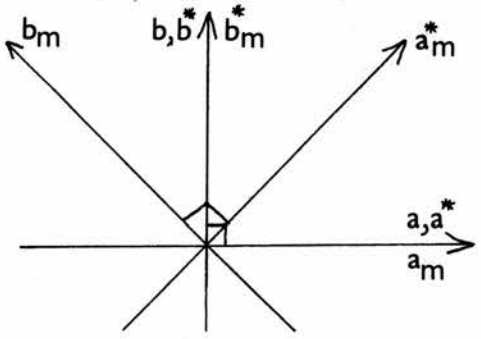

$\gamma_m = 135°$ $\qquad \gamma^*_m = 45°$

$\underline{a}_m = \underline{a}$; $\qquad \underline{b}_m = \underline{b} - \underline{a}$; $\qquad \underline{c}_m = \underline{c}$

$h_m = h$; $\qquad k_m = k - h$; $\qquad l_m = l$

Conditions for reflection are now : hk0; k = 2n. The space group is therefore P2/b with four symmetrically related units, equivalent positions $\pm$ (x,y,z; $\bar{x}$, 1/2 - y, z) and half the MDB molecule as the asymmetric unit. The mercury atoms lie on special positions (0,1/4,z) and $(0,3/4,\bar{z})$.

Strong reflections receiving most of the mercury contribution are k + l = 2n, and hence the Hg's are nearly A-faced centred with equivalent positions (x,y,z) and (x,y + 1/2, z + 1/2). Hg atomic

positions are therefore (0,1/4,~3/4) and (0,3/4,~1/4) which are equivalent to (3/4,1/4,3/8) and (1/4,3/4,1/8) with respect to the original tetragonal unit cell (cf. section 5.3).

It seems likely that the crystals of MDB exist as blocks of single crystals of space group P2/b. These blocks are intermittently turned through 90° about the needle axis c, giving rise to an apparent space group $P4_2/n$ and the two benzyl group orientations seen in figure 5.5.1. Isolation of any one block to determine the true atomic locations would be impossible. In addition, due to radiation damage to the crystal, any accurate determination of intensities would require one crystal per level, which would involve careful correlation between each level of intensity data, especially in view of the high absorption of x-rays.

An accurate determination of the detailed structure of MDB would be difficult, if not impossible, due to the reasons given above, and it was decided that the relative unimportance of the compound did not justify the length of time necessary. The required estimate of the Hg-C bond length had been obtained and the study undertaken so far had provided considerable experience, both experimental and theoretical, for the subsequent structure investigations reported in Chapters 3 and 4.

A1

```
BEGIN RNCD CARD-79
      SF   CARD-7
      SF   CARD-14
      SF   CARD-21
      SF   CARD-28
      SF   CARD-35
      SF   CARD-42
      SF   CARD-45
      SF   CARD-48
      SF   CARD-51
      MF   CARD-50,CARD-49
      MF   CARD-47,CARD-46
      MF   CARD-44,CARD-43
LOOP1 TF   H,CARD-50
      TF   K,CARD-47
      TF   L,CARD-44
      TF   INTS,ZERO7
LOOP2 NOP
BACK  A    INTS,CARD-30
      A    INTS,CARD-16
      A    INTS,CARD-2
      S    INTS,CARD-37
      S    INTS,CARD-23
      S    INTS,CARD-9
      RNCD CARD-79
      SF   CARD-7
      SF   CARD-14
      SF   CARD-21
      SF   CARD-28
      SF   CARD-35
      SF   CARD-42
      SF   CARD-45
      SF   CARD-48
      SF   CARD-51
      MF   CARD-50,CARD-49
      MF   CARD-47,CARD-46
      MF   CARD-44,CARD-43
      C    H,CARD-50
      BNZ  LOOP3
      C    K,CARD-47
      BNZ  LOOP3
      C    L,CARD-44
      BNZ  LOOP3
```

contd.

```
      B    LOOP2
LOOP3 TD   OUT3,ZERO7
      TD   OUT3-3,ZERO7
      TD   OUT3-6,ZERO7
      TF   OUT2+2,H
      CF   OUT2+1
      MF   OUT2+3,OUT2+2
      TF   OUT2+5,K
      CF   OUT2+4
      MF   OUT2+6,OUT2+5
      TF   OUT2+8,L
      CF   OUT2+7
      MF   OUT2+9,OUT2+8
      SF   INTS-5
      TF   OUT5,INTS
      CF   INTS-5
      CF   OUT4+1
      MF   OUT5,INTS
      SF   CARD-58
      TF   OUT1,CARD-54
      CF   OUT1-4
      BNF  NFLAG,OUT5
      TF   OUT5,ZERO7-1
NFLAG WNCD OUT1-4
      PRN  OUT1-4
      C    TEST,H
      BNZ  LOOP1
      H
CARD  DS   80
H     DS   2
K     DS   2
L     DS   2
INTS  DS   7
ZERO7 DC   7,0
OUT1  DS   5
OUT2  DNB  5
OUT3  DS   9
OUT4  DNB  2
OUT5  DS   6
OUT6  DNB  26
OUT7  DNB  27
RECRDMDC   1,@
TEST  DC   2,99
      DEND BEGIN
```

APPENDIX A Computer Programmes

The following programmes were used on an IBM 1620 Model II computer, which has 60,000 digits of core store, card input and output, line printer, digital plotter and three disk drives. All programmes were written by the author in symbolic programming system language (SPS), except A2-A5 which are Computing Department library programmes.

A.1 Data processing for linear diffractometer

For each pair of oscillation cycles using balanced filters, a card is obtained from the linear diffractometer IBM card punch in the form:

column	29			37	43	45	50	52	57	59	64	66	71	73	78
	xx	± xx	± xx	± xxxxxx		xxxxxx		xxxxxx		xxxxxx		xxxxxx		xxxxxx	
	h	k	l	b_1		N_1		b_1'		b_2		N_2		b_2'	

where x represents a digit from 0 to 9.

The net integrated intensity $I(hkl) = [N_1-(b_1 + b_1')]-[N_2-(b_2 + b_2')]$ is calculated and, if more than one card is present for all reflections, the intensities are added together for each reflection. The card output, suitable for input to A2, is of the form:

column	11			19	22	27
	xx	± xx	± xx	±	xxxxxx	
	h	k	l		I(hkl)	

A.2 Intensity data processing programme by E.J. Gabe

This programme reduces the intensity estimates I(hkl) obtained from A1 for linear diffractometer data or measured as

described in section 2.6 from equi-inclination Weissenberg photographs, to a consistent set of $|F_o|^2$ and $|F_o|$ values by applying appropriate scale and Lp^{-1} factors. Reciprocal cell parameters are supplied in directive cards together with $\sin^2\mu$ and a scale factor for each equi-inclination level of data. For each reflection the card output is in the format:

```
col  6     10  11        19  23   26  31       38
     X.XXXX     XX+XX+XX+   XXXX     XXXXXXXX
     sin²θ      h  k  l    |Fo|      |Fo|²
```

A.3 Structure factor and least squares programme (SFLS)

Written by G.A. Mair the programme is in three parts. Part 1, the input routine, interprets a series of directives and stores the input $|F_o|$ data (from A2) on to disk. Part 2 calculates structure factors F_c according to equations (3) (1.1) and (7) or (8) (1.3) and accumulates the least squares totals. The final part calculates parameter shifts from the least squares totals (see 1.4), the new parameters, $\sum w\Delta^2$ and R. Also calculated are positional variances, covariances, new bond lengths and angles and their standard deviations from the equations given in section 1.6. Atoms may be given either isotropic or anisotropic temperature factors, a mixture being permissible, and not all the atoms included in the structure factors calculation need be included in the least squares refinement procedure. Structure factors F_c are stored on disk and may be printed and/or punched together with $|F_o|$, $A_o = |F_o| \cos\phi$ and $B_o = |F_o| \sin\phi$.

Some of the directive cards required are worth mentioning. The "unit cell" directive requires the six R_{ij} values for the cell, calculated from the formula:

$$\sin^2\theta = (\lambda^2/4)\,|d^*(hkl)|^2 \quad (d^*(hkl) \text{ in } \mathring{A}^{-1})$$

$$= (\lambda^2/4)(h^2a^{*2}+k^2b^{*2}+l^2c^{*2}+2klb^*c^*\cos\alpha^*+2hla^*c^*\cos\beta^*+2hka^*b^*\cos\gamma^*)$$

$$= h^2R_{11} + k^2R_{22} + l^2R_{33} + klR_{23} + hlR_{13} + hkR_{23}$$

Values of atomic scattering factor f_o, for each atom included in the F_c calculations, must be given in the "formfactors" directive at intervals of $\sin^2\theta$. Mair has already calculated these for some elements using $CuK\bar{\alpha}$ wavelength from the values of f_o given at intervals of $\sin\theta/\lambda$ in International Tables, Vol. III. Other atomic formfactors required were read off a graph of f_o v. $\sin^2\theta$ (calculated using $CuK\bar{\alpha}$ radiation), and thus in the above formula for the R_{ij}'s, the wavelength λ used, and given in the directive, was 1.5418Å even though Mo was used for all data collection.

Also given in directive cards are the fractional atomic coordinates, temperature factors, the lattice parameters and equivalent positions of the unit cell and the scale factor for the F_o values to put them on the same scale as the F_c's. One of four weighting schemes could be used. For photographic data and initial diffractometer data cycles the scheme given by equation (11), section 1.5 was used, and for the final stages of structure refinement with diffractometer data, equation (12). This latter scheme requires $\sqrt{w(hkl)}$ punched in columns 79 and 80 of the $|F_o|$ data cards as 0.xx.

The number n of parameters in the least squares calculation, for no atoms in special positions, is: 9 x (no. of atoms with anisotropic B_{ij}'s) + 4 x (no. of atoms with isotropic B) + 1 (the scale factor). The fudge factor (section 1.4) was normally chosen as 0.5, increasing to 0.8 as refinement neared completion.

A.4 Fourier programme by G.A. Mair

A three dimensional Fourier synthesis is calculated using the data output from A3. The programme may also be used to compute a Patterson synthesis from the $|F_o|^2$ output of A2, but extra care must be taken with the directives.

The input data cards are sorted so that for sections of x, y or z constant (x_3), h, k or l respectively is the most rapidly moving index (h_3). On each section, the horizontal direction (x_1) has its corresponding index h_1 least rapidly moving.

The equation for the electron density or Patterson function (equation (2) or (4) in section 1.1) must be expanded for the appropriate space group to give a sum of terms of the form:

$$\frac{C}{V}(\pm R_{h_1h_2h_3} \pm R_{h_1\bar{h}_2h_3} \pm R_{h_1h_2\bar{h}_3} \pm R_{\bar{h}_1h_2h_3})\,\mathrm{trg}2\pi h_1x_1\,\mathrm{trg}2\pi h_2x_2\,\mathrm{trg}2\pi h_3x_3$$

where C = constant, V = volume of unit cell and trg = cos or sin. x_1, x_2 and x_3 are fractional coordinates with respect to the unit cell edges. This expansion is shown for the triclinic cases of SiF_4,2Py and $SiCl_4$,2Py.

$$P(u,v,w) = \frac{1}{V}\sum_{hkl=-\infty}^{+\infty}\sum\sum\sum |F(hkl)|^2 \cos 2\pi(hu + kv + lw)$$

$$= \frac{2}{V}\sum_{hkl=o}^{+\infty}\sum\sum\sum |F(hkl)|^2 \cos 2\pi(hu + kv + lw)$$

$$= \frac{2}{V}\sum_{hkl}^{+\infty}\sum\sum\sum [|F(hkl)|^2 + |F(\bar{h}kl)|^2 + |F(h\bar{k}l)|^2 + |F(hk\bar{l})|^2] \cos 2\pi hu \cos 2\pi kv \cos 2\pi lw$$

$$+ [- \quad + \quad + \quad -] \sin 2\pi hu \sin 2\pi kv \cos 2\pi lw$$

$$+ [- \quad + \quad - \quad +] \sin 2\pi hu \cos 2\pi kv \sin 2\pi lw$$

$$+ [- \quad - \quad + \quad +] \cos 2\pi hu \sin 2\pi kv \sin 2\pi lw$$

For P1, $\rho(xyz) = \frac{1}{V}\sum_{hkl=-\infty}^{+\infty}\sum\sum |F(hkl)| \cos[2\pi(hx+ky+lz) - \phi(hkl)]$

$$= \frac{2}{V}\sum_{hkl=o}^{+\infty}\sum\sum\sum |F(hkl)| \cos[2\pi(hx+ky+lz) - \phi(hkl)]$$

$$+ |F(\bar{h}kl)| \cos[2\pi(-hx+ky+lz) - \phi(\bar{h}kl)]$$

$$+ |F(h\bar{k}l)| \cos[2\pi(hx-ky+lz) - \phi(h\bar{k}l)]$$

$$+ |F(hk\bar{l})| \cos[2\pi(hx+ky-lz) - \phi(hk\bar{l})]$$

$$= \frac{2}{V}\sum_{hkl=o}^{+\infty}\sum\sum\sum [A(hkl) + A(\bar{h}kl) + A(h\bar{k}l) + A(hk\bar{l})] \cos 2\pi hx \cos 2\pi ky \cos 2\pi lz$$

$$+ [- \quad + \quad + \quad -] \; s \quad s \quad c$$

$$+ [- \quad + \quad - \quad +] \; s \quad c \quad s$$

$$+ [- \quad - \quad + \quad +] \; c \quad s \quad s$$

$$+ [B(hkl) - B(\bar{h}kl) + B(h\bar{k}l) + B(hk\bar{l})] \; s \quad c \quad c$$

$$+ [+ \quad + \quad - \quad +] \; c \quad s \quad c$$

$$+ [+ \quad + \quad + \quad -] \; c \quad c \quad s$$

$$+ [- \quad + \quad + \quad +] \; s \quad s \quad s$$

$A(hkl) = |F_o(hkl)| \cos\phi(hkl) \qquad B(hkl) = |F_o| \sin\phi(hkl)$

The number of terms in the expansion of P(uvw) or ρ(xyz) is given in the directives and also for each term the signs of the R coefficients (F_o^2 for a Patterson and A and B for a Fourier) together with the trig factors. The R's are chosen to be F_o^2, F_o, A or B according to the setting of further directives. Mesh intervals must be integrals of 1/240 of the cell edges, and for all syntheses intervals of 1/30 of the cell edges were chosen.

A.5 Scan of bonds, angles and intermolecular distances by F.R. Ahmed

This programme carries out scans of intramolecular bond lengths and angles and of intermolecular distances, given the fractional atomic coordinates in the asymmetric unit of the unit cell.

A.6 During structure refinement the latest SFLS card output from A3 is sorted into equi-inclination levels, and at the end of each level a blank card is inserted. Using the whole deck of cards as input, A6 evaluates $\sum|F_o|$ and $\sum|F_c|$ for each level and prints the results as

col 1 8 9 16
xxxxxxxxxxxxxxxx
$\sum|F_o|$ $\sum|F_c|$

Programmes 7 - 11 were written in SPS by the author to find the absolute weights w(h) (equation (12), 1.5), for reflections measured on the linear diffractometer, and to put them into suitable format for input to A3. Decimal points are not punched and all programmes require a blank card at the end of the input data.

A.7 Using the linear diffractometer data cards as input (see A1)

A7

```
CARD    DS    80
B       DS    6
        DC    50,0
IB      DC    30,0
        DC    1,@
BEGIN   RNCD  CARD-79
        SF    CARD-42
        SF    CARD-35
        SF    CARD-28
        SF    CARD-21
        SF    CARD-14
        SF    CARD-7
        CM    CARD-30,0
        BE    END
        A     CARD-37,CARD-23
        S     CARD-37,CARD-16
        S     CARD-37,CARD-2
        TF    B,CARD-37
        A     CARD-37,CARD-30
        S     CARD-37,CARD-9
        S     CARD-30,CARD-9
        S     CARD-30,B
        LD    94,CARD-37
        D     89,CARD-30
        SF    87
        AM    93,5,10
        TF    IB-53,92
        MF    CARD-50,CARD-49
        MF    CARD-47,CARD-46
        MF    CARD-44,CARD-43
        SF    CARD-51
        SF    CARD-48
        SF    CARD-45
        TF    IB-68,CARD50
        TF    IB-65,CARD-47
        TF    IB-62,CARD-44
        MF    IB-67,IB-68
        MF    IB-64,IB-65
        MF    IB-61,IB-62
        CF    IB-29
        CF    IB-79
        WNCD  IB-79
        PRN   IB-79
        B     BEGIN
END     CALL  EXIT
        DEND  BEGIN
```

A6

```
CARD    DS    80
FO      DS    8
FC      DS    8
        DC    1,@
ZERO    DC    8,0
START   TF    FO,ZERO
        TF    FC,ZERO
BEGIN   RNCD  CARD-79
        C     ZERO,CARD-53
        BE    END
        A     FO,CARD-53
        A     FC,CARD-43
        B     BEGIN
END     PRN   FO-7
        DEND  START
```

A8

```
CARD    DS    80
NOF     DC    5,0
SIB     DC    12,0
        DC    1,@
BEGIN   RNCD  CARD-79
        SF    CARD-49
        CM    CARD-42,0,7
        BE    END
        A     SIB,CARD-42
        AM    NOF,1,7
        B     BEGIN
END     PRN   NOF-4
        DEND  BEGIN
```

A9

```
CARD    DS    80
NOF     DC    5,0
FO2     DC    12,0
FOFC2   DC    10,0
        DC    1,@
BEGIN   RNCD  CARD-79
        SF    CARD-57
        CM    CARD-53,0,7
        BE    END
        SF    CARD-47
        S     CARD-43,CARD-53
        M     CARD-53,CARD-53
        A     FO2,99
        M     CARD-43,CARD-43
        A     FOFC2,99
        AM    NOF,1,7
        B     BEGIN
END     PRN   NOF-4
        DEND  BEGIN
```

$(I + B)/(I - B)$ is evaluated for each reflection, where $I = N_1 - N_2$ and $B = (b_1 + b_1') - (b_2 + b_2')$, and the result is given on cards and the line printer as:

1	11	19	22	27
xx±xx±xx±			xx.xxxx	
h k l			(I+B)/(I-B)	

The output from A7 is processed by A2 to form $(K/4Lp)[(I+B)/(I-B)]$ for each reflection as x.xxxxxxx. The scale K/4 for each equi-inclination level of data must be suitably punched in the directives.

A.8. $\sum_1^m \frac{K}{4Lp}\left(\frac{I+B}{I-B}\right)$ is evaluated and given on the line printer in the form:

1	5	6	17
xxxxx		xxxxx.xxxxxxx	
		$\sum$	

A.9 $\sum_1^m |F_o|^2$ and $\sum_1^m (|F_o| - |F_c|)^2$ are calculated from the latest card output of A3 and printed as:

1	5	6	17	18	27
xxxxx		xxxxxxxx.xxxx		xxxxxx.xxxx	
m		$\sum\|F_o\|^2$		$\sum(\|F_o\| - \|F_c\|)^2$	

A.10 $\sqrt{w} = [\frac{K}{4Lp}\left(\frac{I+B}{I-B}\right) + c^2F_o^2]^{-\frac{1}{2}}$ is calculated for each reflection and given on cards and the line printer as:

11	19	20	30
xx±xx±xx±		xxx.xxxxxxxx	
h k l		$\sqrt{w}$	

The input data consists of two cards per reflection, paired on an IBM card sorter. The first card is from the latest SFLS output and the second contains $(K/4Lp)[(I+B)/(I-B)]$ as described above. $c^2 = 0.0xxxxx$ is punched in the appropriate programme card (in the listing given, as 12597 for $SiCl_4$,2Py). If pairing has been done incorrectly then a checking procedure causes no card to be punched for that reflection, and the $\sqrt{w}$ value for the previous

A10

```
CARD1   DS    80
CARD2   DS    80
        DC    50,0
RW      DC    30,0
        DC    1,@
FO2     DS    10
A       DS    11
XN      DS    11
XNPL1   DS    11
XNTEST  DS    11
BEGIN   RNCD  CARD1-79
        CM    CARD1-53,0,7
        BE    END
        MF    CARD1-68,CARD1-67
        MF    CARD1-65,CARD1-64
        MF    CARD1-62,CARD1-61
        M     CARD1-53,CARD1-53
        TF    FO2,99
        MM    FO2,12597,7
        RNCD  CARD2-79
        TF    RW-61,CARD2-61
        TF    RW-64,CARD2-64
        TF    RW-67,CARD2-67
        MF    CARD2-62,CARD2-61
        MF    CARD2-65,CARD2-64
        MF    CARD2-68,CARD2-67
        C     CARD2-68,CARD1-68
        BNE   ERROR
        C     CARD2-65,CARD1-65
        BNE   ERROR
        C     CARD2-62,CARD1-62
        BNE   ERROR
        A     96,CARD2-42
        SF    86
        TF    A,96
        TF    XNPL1,A
SQRT    TF    XN,XNPL1
        TF    XNTEST,XNPL1
        TFM   79,0,7
        LD    92,A
        D     89,XN
        A     XN,88
        MM    XN,50,10
        TF    XNPL1,97
        S     XNTEST,XNPL1
        CF    XNTEST
        CM    XNTEST,5
        BP    SQRT
```

contd.

```
        TFM   79,0,7
        LDM   87,10000,7
        D     87,XNPL1
        SF    77
        AM    88,5,10
        TF    RW-50,87
        CF    RW-29
        WNCD  RW-79
ERROR   PRN   RW-79
        B     BEGIN
END     CALL  EXIT
        DEND  BEGIN
```

A11

```
CARD1   DS    80
CARD2   DS    80
        DC    1,@
BEGIN   RNCD  CARD1-79
        CM    CARD1-50,0,7
        BE    END
        MM    CARD1-50,13714,7
        SF    87
        AM    93,55555,7
        MF    CARD1-68,CARD1-67
        MF    CARD1-65,CARD1-64
        MF    CARD1-62,CARD1-61
        RNCD  CARD2-79
        MF    CARD2-68,CARD2-67
        MF    CARD2-65,CARD2-64
        MF    CARD2-62,CARD2-61
        C     CARD2-68,CARD1-68
        BNE   ERROR
        C     CARD2-65,CARD1-65
        BNE   ERROR
        C     CARD2-62,CARD1-62
        BNE   ERROR
        TF    CARD2,88
        CF    CARD2-1
        MF    CARD2-67,CARD2-68
        MF    CARD2-64,CARD2-65
        MF    CARD2-61,CARD2-62
        WNCD  CARD2-79
ERROR   PRN   CARD2-79
        B     BEGIN
END     CALL  EXIT
        DEND  BEGIN
```

correctly paired reflection is repeated on the line printer.

The direct square root operation in SPS requires numbers to be converted to floating point format and to avoid this, Newton's method was used to find the square root. This is an iterative cyclic procedure given by the formula $x_{n+1} = \frac{1}{2}(A/x_n + x_n)$ where A is the number whose square root is required. x_{n+1} is the improved approximation for $\sqrt{A}$ from x_n, which is initially chosen as A. x_{n+1} becomes x_n for the next cycle, and so on until the difference between x_{n+1} and x_n is less than the least significant digit required for $\sqrt{w}$, when the process is terminated.

A.11 Two paired input cards are again needed for each reflection. The first is $\sqrt{w}$ from A10 and the second, the original $|F_o|$ input card for A3, which requires $\sqrt{w}$ punched as $0.^{79\,80}xx$ on it. This programme multiplies each absolute $\sqrt{w}$ by $D = 0.99/\sqrt{w_{max}}$ and forms a new set of data cards for SFLS calculations, plus a line printer output. D is punched as .xxxxx on a programme card (in the given listing D = 0.13714 for SiF_4,2Py). If the input cards have been incorrectly paired then, for that reflection, no card is punched and $\sqrt{w}$ appears as 00 on the printer.

A.12 This programme finds those reflections which have, on an absolute scale, $|\Delta| = |\,|F_o| - |F_c|\,| > s\sigma$ where $\sigma = 1/\sqrt{w}$. s was taken as 3 or 4 and is given on a programme card. The input data contains two paired cards per reflection and a pairing check is incorporated into the programme. The first card is the latest SFLS output

A12

```
CARD2   DS    80
CARD1   DS    80
        DC    1,@
BEGIN   RNCD  CARD1-79
        CM    CARD1-53,0,7
        BE    END
        MF    CARD1-68,CARD1-67
        MF    CARD1-65,CARD1-64
        MF    CARD1-62,CARD1-61
        S     CARD1-53,CARD1-43
        CF    CARD1-53
        RNCD  CARD2-79
        MF    CARD2-68.CARD2-67
        MF    CARD2-65,CARD2-64
        MF    CARD2-62,CARD2-61
        C     CARD2-68,CARD1-68
        BNE   ERROR
        C     CARD2-65,CARD1-65
        BNE   ERROR
        C     CARD2-62,CARD1-62
        BNE   ERROR
        LDM   92,40000,7
        D     95,CARD2-50
        AM    88,5,10
        S     CARD1-53,87
        BNP   BEGIN
        TFM   CARD1-43,0,7
ERROR   MF    CARD1-67,CARD1-68
        MF    CARD1-64,CARD1-65
        MF    CARD1-61,CARD1-62
        PRN   CARD1-79
        B     BEGIN
END     CALL  EXIT
        DEND  BEGIN
```

A13

```
W       DS    10
D       DS    5
D2      DS    10
CARD    DS    80
        DC    1,@
BEGIN   RNCD  CARD-79
        CM    CARD-53,0,7
        BE    END
        S     CARD-53,CARD-43
        TF    D,CARD-53
        M     CARD-53,CARD-53
```

A13 contd.

```
        TF    D2,99
        RNCD  CARD-79
        M     CARD-50,D
        AM    99,55,10
        SF    87
        TF    CARD-30,97
        AM    CARD-50,5,10
        M     CARD-51,CARD-51
        AM    94,55555,7
        TF    W,89
        M     W,D2
        SF    89
        TF    CARD-50,99
        PRN   CARD-79
        WNCD  CARD-79
        B     BEGIN
END     CALL  EXIT
        DEND  BEGIN
```

A14

```
CARD    DS    80
        DC    50,0
OUTPUT  DC    30,0
        DC    1,@
        BSBA  *+12
        BLXM  *+12,1236(A2)
        CF    OUTPUT-79
        CF    OUTPUT-29
BEGIN   RNCD  CARD-79
        BLXM  *+12,-80(A1)
        SM    CARD-56,100,7
        BNN   NEXT
        SF    OUTPUT+1(A1)
        AM    OUTPUT+5(A1),1,7
        CF    OUTPUT+1(A1)
        BCXM  BEGIN,-1(A2)
        B     NEXT+24
NEXT    BCXM  BEGIN+24,5(A1)
        B     NEXT-24
        WNCD  OUTPUT-79
        PRN   OUTPUT-79
        CALL  EXIT
        DEND  BEGIN-48
```

during the final stage of structure refinement using the correct diffractometer data weighting scheme, and the second data card contains absolute $\sqrt{w}$ (from A10). The value of $(|\Delta| - s\sigma) > 0$ is printed as $\overset{23}{xxx}.\overset{27}{xx}$ together with the indices of the reflection in the usual format. A blank card is required at the end of the data.

A.13 The same input data is used for A13 as for A12 and $\sqrt{w}|\Delta|$ and $w\Delta^2$ are evaluated for each reflection. The results are punched and printed with $w\Delta^2$ in cols 20-30 as xxx.xxxxxxxx and $\sqrt{w}|\Delta|$ in cols 40-50 as xxx.xxxxxxxx (indices in usual format).

A.14 The card output from A13 is used to find the number N of reflections with $w\Delta^2$ values in each of the 16 intervals $0 \rightarrow 0.99$, $1 \rightarrow 1.99$ up to $15 \rightarrow 15.99$ and the values of N are given on the line printer (16 numbers, each of five digits). Index registers are used to modify the addresses of certain instructions and the total number of cards is given in the programme e.g. 1236 for $SiCl_4$,2Py.

A.15 This programme was written for $SiCl_4$,2Py to change the h and k indices (h_L and k_L) on the data cards obtained from the linear diffractometer (see A1) to those of the F cell (h_F and k_F) according to the equations given in section 4.4.

A.16 For $SiCl_4$,2Py the set of $|F_o|$ values from A2 has F cell indices ($h_F k_F l_F$) and A16 changes these to reduced cell indices (hkl) by

A15

```
CARD    DS    80
H       DS    2
K       DS    2
BEGIN   RNCD  CARD-79
        SF    CARD-51
        SF    CARD-48
        SF    CARD-45
        MF    CARD-50,CARD-49
        MF    CARD-47,CARD-46
        MF    CARD-44,CARD-43
        TF    H,CARD-50
        TF    K,CARD-47
        LD    99,CARD-44
        DM    98,2,10
        BD    ODD,99
EVEN    A     CARD-50,H
        CF    CARD-51
        MF    CARD-49,CARD-50
        A     CARD-47,K
        CF    CARD-48
        MF    CARD-46,CARD-47
        CF    CARD-45
        MF    CARD-43,CARD-44
        B     FINISH
ODD     S     CARD-50,99
        S     CARD-47,99
        B     EVEN
FINISH  WNCD  CARD-79
        B     BEGIN
        DEND  BEGIN
```

A16

```
CARD    DS    80
K       DS    2
BEGIN   RNCD  CARD-79
        SF    CARD-49
        CM    CARD-42,0,7
        BE    END
        MF    CARD-68,CARD-67
        MF    CARD-65,CARD-64
        MF    CARD-62,CARD-61
        TF    K,CARD-65
        A     CARD-68,CARD-62
        A     CARD-65,CARD-62
        S     CARD-62,K
        TF    K,CARD-62
        LD    99,CARD-68
        DM    98,2,10
```

A16 contd.

```
        TF    CARD-62,97
        LD    99,CARD-65
        DM    98,2,10
        TF    CARD-68,97
        LD    99,K
        DM    98,2,10
        TF    CARD-65,97
        MF    CARD-67,CARD-68
        MF    CARD-64,CARD-65
        BNF   POS,CARD-62
        CF    CARD-62
        B     FINISH
POS     SF    CARD-61
FINISH  WNCD  CARD-79
        B     BEGIN
END     CALL  EXIT
        DEND  BEGIN
```

A17

```
CARD    DS    80
K       DS    2
BEGIN   RNCD  CARD-79
        MF    CARD-68,CARD-67
        MF    CARD-65,CARD-64
        MF    CARD-62,CARD-61
        SF    CARD-69
        SF    CARD-66
        SF    CARD-63
        TF    K,CARD-65
        TF    CARD-65,CARD-68
        A     CARD-68,CARD-62
        A     CARD-68,CARD-62
        A     CARD-68,K
        TF    CARD-62,CARD-65
        S     CARD-65,K
        A     CARD-62,K
        CF    CARD-69
        CF    CARD-66
        CF    CARD-63
        MF    CARD-61,CARD-62
        MF    CARD-64,CARD-65
        BNF   POS,CARD-68
        CF    CARD-68
        B     FINISH
POS     SF    CARD-67
FINISH  WNCD  CARD-79
        B     BEGIN
        DEND  BEGIN
```

application of the unit cell vector transformation equations given in section 4.3 i.e.

$$\begin{bmatrix} h \\ k \\ l \end{bmatrix} = \begin{bmatrix} 0 & \frac{1}{2} & \frac{1}{2} \\ 0 & -\frac{1}{2} & \frac{1}{2} \\ -\frac{1}{2} & 0 & -\frac{1}{2} \end{bmatrix} \begin{bmatrix} h_F \\ k_F \\ l_F \end{bmatrix}$$

A blank card at the end of the input data terminates the calculations.

A.17 This final SPS programme written by the author converts the reduced cell indices (in cols 11-19) of a deck of cards (e.g. output from A3) back to F cell values. The matrix used is inverse to the one above:

F cell indices \ reduced cell indices →			
	-1	-1	-2
	+1	-1	0
	+1	+1	0

according to the notation in International Tables, Vol.I.

APPENDIX B Calibration of the Stoe precession camera

A Buerger precession camera (Buerger, 1944) was used to photograph layers of the reciprocal lattice of SiF_4,2Py (section 3.3). The original black cardboard in the film cassette between the crystal and film had become buckled and worn and was replaced by cardboard and black paper. Calibration of the crystal to film distance F, set at 60mm for zero level photographs, was therefore necessary.

Quartz has been widely used as a standard for calibration (Bradley and Jay, 1933; Evans et al, 1949; Barnes et al, 1951) and its lattice parameters have been accurately determined by many workers including Miller and Du Mond (1940) and Lipson and Wilson (1941). Although quartz gives differences in lattice spacing, depending on its variety and origin (Keith, 1950 and 1955), these are significant in only the 4th decimal place. Due to inaccuracies in measurement of reciprocal lattice spacings from precession photographs, the minimum error in SiF_4,2Py cell dimensions was 0.005Å, and hence no greater accuracy than ~0.1mm was necessary for the determination of F. Quartz parameters were therefore sufficiently accurate for the purpose required, and a single quartz crystal was supplied by the Geology Department.

Using unfiltered Cu radiation the crystal was aligned on the precession camera by Fisher's method (1952 and 1953), which consists of locating the centre of the circle of precession, formed by the

ends of prominent Laue streaks. The angle μ, between the incident beam and the normal to the plane being photographed, was initially taken as 10°, increasing to 20° and 25° as crystal setting was improved by calculated corrections to the dial and goniometer arcs. Account must be taken of the angles that the arcs make with the horizontal and vertical directions. The crystal was finally set, to within 5' on the dial and 10' on the goniometer arcs, with c* along the dial axis and b as the axis of precession.

h0l was recorded with $CuK\bar{\alpha}$ radiation, $\lambda = 1.54178\text{Å}$, and $\mu = 30°$. The layer screen with annular radius r_s, is set at a distance s from the crystal, where $s = r_s \cot \cos^{-1}(\cos\mu - d^*)$. d^* is the height of the reciprocal level in r.l.u. and hence for zero level photographs, s is simply $r_s \cot\mu$.

The lattice parameters of the quartz hexagonal unit cell are: $a = 4.9027\text{kX}$, $c = 5.3934\text{kX}$ or 4.9126Å and 5.4043Å ($1\text{kX} = 1.00202\text{Å}$). $a^* = 2/a\sqrt{3} = D/nF\lambda$ where D is the distance in mm measured on the film over n spacings parallel to a*. Similarly F may also be found from $c^* = 1/c$. The mean of all F values obtained was $59.74 \pm 0.03\text{mm}$, which was used for subsequent calculations of reciprocal lattice parameters from precession photographs recorded by this camera.

APPENDIX C Calculation of hydrogen positions

For both SiF_4,2Py and $SiCl_4$,2Py the first step was orthogonalisation of the oblique axes of the reduced triclinic unit cell.

Choose standard orthogonal axes x',y',z' such that y' coincides with b, x' is the projection of a on to the plane perpendicular to b and z' is perpendicular to x' and y'. In terms of oblique coordinates (x,y,z) (in Å), orthogonal coordinates (x',y',z') (in Å) are:

$$x' = x\sin\gamma + z(\cos\beta - \cos\alpha\cos\gamma)/\sin\gamma$$

$$y' = x\cos\gamma + y + z\cos\alpha$$

$$z' = z\left[\sin^2\alpha - \left(\frac{\cos\beta - \cos\alpha\cos\gamma}{\sin\gamma}\right)^2\right]^{\frac{1}{2}}$$

For SiF_4,2Py this becomes:

$$\begin{bmatrix} x' \\ y' \\ z' \end{bmatrix} = \begin{bmatrix} 0.9951 & 0 & -0.45171 \\ -0.09928 & 1 & -0.33737 \\ 0 & 0 & 0.82595 \end{bmatrix} \begin{bmatrix} x \\ y \\ z \end{bmatrix}$$

and for $SiCl_4$,2Py

$$\begin{bmatrix} x' \\ y' \\ z' \end{bmatrix} = \begin{bmatrix} 0.91745 & 0 & -0.19805 \\ -0.3979 & 1 & -0.4563 \\ 0 & 0 & 0.8673 \end{bmatrix} \begin{bmatrix} x \\ y \\ z \end{bmatrix}$$

In the pyridine ring shown, N-C3-H3, H1-C1-C4-H4 and H2-C2-C5-H5 are straight lines.

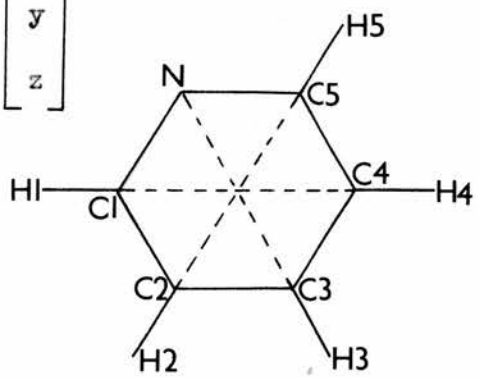

The coordinates of N and C1-C5 were taken from the latest SFLS cycle and were orthogonalised using

the appropriate matrix above. The C-H bond length is 1.08Å (Pauling, 1948) but for calculation of H positions it was assumed to be 1 Å, both for simplicity and because the carbon coordinates used have been calculated with no hydrogens included. To compensate for their absence, the carbon positions have been moved slightly from their true positions towards their corresponding H atom.

Express the orthogonal coordinates of C4 with respect to C1 as origin e.g. $x''_{C4} = x'_{C4} - x'_{C1}$. Now, $x''_{H1}/x''_{C4} = (-1)/C1\text{-}C4$ and $C1\text{-}C4 = \sqrt{(x''_{C4})^2 + (y''_{C4})^2 + (z''_{C4})^2}$. Hence $x'_{H1} = x''_{H1} + x'_{C1}$, the orthogonal x' coordinate of H1 may be calculated. Similarly for y'_{H1} and z'_{H1}. The orthogonal coordinates (x',y',z') of all the hydrogens were found by this method, and then converted to reduced cell oblique coordinates (x,y,z), for inclusion in structure factor calculations, by application of the appropriate inverse matrix below.

SiF_4,2Py:

$$\begin{bmatrix} x \\ y \\ z \end{bmatrix} = \begin{bmatrix} 1.00492 & 0 & 0.54959 \\ 0.09977 & 1 & 0.46303 \\ 0 & 0 & 1.21073 \end{bmatrix} \begin{bmatrix} x' \\ y' \\ z' \end{bmatrix}$$

$SiCl_4$,2Py

$$\begin{bmatrix} x \\ y \\ z \end{bmatrix} = \begin{bmatrix} 1.08998 & 0 & 0.24890 \\ 0.43770 & 1 & 0.62515 \\ 0 & 0 & 1.15300 \end{bmatrix} \begin{bmatrix} x' \\ y' \\ z' \end{bmatrix}$$

APPENDIX D Least squares best plane

A least squares determination of the best plane $lx' + my' + nz' = p$ through the five carbon atoms of the pyridine ring in SiF_4,2Py and $SiCl_4$,2Py was made according to the theory given in section 1.4. Atomic coordinates with respect to the reduced triclinic cell were orthogonalised by the appropriate matrix in Appendix C, and initial approximate values of l, m, n and p were obtained by calculating the plane through C1, C3 and C5. With respect to orthogonal axes x', y', z' this plane has equation:

$$\begin{vmatrix} x' & y' & z' & 1 \\ x'_{C1} & y'_{C1} & z'_{C1} & 1 \\ x'_{C3} & y'_{C3} & z'_{C3} & 1 \\ x'_{C5} & y'_{C5} & z'_{C5} & 1 \end{vmatrix} = 0$$

$$\equiv Ax' + By' + Cz' + D = 0.$$

l, m, n and p were found from the equations:

$$l = -\frac{sA}{E}, \quad m = -\frac{sB}{E}, \quad n = -\frac{sC}{E}, \quad p = \frac{sD}{E}$$

where s = sign of D and $E = (A^2 + B^2 + C^2)^{\frac{1}{2}}$

The deviation of atom i from this plane is $lx'_i + my'_i + nz'_i - p = \Delta_i$, where x'_i, y'_i, z'_i are the orthogonal coordinates in Å of atom i. It is required to minimise $\sum_{i=1}^{5} \Delta_i^2$ with respect to the three independent variables m, n and p. $(l = (1 - m^2 - n^2)^{\frac{1}{2}})$. This occurs when $\sum_{i=1}^{5} \Delta_i \frac{\partial \Delta_i}{\partial u} = 0$ for u = m, n, p.

Δ_i is not linear in m, n and p but $\delta_u = u - u'$, where u' is

the approximate value of m, n or p, and Δ_i can be represented by the first two terms of a Taylor series: $\Delta_i = g_i + \sum_{u=m,n,p} \frac{\partial \Delta_i}{\partial u} \delta_u$.

This gives the 3 normal equations for u = m, n and p:

$$\sum_{i=1}^{5} \frac{\partial \Delta_i}{\partial u} \sum_{u=m,n,p} \frac{\partial \Delta_i}{\partial u} \cdot \delta_u = - \sum_{i=1}^{5} \Delta_i \frac{\partial \Delta_i}{\partial u}$$

It can be shown that $\frac{\partial \Delta_i}{\partial m} = - \frac{mx'_i}{l} + y'_i$;

$\frac{\partial \Delta_i}{\partial n} = - \frac{nx'_i}{l} + z'_i$; $\frac{\partial \Delta_i}{\partial p} = -1$. Hence:

$$\begin{bmatrix} (\frac{m^2}{l^2}\sum x^2 - \frac{2m}{l}\sum xy + \sum y^2) & (\frac{mn}{l^2}\sum x^2 - \frac{n}{l}\sum xy - \frac{m}{l}\sum xz + \sum yz) & (\frac{m}{l}\sum x - \sum y) \\ (\frac{mn}{l^2}\sum x^2 - \frac{n}{l}\sum xy - \frac{m}{l}\sum xy + \sum yz) & (\frac{n^2}{l^2}\sum x^2 - \frac{2n}{l}\sum xz + \sum z^2) & (\frac{n}{l}\sum x - \sum z) \\ (\frac{m}{l}\sum x - \sum y) & (\frac{n}{l}\sum x - \sum z) & 5 \end{bmatrix} \begin{bmatrix} \delta_m \\ \delta_n \\ \delta_p \end{bmatrix} = \begin{bmatrix} \frac{m}{l}\sum \Delta x - \sum \Delta y \\ \frac{n}{l}\sum \Delta x - \sum \Delta z \\ \sum \Delta \end{bmatrix}$$

Using the initial l, m, n and p values and the known orthogonal coordinates of the five carbon atoms, the three simultaneous equations were solved for the shifts δ_m, δ_n and δ_p, giving improved values of l, m, n and p. These, together with the new residuals, Δ, were used for a 2nd cycle, which gave shifts significant in only the 6th or 7th decimal place in all cases.

The best fit plane $lx' + my' + nz' = p$ was found with respect to the oblique axes (x,y,z) of the reduced cell by means of the equations and appropriate matrix given in Appendix C. When $y = z = 0$, $x' = x\sin\gamma$, $y' = x\cos\gamma$ and $z' = 0$. Substitution into $lx' + my' + nz' = p$, gives $x = a$, the intercept on the x axis. Similarly for intercepts b and c on y and z, and the least squares best fit plane $\frac{x}{a} + \frac{y}{b} + \frac{z}{c} = 1$ is obtained.

Table A

SiF_4,2Py

Observed and calculated structure factors for

linear diffractometer (L) and photographic (P) data

H	K	L	$(F_o)_L$	$(F_c)_L$	$(F_o)_P$	$(F_c)_P$
0	0	1	366	464	-	-
0	0	2	714	774	750	742
0	0	3	520	620	624	620
0	0	4	676	682	792	776
0	0	5	-1366	-1350	-1530	-1600
0	0	6	272	314	414	378
0	0	7	204	294	432	378
0	1	1	3160	3000	2976	2962
0	1	-2	664	694	774	698
0	1	2	4476	4334	4242	4394
0	1	3	996	1026	1032	1024
0	1	-3	-2232	-2100	-2232	-2186
0	1	-4	- 552	- 528	- 570	- 632
0	1	4	- 188	- 224	- 198	- 268
0	1	5	180	282	336	314
0	1	-5	690	938	822	1092
0	1	-6	- 130	- 244	-	-
0	1	7	- 226	- 172	- 474	- 258
0	1	-7	262	246	-	-
0	2	0	166	224	-	-
0	2	1	3546	3450	3396	3418
0	2	2	1350	1378	1320	1340
0	2	-2	-1728	-1776	-1134	-1722
0	2	-3	160	194	234	202
0	2	3	1760	1688	1692	1812
0	2	4	524	506	528	466
0	2	-4	-1158	-1000	-1122	-1038
0	2	-5	576	586	642	588
0	2	5	466	478	528	500
0	2	-6	556	558	630	614
0	2	-7	576	570	786	704
0	2	-8	172	136	-	-
0	3	0	134	124	-	-
0	3	1	822	826	960	836
0	3	2	1122	1030	1020	1068
0	3	-3	- 122	- 114	- 450	- 148
0	3	3	784	718	732	662
0	3	4	976	1046	996	1058
0	3	-4	606	582	564	572
0	3	-5	626	550	576	520
0	3	5	368	312	306	398
0	3	-6	988	982	978	1058
0	3	-7	282	294	264	300

0	3	-8	282	280	-	-
0	4	0	144	150	240	192
0	4	1	- 608	- 680	- 600	- 594
0	4	2	444	384	402	342
0	4	3	722	718	678	682
0	4	-3	168	532	540	442
0	4	4	388	390	354	458
0	4	-4	1330	1454	1470	1292
0	4	-5	558	510	492	494
0	4	-6	552	516	552	482
0	4	-7	420	442	366	464
0	4	-8	162	184	-	-
0	5	0	- 562	- 556	- 498	- 480
0	5	-1	430	514	378	434
0	5	-2	-	-	426	472
0	5	-3	460	666	546	544
0	5	-4	526	580	558	476
0	5	-5	958	962	924	834
0	5	-6	204	180	222	174
0	5	-7	186	132	-	-
0	6	0	248	246	192	134
0	6	-1	220	220	150	144
0	6	2	-	-	- 120	- 76
0	6	-2	566	652	420	484
0	6	-3	-	-	390	520
0	6	-4	282	354	282	282
0	6	-5	312	278	240	230
0	6	-6	272	256	246	218
0	7	0	246	236	174	148
0	7	1	188	86	-	-
0	7	-1	352	354	252	224
0	7	-2	290	304	222	208
0	7	-3	-	-	180	238
0	7	-4	188	254	168	184
0	7	-5	116	80	-	-
0	7	-6	144	90	-	-
1	0	1	1900	1802	1836	1804
1	0	2	1080	1034	1044	1064
-1	0	2	1390	1340	1386	1372
1	0	3	490	522	528	534
-1	0	3	582	578	630	604
1	0	4	316	272	390	316
-1	0	4	142	56	-	-
-1	0	5	- 216	- 168	- 372	- 160
1	0	6	298	262	390	322
-1	0	6	166	24	-	-
1	0	7	174	162	-	-

1	1	0	2068	1946	-	-
-1	1	0	2764	3024	-	-
1	1	1	1868	1874	1788	1896
1	1	-1	2150	2210	-	-
-1	1	1	2188	1984	1548	1966
-1	1	-1	782	792	-	-
1	1	2	2006	1928	2082	2010
1	1	-2	464	490	-	-
-1	1	2	1862	1812	1818	1830
1	1	3	676	678	690	704
1	1	-3	-1198	-1100	-1266	-1144
-1	1	3	1404	1388	1476	1404
-1	1	-3	388	388	444	414
1	1	-4	- 388	- 356	- 468	- 360
-1	1	4	570	564	600	630
-1	1	-4	614	596	588	642
1	1	5	226	232	-	-
1	1	-5	282	250	-	-
-1	1	-5	194	124	-	-
-1	1	-6	320	380	-	-
1	1	-7	364	368	-	-
-1	1	-7	262	260	-	-
1	1	-8	376	372	-	-
1	2	0	780	744	804	750
-1	2	0	658	778	-	-
1	2	1	2164	2032	2124	2074
1	2	-1	576	542	-	-
-1	2	1	908	950	852	946
-1	2	-1	506	430	-	-
1	2	2	1006	998	978	978
-1	2	2	-	-	2256	2184
1	2	-2	-1082	-1130	-	-
-1	2	-2	768	784	738	782
1	2	3	908	660	954	730
1	2	-3	- 268	- 192	- 246	- 246
-1	2	3	-	-	954	886
-1	2	-3	- 288	- 194	- 252	- 224
1	2	4	-	-	426	312
1	2	-4	- 896	- 784	- 930	- 802
-1	2	4	640	402	684	418
-1	2	-4	666	644	678	660
1	2	5	346	280	372	326
1	2	-5	506	482	552	468
-1	2	5	224	300	342	326
-1	2	-5	710	692	786	780
1	2	-6	748	674	810	756
-1	2	6	152	176	-	-

1	2	-7	570	598	708	684
-1	2	-7	184	166	-	-
1	2	-8	184	276	294	312
1	3	0	-	-	- 186	- 40
-1	3	0	- 92	- 82	-	-
1	3	1	950	932	882	908
1	3	-1	-1386	-1242	-1290	-1160
-1	3	1	810	792	750	804
1	3	2	754	588	678	612
-1	3	2	632	618	630	586
-1	3	-2	176	190	-	-
1	3	3	430	388	396	356
1	3	-3	- 80	- 116	-	-
-1	3	3	-	-	816	786
-1	3	-3	950	936	864	884
1	3	4	528	590	618	632
1	3	-4	434	434	480	368
-1	3	4	362	324	348	268
-1	3	-4	250	258	-	-
1	3	5	362	286	288	330
1	3	-5	724	678	708	726
-1	3	5	460	470	438	504
-1	3	-5	558	620	564	594
1	3	-6	1090	1086	1098	1084
-1	3	6	208	176	-	-
-1	3	-6	214	190	-	-
1	3	-7	454	436	420	484
-1	3	-7	250	254	-	-
1	3	-8	392	406	444	486
1	4	0	696	696	624	662
-1	4	0	200	246	156	226
1	4	1	- 646	- 662	- 612	- 642
1	4	-1	- 238	- 260	- 162	- 320
-1	4	1	878	968	876	910
1	4	2	308	314	294	296
1	4	-2	- 634	- 564	- 642	- 510
-1	4	-2	496	944	792	828
1	4	3	584	584	564	562
1	4	-3	168	422	450	390
-1	4	3	238	174	252	142
-1	4	-3	822	978	924	856
1	4	4	376	354	384	400
1	4	-4	1556	1788	1758	1606
-1	4	4	546	532	354	540
-1	4	-4	168	162	-	-
1	4	-5	- 476	- 100	- 516	- 128
-1	4	5	308	340	336	372

-1	4	-5	250	240	-	-
1	4	-6	690	672	654	698
-1	4	-6	402	424	-	-
1	4	-7	678	642	654	650
1	4	-8	250	224	-	-
1	5	0	- 862	- 820	- 714	- 750
-1	5	0	1018	1086	816	946
1	5	1	238	238	180	206
1	5	-1	496	510	432	448
-1	5	1	- 574	- 544	- 540	- 502
-1	5	-1	322	614	378	454
1	5	2	282	226	240	186
1	5	-2	724	752	654	578
-1	5	2	376	364	342	338
1	5	-3	604	470	606	372
-1	5	3	316	374	306	334
-1	5	-3	90	50	-	-
1	5	-4	342	390	384	380
-1	5	-4	1024	1048	966	886
1	5	-5	1516	1522	1464	1318
-1	5	-5	- 204	- 200	-	-
1	5	-6	156	238	210	200
-1	5	-7	172	244	-	-
1	6	0	202	196	144	130
1	6	1	132	154	120	124
1	6	-1	208	252	186	192
-1	6	1	484	458	360	350
-1	6	-1	248	388	252	284
1	6	2	- 214	- 160	- 192	- 166
1	6	-2	398	374	318	280
-1	6	2	288	294	252	236
-1	6	-2	-	-	96	406
1	6	-3	958	1040	648	802
-1	6	3	- 144	- 36	-	-
-1	6	-3	126	126	-	-
1	6	-4	456	478	390	348
-1	6	-4	- 214	- 196	- 192	- 148
1	6	-5	178	196	150	182
-1	6	-5	600	542	-	-
1	6	-6	334	316	258	260
-1	6	-6	178	130	-	-
1	6	-7	144	174	144	134
-1	6	-7	-	-	186	48
1	7	0	378	344	258	242
-1	7	0	88	132	84	60
1	7	-1	172	166	126	100
-1	7	1	322	284	252	198

-1	7	-1	206	238	-	-
1	7	-2	562	528	414	386
-1	7	-2	- 44	- 54	-	-
1	7	-3	228	244	186	160
1	7	-4	390	444	318	324
1	7	-6	122	154	114	106
-1	7	-6	172	156	-	-
2	0	0	-3482	-3270	-2628	-3236
2	0	1	- 756	- 676	- 774	- 750
-2	0	1	4570	4536	4116	4646
2	0	2	1378	1332	1476	1412
-2	0	2	- 136	- 108	-	-
2	0	3	1024	1038	1188	1178
-2	0	3	- 402	- 318	- 396	- 334
2	0	4	- 166	- 52	-	-
-2	0	4	844	896	918	934
2	0	5	850	882	1080	1100
-2	0	5	1676	1694	1836	1890
2	0	6	390	454	600	578
-2	0	6	- 416	- 408	- 552	- 528
-2	0	7	366	374	390	426
-2	0	8	-	-	522	494
2	1	0	- 632	- 568	- 684	- 600
-2	1	0	4758	4662	-	-
2	1	1	1492	1394	1548	1466
-2	1	1	-3536	-3338	-3438	-3338
-2	1	-1	- 408	- 350	- 462	- 320
2	1	2	- 652	- 536	- 714	- 604
2	1	-2	934	928	978	980
-2	1	2	- 902	- 814	- 942	- 794
-2	1	-2	332	354	336	360
2	1	3	364	422	420	514
2	1	-3	2432	2338	2490	2372
-2	1	3	1154	1142	1224	1220
-2	1	-3	1316	1340	1428	1424
2	1	4	444	398	522	428
2	1	-4	- 326	- 260	- 390	- 312
-2	1	4	1140	1084	1176	1162
-2	1	-4	1806	1192	1896	1390
2	1	5	588	536	618	638
2	1	-5	752	774	858	748
-2	1	5	- 526	- 466	- 558	- 556
-2	1	-5	- 206	- 186	-	-
2	1	-6	790	790	900	898
-2	1	6	764	806	888	946
-2	1	-6	376	410	-	-
2	1	-7	268	292	336	362

-2	1	7	394	414	498	488
2	2	0	1140	1092	1086	1072
-2	2	0	- 230	- 190	-	-
2	2	1	166	60	222	36
2	2	-1	- 486	- 398	- 462	- 398
-2	2	1	- 544	- 476	- 540	- 512
-2	2	-1	2086	1910	1866	1928
2	2	2	416	312	444	426
2	2	-2	2240	2068	2124	1994
-2	2	2	1344	1204	1320	1220
-2	2	-2	2740	2542	2616	2596
2	2	3	- 140	- 182	-	-
2	2	-3	562	584	564	496
-2	2	3	- 558	- 538	- 630	- 568
-2	2	-3	602	554	606	596
2	2	4	474	486	558	532
2	2	-4	1318	1240	1182	1264
-2	2	-4	942	834	990	868
2	2	5	160	122	-	-
-2	2	5	434	432	450	460
-2	2	-5	736	746	810	854
2	2	-6	826	826	864	884
-2	2	6	376	432	468	472
2	2	-7	152	180	-	-
2	2	-8	416	392	510	520
-2	2	8	-	-	336	334
2	3	0	1208	1196	1074	1164
-2	3	0	460	540	444	506
2	3	-1	1060	1056	948	894
-2	3	1	1128	1206	1038	1148
-2	3	-1	2496	2390	2226	2286
2	3	2	146	174	-	-
2	3	-2	- 270	- 214	- 306	- 214
-2	3	2	- 196	- 166	- 342	- 160
-2	3	-2	1270	1232	1128	1234
2	3	3	392	446	390	440
2	3	-3	938	922	906	856
-2	3	3	270	226	288	274
-2	3	-3	1522	1468	1368	1464
2	3	-4	1128	1206	1116	1102
-2	3	4	- 176	- 204	- 324	- 246
2	3	-5	276	294	330	356
-2	3	5	362	394	396	404
-2	3	-5	318	320	282	330
2	3	-6	466	406	414	400
2	3	-7	614	648	654	726
-2	3	-7	176	114	-	-

2	3	-8	238	208	-	-
2	4	0	- 188	- 256	- 216	- 226
-2	4	0	1300	1518	1368	1314
2	4	1	628	620	624	518
2	4	-1	1086	990	888	922
-2	4	1	1130	1254	1206	1176
-2	4	-1	602	596	510	570
2	4	2	352	382	318	358
2	4	-2	778	768	654	612
-2	4	2	238	206	156	182
-2	4	-2	1248	1176	1134	1044
2	4	-3	326	358	342	360
-2	4	-3	590	566	558	518
2	4	-4	294	306	282	292
-2	4	4	332	336	396	294
2	4	-5	1142	1034	1110	938
-2	4	-5	- 156	- 116	-	-
2	4	-6	156	176	-	-
-2	4	-6	126	178	-	-
2	4	-7	282	272	-	-
2	4	-8	200	258	-	-
2	5	0	460	452	444	348
-2	5	0	1138	630	924	566
2	5	1	364	316	246	282
-2	5	1	348	316	234	266
-2	5	-1	700	716	552	546
2	5	-2	580	592	528	536
-2	5	2	628	636	576	516
-2	5	-2	84	110	-	-
2	5	-3	610	660	558	534
-2	5	3	408	418	270	366
2	5	-4	418	394	396	398
-2	5	-4	276	266	222	208
2	5	-5	348	350	336	290
-2	5	-5	- 162	- 194	-	-
2	5	-6	562	548	492	484
-2	5	-6	198	90	-	-
2	5	-7	186	150	-	-
-2	5	-7	246	216	-	-
2	6	0	330	274	180	224
-2	6	0	132	106	234	88
2	6	1	138	110	-	-
2	6	-1	294	286	222	226
-2	6	1	572	554	408	380
-2	6	-1	224	332	222	266
2	6	-2	300	282	240	234
-2	6	2	416	438	336	386

-2	6	-2	80	74	-	-
2	6	-3	370	426	300	342
-2	6	3	202	208	180	154
-2	6	-3	- 138	- 150	- 114	- 158
2	6	-4	490	472	366	364
-2	6	-4	- 126	- 56	-	-
2	6	-5	166	150	204	144
-2	6	-5	334	298	150	238
2	6	-6	266	230	186	174
-2	6	-6	-	-	210	98
2	6	-7	132	154	132	118
-2	7	0	162	164	108	88
2	7	-1	156	206	144	142
-2	7	1	150	192	150	152
2	7	-2	284	230	174	166
-2	7	-2	66	28	-	-
2	7	-3	272	220	174	170
-2	7	-3	78	88	-	-
2	7	-4	240	248	156	152
-2	7	-4	100	78	-	-
2	7	-5	156	142	108	104
-2	7	-5	206	186	-	-
3	0	0	-1440	-1398	-1566	-1482
3	0	1	- 472	- 448	- 630	- 476
-3	0	1	- 762	- 726	- 870	- 816
3	0	2	576	554	684	624
-3	0	2	- 266	- 262	- 264	- 278
3	0	3	782	768	1002	900
-3	0	3	596	570	672	650
3	0	4	540	612	750	718
-3	0	4	1534	1496	1584	1614
3	0	5	502	520	618	702
-3	0	5	1520	1556	1632	1612
-3	0	6	682	696	810	798
-3	0	7	484	500	570	616
3	0	-8	-	-	390	282
3	1	0	- 952	- 850	-1026	- 930
-3	1	0	- 682	- 682	- 714	- 738
3	1	1	- 206	- 194	-	-
3	1	-1	- 118	- 120	-	-
-3	1	1	- 770	- 736	- 756	- 716
-3	1	-1	496	498	480	486
3	1	2	- 358	- 338	- 432	- 412
3	1	-2	1122	1172	1188	1180
-3	1	2	-1398	-1344	-1482	-1376
-3	1	-2	1316	1274	1398	1422
3	1	3	218	250	354	300

3	1	-3	2332	2328	2400	2338
-3	1	3	- 212	- 228	- 288	- 216
-3	1	-3	1254	1270	1494	1482
3	1	4	382	376	474	476
3	1	-4	1404	1376	1530	1470
-3	1	4	596	598	630	596
-3	1	-4	676	692	786	822
3	1	5	370	390	462	522
3	1	-5	1378	1388	1518	1488
-3	1	5	952	450	1080	566
-3	1	-5	420	458	492	536
3	1	-6	914	934	1050	1018
-3	1	6	608	628	630	690
-3	1	-6	174	198	-	-
3	1	-7	162	198	-	-
-3	1	7	538	550	624	622
3	1	-8	156	34	-	-
3	2	0	306	356	192	306
-3	2	0	1434	1308	1596	1384
3	2	1	- 288	- 236	- 342	- 302
3	2	-1	678	702	690	712
-3	2	1	- 562	- 520	- 594	- 602
-3	2	-1	1760	1652	1758	1702
3	2	-2	-	-	2448	2404
-3	2	2	-	-	-1116	-1016
-3	2	-2	1370	1272	1398	1346
3	2	3	-	-	- 324	- 304
3	2	-3	2016	1844	1866	1836
-3	2	3	- 160	- 200	- 258	- 226
-3	2	-3	1300	1242	1314	1354
3	2	4	204	216	378	262
3	2	-4	1920	1816	1698	1792
-3	2	4	- 146	- 110	-	-
-3	2	-4	864	820	906	978
3	2	-5	602	568	648	674
3	2	-6	498	512	540	510
-3	2	6	448	482	516	564
-3	2	7	498	404	342	478
3	2	-8	166	150	-	-
3	3	0	1412	1424	1278	1422
-3	3	0	1718	1732	1590	1664
3	3	-1	1312	1288	1182	1154
-3	3	1	460	516	468	462
-3	3	-1	1608	1474	1536	1510
3	3	2	- 160	- 128	-	-
3	3	-2	956	992	906	1010
-3	3	2	508	508	522	480

-3	3	-2	1742	1656	1608	1676
3	3	3	170	132	-	-
3	3	-3	1698	1604	1458	1588
-3	3	3	- 496	- 522	- 540	- 528
-3	3	-3	312	320	318	322
3	3	-4	1344	1310	1254	1266
-3	3	4	- 184	- 80	-	-
-3	3	-4	324	346	246	334
3	3	-5	- 116	- 42	-	-
-3	3	-5	-	-	150	92
-3	3	6	214	216	378	108
3	3	-6	-	-	252	256
3	3	-7	264	300	306	306
-3	4	0	904	902	780	790
3	4	1	684	648	606	626
3	4	-1	1720	1606	1542	1542
-3	4	1	1060	1068	972	1004
-3	4	-1	1676	1532	1446	1456
3	4	2	376	366	402	332
3	4	-2	1224	1064	1044	918
-3	4	2	708	584	726	528
-3	4	-2	622	546	558	548
3	4	-3	338	354	372	356
-3	4	3	220	198	-	-
-3	4	-3	206	182	168	174
3	4	-4	- 206	- 152	-	-
-3	4	4	- 276	- 280	-	-
-3	4	-4	- 106	- 122	-	-
3	4	-5	942	968	864	896
3	4	-6	- 358	- 378	- 408	- 364
3	4	-7	- 138	- 40	-	-
3	4	-8	250	254	324	286
3	5	0	730	704	630	620
-3	5	0	736	682	594	620
3	5	1	586	526	504	480
3	5	-1	172	178	228	174
-3	5	1	1390	1406	1170	1222
3	5	-2	370	378	360	362
-3	5	2	144	142	-	-
3	5	-3	508	574	480	502
-3	5	3	294	322	318	254
-3	5	-3	376	414	330	364
-3	5	4	298	302	258	284
-3	5	-4	- 310	- 308	- 264	- 304
3	5	-5	- 412	- 362	- 354	- 242
3	5	-6	526	520	498	452
-3	5	-6	334	288	-	-

3	5	-7	204	196	198	166
3	6	0	456	402	342	348
-3	6	0	582	562	426	478
3	6	-1	150	114	-	-
-3	6	1	- 104	- 158	- 228	- 148
-3	6	-1	224	218	-	-
3	6	-2	300	242	162	236
-3	6	2	618	598	468	484
-3	6	-2	- 156	- 126	-	-
3	6	-3	- 156	- 152	- 174	- 122
-3	6	3	490	434	324	352
-3	6	-3	- 282	- 280	- 204	- 242
3	6	-4	352	346	240	290
-3	6	-4	594	578	408	478
3	6	-6	232	206	144	170
-3	6	-6	138	132	174	102
3	6	-7	162	148	138	114
3	6	-8	398	334	306	280
-3	7	1	222	212	168	148
3	7	-2	- 128	- 84	-	-
-3	7	2	272	264	246	200
-3	7	-2	262	246	150	170
3	7	-3	156	84	-	-
-3	7	-3	100	58	-	-
3	7	-4	134	116	-	-
-3	7	-4	100	46	-	-
3	7	-5	272	228	174	148
-3	7	-5	334	306	-	-
3	7	-7	-	-	258	210
4	0	0	- 458	- 474	- 534	- 608
4	0	1	1068	1036	1218	1148
-4	0	1	-1286	-1208	-1404	-1296
4	0	2	210	226	306	276
-4	0	2	1080	1062	1146	1118
4	0	3	148	232	432	302
-4	0	3	1322	1312	1458	1350
4	0	4	452	490	636	620
-4	0	4	260	308	270	320
4	0	5	322	308	414	414
-4	0	5	1160	1180	1248	1308
-4	0	6	1366	1382	1548	1632
4	1	0	596	566	612	562
-4	1	0	-1084	- 996	-1164	- 988
4	1	1	- 488	- 248	- 552	- 338
4	1	-1	- 432	- 382	- 462	- 470
-4	1	1	2646	2580	2688	2646
-4	1	-1	188	238	-	-

4	1	2	376	350	456	462
4	1	-2	1442	1446	1554	1468
-4	1	2	-1322	-1232	-1410	-1360
-4	1	-2	996	948	1050	1068
4	1	3	150	52	-	-
4	1	-3	1022	1060	1122	1134
-4	1	3	- 538	- 494	- 570	- 546
-4	1	-3	996	1010	1080	1256
4	1	4	444	452	522	576
4	1	-4	2250	2204	2334	2412
-4	1	4	720	750	798	842
-4	1	-4	- 344	- 300	- 396	- 416
4	1	-5	532	572	660	662
-4	1	5	1530	1494	1692	1666
-4	1	-5	358	376	420	484
4	1	-6	796	824	900	924
-4	1	6	- 232	- 202	-	-
4	1	-7	218	150	-	-
-4	1	7	664	678	768	834
-4	1	8	-	-	534	538
4	2	0	594	618	600	610
-4	2	0	2240	2078	2130	2150
4	2	1	- 128	- 90	-	-
4	2	-1	1056	1098	1122	1072
-4	2	1	- 928	- 870	- 936	- 878
-4	2	-1	908	882	978	966
4	2	2	-	-	- 270	- 268
4	2	-2	454	478	540	556
-4	2	-2	146	184	-	-
-4	2	2	-	-	- 396	- 328
4	2	3	312	366	432	394
4	2	-3	2182	2044	2064	2142
-4	2	3	716	684	708	714
-4	2	-3	480	456	396	486
4	2	-4	1478	1436	1494	1488
-4	2	4	198	260	-	-
-4	2	-4	742	716	750	868
4	2	-5	672	580	744	722
-4	2	5	- 230	- 204	- 318	- 208
-4	2	-5	- 218	- 198	-	-
4	2	-6	128	40	-	-
-4	2	6	710	674	834	786
4	2	-7	312	322	264	386
-4	2	7	460	448	486	526
-4	3	0	864	810	810	820
4	3	1	404	414	396	368
4	3	-1	1496	688	1362	738

-4	3	1	356	396	366	346
-4	3	-1	662	610	612	658
4	3	2	264	252	240	234
4	3	-2	1416	1416	1290	1384
-4	3	2	1006	988	990	986
-4	3	-2	920	864	864	890
4	3	-3	730	666	678	762
-4	3	3	- 312	- 92	- 282	- 118
-4	3	-3	- 170	- 132	-	-
4	3	-4	440	384	378	456
-4	3	-4	214	224	-	-
4	3	-5	822	1238	768	1190
-4	3	-5	232	206	276	226
4	3	-6	- 404	- 424	- 216	- 342
-4	3	6	306	286	288	318
4	3	-7	- 140	- 132	- 276	- 148
4	3	-8	140	162	-	-
4	3	-9	154	204	-	-
4	4	0	828	788	804	766
-4	4	0	-	-	390	140
4	4	1	408	408	444	418
4	4	-1	352	342	240	346
-4	4	1	892	746	816	676
-4	4	-1	796	696	660	630
4	4	-2	992	916	930	948
-4	4	2	470	486	432	458
-4	4	-2	118	114	204	140
4	4	-3	634	584	552	546
-4	4	3	376	372	366	328
-4	4	-3	282	266	288	258
4	4	-5	- 382	- 338	- 366	- 334
-4	4	5	244	266	-	-
-4	4	-5	358	318	384	368
4	4	-6	320	306	240	280
4	5	0	478	474	366	456
-4	5	0	352	374	318	288
4	5	-1	436	400	372	390
-4	5	1	610	590	534	558
-4	5	-1	- 106	- 110	-	-
4	5	-2	186	196	264	186
-4	5	2	238	170	240	124
-4	5	-2	222	222	198	182
-4	5	3	276	258	204	222
-4	5	-3	360	344	324	334
-4	5	4	360	348	-	-
-4	5	-4	132	114	-	-
4	5	-5	- 172	- 218	- 174	- 130

-4	5	-5	250	204	252	200
4	5	-6	172	110	-	-
4	5	-7	316	264	258	234
4	5	-8	304	272	-	-
-4	6	0	364	292	246	270
4	6	-1	266	192	156	166
-4	6	-1	166	178	-	-
-4	6	2	272	266	222	186
4	6	-3	- 156	- 58	- 126	- 28
-4	6	3	294	272	204	240
-4	6	-3	220	188	-	-
-4	6	-4	386	406	306	350
4	6	-5	184	136	84	102
-4	6	-5	138	108	-	-
4	6	-6	126	106	-	-
4	6	-7	322	310	252	250
-4	7	0	- 128	- 46	-	-
-4	7	1	134	146	-	-
-4	7	-1	212	226	150	160
-4	7	-2	256	238	138	184
-4	7	-3	-	-	138	80
-4	7	-4	188	152	-	-
4	7	-5	212	228	150	124
4	7	-6	162	184	162	156
5	0	0	650	702	876	824
5	0	1	676	738	924	856
-5	0	1	626	662	834	752
5	0	2	322	314	360	384
-5	0	2	936	964	1062	994
5	0	3	166	146	-	-
-5	0	3	738	790	906	794
-5	0	4	316	282	330	406
-5	0	5	434	424	576	530
-5	0	6	508	516	810	588
5	1	0	790	798	876	876
-5	1	0	608	646	684	708
5	1	1	414	416	438	472
5	1	-1	500	538	588	570
-5	1	1	908	898	942	978
-5	1	-1	450	462	558	574
5	1	2	444	460	576	580
5	1	-2	764	758	870	846
-5	1	2	1034	1028	1056	1116
-5	1	-2	282	280	-	-
5	1	3	174	158	-	-
5	1	-3	464	466	528	528
-5	1	3	620	590	702	670

5	1	-4	732	754	822	810
-5	1	4	588	586	660	620
5	1	-5	162	212	-	-
-5	1	5	450	480	474	486
5	1	-6	306	306	396	408
-5	1	6	268	264	-	-
5	1	-7	268	222	-	-
-5	1	7	144	162	-	-
5	1	-8	232	154	-	-
5	2	0	122	710	756	792
-5	2	0	346	316	354	344
5	2	1	332	338	378	388
5	2	-1	508	500	534	490
-5	2	1	1190	1110	1212	1256
5	2	2	178	158	-	-
-5	2	2	628	618	672	628
-5	2	-2	166	94	-	-
5	2	3	780	782	900	910
-5	2	3	684	668	726	726
5	2	-4	498	482	588	564
-5	2	4	658	666	702	672
5	2	-5	178	196	342	242
-5	2	5	524	480	630	592
5	2	-6	146	70	-	-
5	2	-7	320	344	300	368
-5	2	7	192	228	408	284
5	3	0	- 154	- 158	- 264	- 166
-5	3	0	264	356	480	416
5	3	1	330	316	336	352
5	3	-1	932	938	912	1044
-5	3	1	300	312	312	284
-5	3	-1	170	164	198	122
5	3	2	288	352	324	382
5	3	-2	454	472	468	446
-5	3	2	362	254	420	292
-5	3	-2	- 288	- 232	- 258	- 288
5	3	-3	-	-	228	118
-5	3	3	902	924	882	906
-5	3	-3	244	166	-	-
5	3	-4	-	-	390	236
-5	3	4	416	378	408	428
-5	3	-4	300	294	294	388
5	3	-5	858	810	810	814
-5	3	5	306	348	318	358
5	3	-6	- 214	- 228	-	-
-5	3	6	208	226	-	-
5	3	-7	-	-	390	158

5	3	-8	288	366	372	400
5	4	0	484	448	336	458
-5	4	0	262	236	258	208
5	4	1	370	314	336	330
5	4	-1	- 262	- 208	-	-
-5	4	-1	- 188	- 170	-	-
5	4	-2	452	448	432	506
-5	4	2	438	400	318	402
-5	4	-2	270	276	312	264
5	4	-3	476	480	444	460
-5	4	3	276	276	-	-
-5	4	4	470	490	462	518
-5	4	-4	396	388	366	438
5	4	-5	- 300	- 308	- 348	- 192
5	4	-6	840	760	774	688
5	4	-7	132	102	-	-
5	4	-8	220	110	-	-
-5	5	0	- 246	- 246	- 234	- 284
5	5	-1	166	180	-	-
-5	5	-1	282	298	210	274
-5	5	2	288	358	270	310
-5	5	-2	364	376	318	372
5	5	-3	- 138	- 68	-	-
-5	5	-3	232	214	216	234
5	5	-4	400	418	372	372
-5	5	-4	334	268	228	250
5	5	-7	352	354	264	310
5	5	-8	370	396	-	-
-5	6	0	156	146	120	138
-5	6	1	380	380	318	324
-5	6	-1	126	100	-	-
-5	6	2	- 370	- 382	- 270	- 340
-5	6	-2	242	188	-	-
5	6	-3	150	168	-	-
-5	6	-3	600	620	456	570
5	6	-4	162	52	-	-
-5	6	-4	214	34	-	-
5	6	-5	300	336	156	258
5	6	-7	416	374	252	324
-5	7	0	272	250	204	198
-5	7	1	- 122	- 144	-	-
-5	7	-1	362	360	264	280
-5	7	-2	200	194	162	136
6	0	0	1186	1256	1404	1556
6	0	1	-	-	408	290
-6	0	1	688	694	834	824
6	0	2	260	272	372	364

-6	0	2	850	152	1032	162
-6	0	3	452	314	618	430
-6	0	4	670	630	792	742
-6	0	5	- 466	- 514	- 564	- 568
-6	0	7	-	-	366	270
6	1	0	670	696	744	852
-6	1	0	376	426	522	476
6	1	1	588	578	720	806
6	1	-1	858	908	1062	1080
-6	1	1	238	222	336	378
-6	1	-1	620	622	672	736
6	1	-2	- 188	- 96	-	-
-6	1	2	1974	1156	2178	1320
6	1	-3	546	544	660	620
-6	1	3	858	824	978	924
-6	1	-3	- 300	- 294	- 426	- 456
6	1	-4	- 226	- 214	- 300	- 210
6	1	-5	124	32	-	-
-6	1	5	218	212	-	-
-6	1	6	602	544	588	678
6	1	-7	332	430	528	518
-6	1	7	- 394	- 442	- 528	- 524
-6	2	0	- 212	- 160	-	-
6	2	1	448	426	420	504
6	2	-1	704	664	798	800
-6	2	1	1736	1722	1848	1902
-6	2	-1	- 236	- 254	- 336	- 364
6	2	-2	-	-	294	242
-6	2	2	-	-	318	238
6	2	-3	- 460	- 484	- 504	- 446
-6	2	3	684	664	750	770
-6	2	-3	346	362	390	454
-6	2	4	966	998	1092	1160
6	2	-5	466	484	582	520
-6	2	5	748	718	804	798
-6	2	6	- 422	- 412	- 462	- 470
6	2	-7	198	250	384	302
-6	2	7	274	244	-	-
6	2	-8	524	524	390	616
6	3	0	380	366	384	406
-6	3	0	270	246	318	234
6	3	-1	- 318	- 338	- 348	- 358
-6	3	1	- 196	- 224	- 258	- 220
-6	3	-1	134	84	-	-
6	3	-2	306	240	270	316
-6	3	2	330	336	342	342
-6	3	-2	- 220	- 234	-	-
-6	3	3	1054	1046	1050	1170

-6	3	-3	170	152	-	-
6	3	-4	- 128	- 22	240	50
-6	3	4	496	474	504	512
-6	3	5	238	302	366	356
6	3	-6	846	852	762	888
-6	3	6	368	366	390	412
6	3	-7	276	226	468	300
6	3	-8	318	300	366	336
-6	4	1	- 226	- 226	- 276	- 266
-6	4	2	370	316	342	332
-6	4	-2	358	368	360	388
6	4	-3	182	148	-	-
-6	4	3	194	116	-	-
-6	4	-3	132	118	-	-
6	4	-4	364	366	414	344
-6	4	4	502	466	432	482
6	4	-5	352	258	336	334
-6	4	5	250	250	270	278
6	4	-6	408	380	414	332
6	4	-7	540	520	528	524
6	4	-8	276	278	-	-
-6	5	0	- 162	- 128	- 150	- 110
-6	5	1	132	58	-	-
-6	5	-1	342	340	216	288
6	5	-2	156	48	-	-
-6	5	-2	222	280	318	316
6	5	-3	246	164	-	-
-6	5	-3	246	272	288	276
6	5	-4	250	312	234	262
6	5	-5	484	442	408	400
6	5	-6	264	204	216	246
6	5	-7	390	364	240	332
-6	6	0	-	-	180	150
-6	6	1	242	198	198	186
-6	6	-1	138	150	-	-
-6	6	2	- 144	- 116	-	-
-6	6	-2	272	274	-	-
7	0	0	458	516	618	660
7	0	1	210	202	342	272
-7	0	1	534	504	654	688
-7	0	2	440	458	690	666
-7	0	3	348	338	510	456
-7	0	4	260	242	342	272
-7	0	5	- 204	- 166	-	-
-7	0	7	266	202	-	-
7	1	0	370	412	546	580
-7	1	0	294	312	480	438

7	1	1	294	320	456	458
7	1	-1	382	418	546	558
-7	1	1	364	420	420	530
-7	1	-1	232	212	-	-
-7	1	2	640	648	726	814
7	1	-3	200	222	378	334
-7	1	3	558	588	720	734
7	1	-4	- 124	- 104	-	-
-7	1	4	238	238	414	424
7	1	-5	144	64	-	-
-7	1	5	180	130	-	-
-7	1	6	144	124	-	-
7	1	-7	288	334	486	390
7	1	-8	-	-	348	304
-7	2	0	178	136	-	-
7	2	-1	466	468	558	620
-7	2	1	198	214	-	-
-7	2	-1	152	118	-	-
-7	2	2	692	654	786	814
-7	2	-2	184	168	-	-
7	2	-3	- 300	- 266	- 342	- 258
-7	2	3	396	422	498	546
-7	2	4	440	434	576	536
7	2	-5	428	416	402	432
-7	2	5	242	314	372	362
7	2	-6	192	124	-	-
-7	2	6	198	178	-	-
7	2	-7	288	326	300	488
-7	2	7	- 184	- 48	-	-
7	2	-8	498	518	432	624
-7	3	0	146	100	-	-
7	3	-1	- 250	- 328	- 324	- 354
-7	3	1	356	312	306	384
-7	3	-1	128	24	-	-
7	3	-2	250	250	192	306
-7	3	2	154	132	-	-
-7	3	-2	134	196	-	-
7	3	-3	208	174	-	-
-7	3	3	270	270	354	358
-7	3	4	484	508	492	544
-7	3	5	324	306	396	424
7	3	-6	894	944	912	986
7	3	-7	264	248	264	276
7	3	-8	140	220	324	326
-7	4	1	144	150	-	-
-7	4	-1	314	326	312	334
7	4	-2	- 144	- 104	-	-

-7	4	-2	226	84	-	-
-7	4	3	338	322	300	322
7	4	-4	514	524	474	530
7	4	-5	432	342	306	338
-7	4	5	200	274	-	-
7	4	-6	232	188	-	-
7	4	-7	590	554	558	580
-7	5	0	352	340	180	342
-7	5	-2	190	204	288	220
-7	5	3	166	118	-	-
-7	5	4	180	126	-	-
-7	6	1	184	126	-	-
-8	0	1	304	348	468	494
-8	0	3	416	372	528	496
-8	0	5	390	394	570	528
-8	0	7	334	332	420	406
-8	1	0	344	392	462	522
8	1	-1	206	298	396	426
8	1	-2	232	264	420	348
-8	1	2	- 174	- 52	-	-
8	1	-3	- 138	- 142	-	-
-8	1	3	206	344	426	510
8	1	-4	226	344	510	426
-8	1	4	414	364	468	474
8	1	-5	300	364	378	420
8	1	-6	144	156	-	-
-8	1	6	206	164	-	-
8	1	-7	162	178	-	-
-8	1	7	294	366	480	492
-8	2	1	- 152	- 182	-	-
-8	2	-1	320	326	468	432
8	2	-2	346	362	420	506
-8	2	2	704	738	786	896
8	2	-3	224	252	306	276
8	2	-4	140	86	-	-
8	2	-5	166	132	-	-
-8	2	5	178	226	-	-
8	2	-6	634	686	786	780
-8	2	6	448	432	390	552
-8	3	0	226	158	-	-
-8	3	1	520	600	636	704
-8	3	-1	214	70	-	-
-8	3	2	- 190	- 184	- 252	- 198
8	3	-3	196	258	228	308
8	3	-4	324	340	402	372
-8	3	4	356	322	-	-
8	3	-5	288	248	588	334

-8	3	5	184	160	-	-
8	3	-6	244	190	-	-
-8	4	0	276	270	-	-
-8	4	1	174	134	-	-
-8	4	2	150	118	-	-
-8	4	3	320	292	354	352
-8	4	4	- 156	- 22	-	-
-8	5	2	-	-	270	266
9	0	-3	-	-	408	244
9	0	-4	-	-	348	272
9	0	-5	-	-	420	440
9	1	-4	-	-	462	514
9	1	-5	-	-	420	480
-9	3	2	244	254	276	352

Table B

$SiCl_4, 2Py$

Observed and calculated structure factors

H	K	L	(F_o)	(F_c)	H	K	L	(F_o)	(F_c)
0	0	-1	2644	3114	0	0	-2	-3988	-4844
0	0	-4	284	194	0	0	-5	- 622	- 536
0	0	-6	1088	1012	0	0	-7	1564	1452
0	0	-8	346	322	0	-1	-1	816	946
0	-1	2	2030	2048	0	-1	-2	358	332
0	-1	3	- 852	- 810	0	-1	-3	916	1108
0	-1	4	1046	794	0	-1	-4	- 318	- 290
0	-1	5	1156	1064	0	-1	-5	- 860	- 942
0	-1	6	420	220	0	-1	-6	842	1030
0	-1	7	870	774	0	-1	-7	1050	1464
0	-1	8	450	446	0	-2	0	- 166	- 50
0	-2	1	1078	958	0	-2	2	-4150	-4840
0	-2	-2	3372	3444	0	-2	3	- 898	- 800
0	-2	-3	2006	2062	0	-2	4	4888	5808
0	-2	-4	- 554	- 562	0	-2	5	2704	2716
0	-2	-5	- 308	- 114	0	-2	6	- 748	- 746
0	-2	-6	392	364	0	-2	7	- 328	- 190
0	-2	8	240	216	0	-3	0	-1622	-1474
0	-3	-1	136	214	0	-3	2	254	316
0	-3	-2	3334	3476	0	-3	-3	2366	2406
0	-3	4	922	888	0	-3	-4	- 750	- 736
0	-3	5	2582	2772	0	-3	-5	- 730	- 702
0	-3	6	1140	1168	0	-3	-6	354	294
0	-3	7	- 886	- 920	0	-3	9	550	472
0	-4	0	-1682	-1594	0	-4	-1	1314	1360
0	-4	2	3418	3472	0	-4	-2	1218	1182
0	-4	3	1198	1108	0	-4	-3	- 564	- 522
0	-4	4	140	240	0	-4	-4	454	422
0	-4	5	1064	1134	0	-4	-5	916	922
0	-4	6	- 786	- 738	0	-4	7	- 840	- 920
0	-4	8	1036	998	0	-4	9	998	1074
0	-5	0	-1494	-1456	0	-5	1	1470	1424
0	-5	-1	- 978	-1032	0	-5	2	3640	3580
0	-5	-2	238	286	0	-5	3	2138	2106
0	-5	-3	244	252	0	-5	4	- 378	- 324
0	-5	-4	796	798	0	-5	5	- 624	- 568
0	-5	6	298	202	0	-5	8	- 308	- 82
0	-5	9	1076	1112	0	-6	0	760	714
0	-6	1	-1098	-1046	0	-6	-1	978	952
0	-6	2	1310	1236	0	-6	-2	- 486	- 558
0	-6	3	2680	2614	0	-6	4	- 618	- 580
0	-6	5	-1112	-1054	0	-6	6	1122	1024
0	-6	7	830	780	0	-6	9	352	530
0	-7	0	1484	1454	0	-7	1	992	1012
0	-7	-1	778	804	0	-7	2	320	328
0	-7	3	- 594	- 624	0	-7	4	- 868	- 816

0	-7	6	1132	1132
0	-7	8	334	474
0	-8	1	892	838
0	-8	3	382	254
0	-8	5	- 850	- 862
0	-8	7	1800	1736
0	-9	5	1048	1056
-1	0	1	3246	2674
-1	0	2	3378	3736
-1	0	3	1882	1788
-1	0	4	- 774	- 646
-1	0	5	-1284	-1168
-1	0	6	480	546
-1	0	7	1330	1228
-1	0	8	332	250
-1	-1	0	4062	6174
-1	1	-1	2782	2662
1	-1	-2	3978	4154
-1	-1	2	-3994	-4834
1	-1	-3	2666	2562
-1	-1	3	814	812
1	-1	-4	-2100	-1974
-1	-1	4	2136	2064
1	-1	-5	-1188	-1152
-1	-1	5	- 360	- 368
1	-1	-6	1036	956
-1	-1	6	932	910
1	-1	-7	596	538
-1	-1	-7	750	684
1	-2	0	-2164	-2400
1	-2	1	414	582
1	-2	2	3364	3722
-1	-2	2	-3106	-3498
1	-2	3	838	780
-1	-2	3	-1768	-1812
1	-2	4	820	898
-1	-2	-4	- 646	- 604
1	-2	-5	608	106
-1	-2	-5	-1378	-1386
1	-2	-6	464	622
-1	-2	-6	592	574
-1	-2	7	1052	980
-1	-2	8	466	356
-1	-3	0	618	580
1	-3	-1	- 422	- 344
-1	-3	-1	740	752
1	-3	-2	2766	2674

0	-7	7	1572	1528
0	-8	0	1364	1368
0	-8	2	- 620	- 588
0	-8	4	350	438
0	-8	6	484	408
0	-9	4	854	824
0	-9	6	364	372
-1	0	-1	788	1048
-1	0	-2	-3006	-3392
-1	0	-3	-1446	-1502
-1	0	-4	1974	2338
-1	0	-5	1090	1460
-1	0	-6	386	336
-1	0	-7	704	866
1	-1	0	4162	4550
1	-1	-1	610	588
-1	-1	-1	848	926
-1	1	-2	-4454	-4888
-1	-1	-2	- 554	- 598
-1	1	-3	-1976	-1820
-1	-1	-3	850	860
-1	1	-4	2544	2542
-1	-1	-4	492	438
-1	1	-5	2006	1928
-1	-1	-5	- 250	- 38
-1	1	-6	438	306
-1	-1	-6	518	560
-1	-1	7	1744	1690
-1	1	-8	262	228
-1	-2	0	3994	4940
-1	-2	-1	2046	2088
1	-2	-2	2112	2616
-1	-2	-2	750	778
1	-2	-3	1270	1550
-1	-2	-3	1416	1390
-1	-2	4	872	924
1	-2	5	2016	2060
-1	-2	5	1636	1692
1	-2	6	- 540	- 252
-1	-2	6	1172	1156
1	-2	7	-1040	-1066
1	-2	8	580	416
1	-3	0	-4942	-4924
1	-3	1	154	198
-1	-3	1	2126	2094
1	-3	2	4050	4160
-1	-3	2	- 616	- 616

-1	-3	-2	1918	1936
1	-3	-3	854	812
-1	-3	-3	602	544
1	-3	-4	996	882
-1	-3	-4	- 678	- 712
1	-3	-5	1382	1348
1	-3	6	- 784	- 744
1	-3	7	-1192	-1190
-1	-3	8	784	766
1	-4	0	- 992	- 854
1	-4	1	- 356	- 350
-1	-4	1	798	736
1	-4	2	2758	2678
-1	-4	2	802	756
1	-4	3	2690	2648
-1	-4	3	918	890
1	-4	4	- 714	- 650
-1	-4	4	2462	2446
1	-4	-5	904	862
1	-4	6	1222	1156
-1	-4	7	-1194	-1190
-1	-4	9	690	688
-1	-5	0	-1610	-1594
1	-5	-1	1504	1488
-1	-5	-1	844	820
1	-5	-2	-1314	-1246
-1	-5	-2	1342	1304
1	-5	-3	- 870	- 828
-1	-5	-3	624	528
1	-5	-4	1028	1052
1	-5	5	-1300	-1186
1	-5	6	924	930
1	-5	7	968	978
1	-5	8	726	782
1	-5	9	720	712
1	-6	0	1538	1538
1	-6	1	1566	1544
-1	-6	1	868	852
1	-6	2	1026	966
-1	-6	2	2166	2076
1	-6	3	880	802
-1	-6	3	622	536
-1	-6	4	- 642	- 576
1	-6	6	550	580
1	-6	7	1726	1794
1	-6	8	442	386
1	-6	9	- 358	- 160
1	-3	3	1988	1788
-1	-3	3	-1692	-1584
1	-3	4	2292	2108
-1	-3	4	2404	2524
1	-3	5	1682	1706
-1	-3	5	2000	2098
-1	-3	6	- 764	- 708
1	-3	8	286	232
-1	-3	9	- 338	- 174
-1	-4	0	-1490	-1506
1	-4	-1	580	524
-1	-4	-1	- 922	-1020
1	-4	-2	946	888
-1	-4	-2	2022	2028
1	-4	-3	470	452
-1	-4	-3	1678	1630
1	-4	-4	636	766
1	-4	5	- 368	- 348
-1	-4	5	1942	1962
-1	-4	6	- 382	- 302
1	-4	9	928	904
1	-5	0	1578	1506
1	-5	1	582	526
-1	-5	1	-1016	-1076
1	-5	2	2800	2734
-1	-5	2	2190	2002
1	-5	3	1732	1606
-1	-5	3	1532	1482
1	-5	4	-2094	-2038
-1	-5	4	502	472
-1	-5	5	1600	1556
-1	-5	6	324	316
-1	-5	7	-1078	-1158
-1	-5	8	232	210
-1	-5	9	924	922
-1	-6	0	- 452	- 428
1	-6	-1	212	258
-1	-6	-1	466	376
1	-6	-2	- 862	- 904
-1	-6	-2	222	264
1	-6	-3	- 364	- 398
1	-6	4	- 194	- 296
1	-6	5	-1252	-1234
-1	-6	6	308	308
-1	-6	7	196	128
-1	-6	8	446	456
1	-7	0	1940	1874

-1	-7	0	564	576
1	-7	-1	338	284
1	-7	2	-1404	-1318
-1	-7	2	1466	1384
-1	-7	3	1942	1746
-1	-7	4	- 824	- 812
1	-7	6	1054	1014
1	-7	7	1320	1342
-1	-7	8	272	238
1	-8	1	234	272
1	-8	2	- 920	- 928
1	-8	3	- 888	- 896
1	-8	4	746	756
1	-8	5	1476	1504
1	-8	6	726	756
1	-8	7	518	580
1	-9	2	- 344	- 330
1	-9	4	1284	1192
1	-9	6	- 360	- 254
-2	0	1	568	576
-2	0	2	3726	4034
-2	0	3	2740	2680
-2	0	4	-1522	-1500
-2	0	5	-1014	- 948
-2	0	6	1402	1328
-2	0	8	- 276	- 180
-2	-1	0	4284	4890
-2	1	-1	506	584
-2	-1	-1	3044	3104
-2	1	-2	298	330
-2	-1	-2	-2244	-2280
-2	1	-3	- 474	- 450
-2	-1	-3	-1332	-1260
-2	1	-4	2130	2344
-2	-1	-4	1346	1352
-2	1	-5	2328	2666
-2	-1	-5	764	770
-2	-1	6	954	986
-2	1	-7	- 668	- 920
-2	-1	8	370	378
-2	-2	0	3300	3894
-2	-2	-1	288	358
-2	2	-2	4226	4050
2	-2	-3	1076	954
-2	-2	3	- 480	- 474
2	-2	-4	- 230	- 176
-2	-2	4	278	292

1	-7	1	274	280
-1	-7	1	532	418
1	-7	-2	- 298	- 282
1	-7	3	528	488
1	-7	4	1032	956
-1	-7	5	-1624	-1572
-1	-7	6	664	626
-1	-7	7	1076	960
1	-8	0	900	938
-1	-8	1	306	102
-1	-8	2	316	306
-1	-8	3	590	542
-1	-8	4	- 306	- 166
-1	-8	5	- 236	- 138
-1	-8	6	628	588
-1	-8	7	678	712
1	-9	3	- 488	- 444
1	-9	5	1044	966
-2	0	0	238	162
-2	0	-1	366	372
-2	0	-2	-1088	- 820
-2	0	-3	402	302
-2	0	-4	1990	1954
-2	0	-5	1416	1398
-2	0	7	708	626
-2	1	0	-3262	-2616
-2	1	1	- 204	- 44
-2	-1	1	370	374
-2	1	2	4134	4142
-2	-1	2	354	356
-2	1	3	2606	2394
-2	-1	3	1674	1680
-2	1	4	236	98
-2	-1	4	- 800	- 676
-2	1	5	436	118
-2	-1	5	-1296	-1246
-2	1	-6	- 276	- 248
-2	1	7	- 326	- 380
-2	-1	7	1560	1566
2	-2	0	-4742	-4514
2	-2	-1	498	368
2	-2	-2	4154	4010
-2	-2	-2	- 920	- 938
-2	2	-3	1924	1652
-2	-2	-3	216	126
-2	2	-4	360	316
2	-2	-5	1098	1036

-2	2	-5	832	842
-2	2	-6	252	196
-2	-2	-6	542	488
-2	2	-7	- 412	- 490
-2	2	-8	302	176
-2	-3	0	2370	2472
2	-3	-1	520	638
-2	-3	-1	818	782
2	-3	-2	- 552	- 718
2	-3	3	2462	2728
-2	-3	3	266	322
2	-3	4	- 742	- 650
-2	-3	4	2262	2404
2	-3	5	- 392	- 346
-2	-3	5	788	812
2	-3	6	298	150
-2	-3	7	952	978
-2	-3	8	446	408
2	-4	0	- 506	- 300
2	-4	1	748	630
-2	-4	1	810	786
2	-4	2	4174	4102
-2	-4	-2	1508	1514
2	-4	-3	- 442	- 428
-2	-4	-3	1170	1138
2	-4	-4	1576	1470
2	-4	5	-1310	-1222
-2	-4	5	2592	2782
-2	-4	6	232	242
-2	-4	7	- 332	- 354
-2	-4	9	- 324	- 146
-2	-5	0	- 844	- 834
2	-5	-1	1264	1168
-2	-5	-1	308	284
2	-5	-2	-1100	-1138
-2	-5	-2	1546	1550
2	-5	-3	- 482	- 326
2	-5	-4	804	856
2	-5	5	-1014	-1006
2	-5	6	1088	1030
2	-5	7	1736	1836
2	-5	8	446	406
2	-6	0	2728	2612
2	-6	1	1292	1212
-2	-6	1	324	272
2	-6	-2	- 366	- 408
2	-6	3	- 552	- 432
-2	-2	5	- 368	- 358
-2	-2	6	866	914
2	-2	-7	- 534	- 578
-2	-2	7	1770	1778
-2	-2	8	346	242
2	-3	1	420	364
-2	-3	1	300	340
2	-3	2	3502	4194
-2	-3	-2	532	534
2	-3	-3	- 346	- 418
-2	-3	-3	804	840
2	-3	-4	1036	1610
-2	-3	-4	- 386	- 310
2	-3	-5	1062	1618
-2	-3	-5	- 350	- 388
2	-3	7	- 392	- 348
2	-3	8	496	430
-2	-3	9	- 554	- 520
-2	-4	0	364	348
2	-4	-1	660	660
-2	-4	-1	334	354
2	-4	-2	- 876	- 772
2	-4	3	2598	2432
-2	-4	3	-1372	-1352
2	-4	4	-1610	-1512
-2	-4	4	1902	1986
2	-4	-5	974	1016
2	-4	6	968	916
2	-4	7	906	928
2	-4	8	346	240
2	-5	0	3054	2986
2	-5	1	686	676
-2	-5	1	332	314
2	-5	2	- 904	- 734
-2	-5	2	514	516
2	-5	3	1070	974
-2	-5	-3	476	484
-2	-5	4	1370	1468
-2	-5	5	1392	1436
-2	-5	6	- 282	- 298
-2	-5	7	- 432	- 488
-2	-5	8	426	454
-2	-6	0	- 764	- 812
2	-6	-1	634	652
2	-6	2	- 870	- 790
-2	-6	2	1598	1554
2	-6	-3	324	390

-2	-6	3	938	878
-2	-6	4	234	304
-2	-6	5	922	886
2	-6	7	1608	1646
2	-6	8	266	266
2	-6	9	- 506	- 500
-2	-7	0	- 654	- 644
2	-7	-1	650	564
2	-7	2	-1176	-1174
-2	-7	2	1554	1632
-2	-7	3	1190	1244
-2	-7	4	- 306	- 310
2	-7	6	216	20
2	-7	7	676	686
2	-8	0	- 232	- 74
2	-8	-1	- 244	- 218
2	-8	3	- 462	- 402
2	-8	4	1704	1610
2	-8	5	1850	1798
2	-8	6	250	236
2	-8	7	- 370	- 408
2	-9	3	390	456
2	-9	5	1096	1078
-3	0	0	-1746	-1574
-3	0	-1	1008	1036
-3	0	-2	958	764
-3	0	-3	- 254	- 132
-3	0	5	- 188	- 44
-3	0	6	470	420
-3	0	7	- 344	- 268
-3	-1	0	766	758
-3	1	-1	-1042	- 924
-3	-1	-1	468	492
-3	1	-2	3492	3334
-3	-1	-2	-1072	-1066
-3	1	-3	1898	1794
-3	1	4	400	410
-3	-1	4	-1854	-1796
-3	1	5	1528	1390
-3	-1	5	- 596	- 592
-3	-1	6	1250	1270
-3	1	-7	- 408	- 562
-3	2	0	- 998	- 730
-3	2	1	480	384
-3	-2	1	442	486
-3	2	2	326	268
-3	-2	2	342	760
2	-6	4	- 288	- 246
2	-6	5	234	78
2	-6	6	1426	1412
-2	-6	7	-1050	-1054
-2	-6	8	292	148
2	-7	0	1396	1358
2	-7	1	664	642
-2	-7	1	- 402	- 176
2	-7	-2	390	316
2	-7	3	- 468	- 432
2	-7	4	1734	1692
2	-7	5	1146	1096
-2	-7	6	306	210
2	-7	8	362	408
2	-8	1	634	566
2	-8	2	- 428	- 456
-2	-8	3	552	490
-2	-8	4	- 254	- 324
-2	-8	5	- 524	- 430
-2	-8	6	560	522
2	-9	1	- 412	- 256
2	-9	4	946	924
2	-9	7	- 654	- 620
-3	0	1	- 998	- 936
-3	0	2	2956	3066
-3	0	3	2790	2878
-3	0	-4	1342	1412
-3	0	-5	1652	1686
-3	0	-6	- 268	- 96
-3	1	0	-4728	-4584
-3	1	1	1394	1234
-3	-1	1	1014	1028
-3	1	2	3810	3774
-3	-1	2	3322	3350
-3	1	3	822	774
-3	-1	3	1626	1584
-3	1	-4	638	654
-3	-1	-4	1588	1578
-3	1	-5	716	794
-3	-1	-5	906	980
-3	1	7	- 870	- 810
-3	-1	7	598	568
-3	-2	0	2544	2526
-3	2	-1	1358	1202
-3	-2	-1	1424	1378
-3	2	-2	3092	3032
-3	-2	-2	-1258	-1270

-3	2	3	- 318	- 148
-3	-2	3	1788	1816
-3	2	4	2086	1714
-3	-2	-4	754	758
-3	-2	5	-1650	-1642
-3	2	6	- 510	- 356
-3	2	7	- 732	- 564
-3	-2	8	250	324
-3	-3	0	2656	2868
-3	3	-1	412	392
-3	-3	-1	436	310
-3	3	-2	4204	3788
3	-3	-3	- 858	- 784
-3	-3	3	- 160	- 180
3	-3	-4	1494	1422
-3	-3	4	556	600
3	-3	-5	1380	1240
-3	-3	5	174	52
-3	3	-6	976	916
-3	3	-7	1116	1046
-3	3	-8	504	364
3	-4	0	2592	3390
3	-4	1	984	1254
-3	-4	1	262	288
3	-4	2	220	312
-3	-4	2	-1112	-1274
3	-4	3	732	858
-3	-4	-3	360	386
-3	-4	4	1274	1450
3	-4	-5	308	554
3	-4	6	650	670
3	-4	7	1136	1304
3	-4	8	382	452
3	-5	0	2790	2632
3	-5	1	1120	1046
-3	-5	1	914	928
-3	-5	2	- 812	- 928
3	-5	-3	504	540
3	-5	-4	238	24
3	-5	-5	- 484	- 388
3	-5	6	1372	1288
-3	-5	8	276	346
-3	-6	0	- 666	- 704
3	-6	-1	804	760
3	-6	-2	274	278
3	-6	3	- 774	- 864
-3	-6	3	406	482

-3	2	-3	1612	1554
-3	-2	-3	- 840	- 854
-3	-2	4	- 372	- 366
-3	2	5	1998	1724
-3	-2	-5	802	798
-3	-2	6	628	702
-3	-2	7	1742	1764
3	-3	0	958	932
3	-3	-1	1470	1234
-3	-3	1	1374	1442
3	-3	-2	-1144	-1060
-3	-3	-2	- 812	- 846
-3	3	-3	3162	2826
-3	-3	-3	446	430
-3	3	-4	-2060	-1838
-3	-3	-4	486	414
-3	3	-5	-1822	-1614
3	-3	-6	296	122
-3	-3	6	920	928
-3	-3	7	1326	1322
-3	-3	8	334	80
-3	-4	0	1374	1356
3	-4	-1	814	1058
-3	-4	-1	880	936
3	-4	-2	-1334	-1912
-3	-4	-2	636	674
3	-4	-3	- 410	- 436
3	-4	-4	1044	1418
3	-4	5	- 492	- 676
-3	-4	5	738	768
-3	-4	6	398	328
-3	-4	7	994	1086
-3	-4	8	508	454
-3	-5	0	600	562
3	-5	-1	902	792
3	-5	2	-1130	-1070
-3	-5	-2	770	794
3	-5	4	548	454
-3	-5	4	1624	1714
-3	-5	5	1210	1882
3	-5	7	1788	1740
3	-6	0	2090	2180
3	-6	1	912	792
3	-6	2	-2056	-2000
-3	-6	2	636	686
3	-6	-3	622	590
3	-6	4	1856	1786

3	-6	-4	- 252	- 164
3	-6	5	1508	1488
3	-6	6	518	490
-3	-6	7	- 506	- 538
3	-7	1	808	788
3	-7	-2	1302	1306
3	-7	3	- 556	- 486
3	-7	4	1438	1462
3	-7	5	1828	1766
3	-7	6	222	192
3	-8	2	232	280
3	-8	4	1564	1556
3	-8	6	- 392	- 432
3	-9	1	274	96
3	-9	3	784	624
3	-9	7	- 702	- 670
-4	0	0	-2166	-2080
-4	0	-1	1144	1094
-4	0	-2	2268	2250
-4	0	-4	424	378
-4	0	-5	448	550
-4	0	7	- 698	- 716
-4	-1	0	-1186	-1042
-4	1	-1	270	304
-4	-1	-1	- 334	- 208
-4	1	-2	3238	3208
-4	-1	-2	412	372
-4	1	-3	2472	2472
-4	1	4	1646	1602
-4	-1	4	- 456	- 434
-4	1	5	2038	2038
-4	-1	5	- 438	- 446
-4	1	-6	260	150
-4	1	7	- 722	- 704
-4	2	0	266	224
-4	2	1	1844	1654
-4	-2	1	- 242	- 204
-4	2	2	-1282	-1232
-4	-2	2	2380	2316
-4	2	3	- 478	- 462
-4	-2	3	2558	2574
-4	2	-4	- 860	- 800
-4	-2	-4	1258	1302
-4	2	-5	- 498	- 428
-4	2	6	- 356	- 448
-4	-2	6	962	942
-4	-2	7	274	306

-3	-6	4	760	778
-3	-6	5	900	990
3	-6	7	640	656
3	-6	8	430	328
3	-7	2	- 292	- 150
-3	-7	2	870	808
-3	-7	3	418	426
-3	-7	4	510	488
-3	-7	5	976	890
3	-8	0	- 544	- 590
3	-8	3	596	614
3	-8	5	1376	1328
3	-8	7	- 888	- 928
3	-9	2	1384	1380
3	-9	5	714	674
3	-10	5	- 466	- 448
-4	0	1	288	266
-4	0	2	2682	2618
-4	0	-3	588	524
-4	0	5	1608	1604
-4	0	-6	- 280	- 176
-4	1	0	-1222	-1112
-4	1	1	- 718	- 592
-4	-1	1	1174	1106
-4	1	2	- 182	- 190
-4	-1	2	3306	3218
-4	1	3	282	210
-4	-1	3	1832	1838
-4	1	-4	- 330	- 318
-4	-1	-4	854	820
-4	1	-5	- 522	- 504
-4	-1	-5	1250	1320
-4	-1	6	250	302
-4	-1	8	250	76
-4	-2	0	414	390
-4	2	-1	- 772	- 598
-4	-2	-1	422	342
-4	2	-2	2762	2656
-4	-2	-2	- 940	- 964
-4	2	-3	1908	1904
-4	2	4	2480	2364
-4	-2	4	- 874	- 844
-4	2	5	1288	1250
-4	-2	5	- 882	- 846
-4	2	-6	688	606
-4	2	-7	454	400
-4	3	0	3522	3188

-4	-3	0	1402	1390
-4	3	-1	1828	1606
-4	-3	-1	1026	1126
-4	3	-2	- 442	- 200
-4	-3	-2	- 586	- 504
-4	-3	3	560	556
-4	3	4	1014	796
-4	-3	4	- 308	- 310
-4	3	-5	- 750	- 752
-4	3	-6	894	960
-4	3	-7	1230	1560
4	-4	0	4416	4232
4	-4	-1	832	644
-4	-4	1	1146	1164
4	-4	-2	-1366	-1298
-4	-4	2	- 944	-1028
4	-4	-3	538	346
4	-4	-4	310	246
4	-4	-5	- 394	- 324
-4	-4	5	- 542	- 542
-4	-4	6	662	678
-4	-4	7	1656	1686
-4	-4	8	322	286
-4	-5	0	1046	1088
4	-5	-1	588	492
-4	-5	-1	330	222
4	-5	-2	414	570
4	-5	3	- 326	- 474
4	-5	4	1400	1602
4	-5	5	1322	1556
-4	-5	5	536	558
-4	-5	7	270	448
4	-6	0	230	10
4	-6	-1	302	208
4	-6	-2	1990	1948
4	-6	3	- 666	- 644
-4	-6	3	- 346	- 360
4	-6	-4	- 576	- 536
-4	-6	5	1372	1418
4	-6	8	- 260	- 94
4	-7	1	244	204
4	-7	-2	1190	1220
4	-7	-3	694	654
4	-7	5	1344	1416
4	-7	7	- 740	- 760
4	-8	1	318	208
4	-8	2	1946	2030

-4	3	1	1966	1634
-4	-3	1	412	356
-4	3	2	-1164	- 930
-4	-3	2	424	416
-4	3	3	- 602	- 674
-4	-3	-3	- 432	- 350
-4	3	-4	- 604	- 392
-4	3	5	496	442
-4	-3	5	- 438	- 404
-4	-3	6	946	952
-4	-3	7	1274	1366
-4	-4	0	2084	2232
-4	4	-1	1876	1630
-4	-4	-1	410	466
-4	4	-2	-1424	-1270
-4	-4	-2	- 238	- 336
-4	4	-3	258	182
-4	-4	4	334	400
-4	4	-5	- 556	- 456
-4	4	-6	1024	988
-4	4	-7	1456	1418
-4	4	-8	294	298
4	-5	0	916	1266
4	-5	1	608	694
-4	-5	1	494	480
4	-5	2	- 772	- 912
-4	-5	2	- 466	- 514
4	-5	-3	690	972
-4	-5	4	654	770
4	-5	-5	- 392	- 480
-4	-5	6	288	218
4	-5	8	340	196
4	-6	1	612	504
4	-6	2	-1366	-1326
-4	-6	2	- 350	- 340
4	-6	-3	1142	1094
4	-6	4	2528	2500
4	-6	5	2250	2096
4	-6	7	- 234	- 156
4	-7	0	- 512	- 410
4	-7	2	620	554
4	-7	3	370	316
4	-7	4	894	858
4	-7	6	230	224
4	-8	0	-1008	-1084
4	-8	-1	336	182
4	-8	3	1082	992

4	-8	5	608	468
4	-8	7	- 734	- 704
4	-9	2	1230	1280
4	-9	5	- 294	- 374
4	-10	4	- 452	- 586
-5	0	0	- 504	- 452
-5	0	-1	-1272	-1202
-5	0	-2	1612	1560
-5	0	4	1404	1404
-5	0	5	1392	1398
-5	0	7	- 778	- 710
-5	-1	0	-2260	-2208
-5	1	-1	1728	1620
-5	-1	-1	592	532
-5	1	-2	2308	2242
-5	-1	-2	1488	1508
-5	1	-3	362	228
-5	-1	-3	888	862
-5	1	-4	-1094	-1112
-5	-1	-4	586	590
-5	1	-5	- 336	- 390
-5	1	6	- 484	- 420
-5	1	7	406	420
-5	2	0	2782	2692
-5	2	1	442	518
-5	-2	1	562	538
-5	2	2	-1822	-1704
-5	-2	2	1606	1556
-5	2	3	- 676	- 684
-5	-2	3	184	174
-5	2	5	1134	1066
-5	-2	5	804	794
-5	2	-6	438	374
-5	-2	7	- 262	- 222
-5	-3	0	744	732
-5	3	-1	444	508
-5	-3	-1	386	328
-5	3	-2	-1120	-1020
-5	3	3	1312	1228
-5	3	4	1278	1164
-5	-3	4	-1204	-1190
-5	3	-5	794	664
-5	3	-6	972	884
-5	3	-7	372	550
-5	4	0	1630	1410
-5	4	1	1794	1584
-5	4	2	2072	1778
4	-8	6	- 538	- 472
4	-9	0	- 490	- 456
4	-9	3	1166	1182
4	-10	3	720	746
4	-10	5	- 402	- 524
-5	0	1	1726	1674
-5	0	2	706	546
-5	0	-3	1626	1598
-5	0	-4	- 348	- 208
-5	0	6	- 236	- 222
-5	1	0	1110	958
-5	1	1	1266	1146
-5	-1	1	-1272	-1246
-5	1	2	-1100	-1048
-5	-1	2	2356	2298
-5	1	3	-1226	-1154
-5	-1	3	1702	1720
-5	1	4	1656	1670
-5	-1	4	538	502
-5	1	5	1206	1228
-5	-1	5	1328	1234
-5	1	-6	368	442
-5	-1	7	- 964	- 968
-5	-2	0	- 744	- 730
-5	2	-1	1248	1142
-5	-2	-1	492	460
-5	2	-2	700	562
-5	-2	-2	640	652
-5	2	-3	1658	1626
-5	2	4	938	914
-5	2	-5	-1366	-1412
-5	2	6	612	622
-5	-2	6	508	500
-5	3	0	3040	2970
-5	3	1	660	584
-5	-3	1	478	472
-5	3	2	-1234	-1210
-5	-3	2	1538	1546
-5	-3	3	1704	1676
-5	3	-4	556	512
-5	3	5	- 702	- 692
-5	-3	5	-1530	-1536
-5	-3	6	976	958
-5	-3	7	996	984
-5	-4	0	1070	1128
-5	4	-1	690	604
-5	4	-2	-1914	-1716

-5	-4	2	636	688
-5	4	-3	-1358	-1140
-5	4	4	- 966	- 776
-5	-4	4	- 252	- 252
-5	4	-5	1308	1274
-5	4	-6	658	520
-5	4	-7	796	898
5	-5	0	1364	1364
-5	5	-1	1712	1622
-5	5	-2	-1372	-1252
5	-5	-3	1096	1110
5	-5	-4	- 668	- 686
-5	-5	4	546	602
-5	5	-6	324	134
5	-6	0	-1110	-1642
5	-6	2	1256	1822
5	-6	3	948	1216
5	-6	4	736	916
5	-6	7	- 796	- 970
5	-7	2	1182	1176
5	-7	3	820	656
5	-7	5	1106	1122
5	-7	7	- 828	- 764
5	-8	3	1142	1180
5	-8	5	- 708	- 692
5	-8	7	370	412
5	-9	2	1096	1156
5	-9	4	- 762	- 762
-6	0	1	- 318	- 256
-6	0	2	- 600	- 544
-6	0	3	- 262	- 242
-6	0	4	1672	1610
-6	1	0	2292	2288
-6	1	1	1306	1264
-6	-1	1	994	926
-6	1	2	-1048	-1104
-6	-1	2	- 352	- 354
-6	1	-3	994	980
-6	-1	-3	686	766
-6	-1	4	1288	1326
-6	-1	5	1582	1652
-6	-1	7	- 354	- 346
-6	-2	0	- 690	- 736
-6	2	-1	1314	1238
-6	2	2	- 522	- 618
-6	-2	2	1746	1682
-6	2	-3	- 946	- 852

-5	4	3	846	626
-5	-4	3	852	868
-5	4	-4	1464	1444
-5	4	5	- 884	- 680
-5	-4	5	- 372	- 404
-5	-4	6	310	348
-5	-4	7	516	510
5	-5	-1	- 362	- 324
5	-5	-2	1174	1126
-5	-5	2	- 346	- 394
-5	5	-3	- 670	- 708
-5	5	-4	1804	1696
-5	5	-5	1544	1424
-5	-5	6	470	462
5	-6	1	- 478	- 298
5	-6	-2	852	1414
5	-6	-3	450	808
5	-6	5	944	1274
5	-7	0	-1362	-1354
5	-7	-2	1072	1112
5	-7	4	1214	1230
5	-7	6	- 406	- 458
5	-8	2	1360	1460
5	-8	4	- 788	- 792
5	-8	6	648	688
5	-9	1	354	312
5	-9	3	874	856
5	-9	5	- 706	- 728
-6	0	-1	1036	908
-6	0	-2	1608	1640
-6	0	-3	966	952
-6	0	5	1536	1540
-6	-1	0	- 414	- 248
-6	1	-1	- 232	- 250
-6	-1	-1	220	184
-6	1	-2	- 378	- 322
-6	-1	-2	1646	1682
-6	-1	3	- 978	- 932
-6	1	4	1224	1192
-6	1	5	292	306
-6	1	6	286	68
-6	2	0	2732	2770
-6	2	1	1244	1284
-6	-2	1	254	164
-6	2	-2	- 610	- 546
-6	-2	-2	738	722
-6	-2	3	1056	1032

-6	2	4	404	354
-6	-2	4	- 208	- 242
-6	2	-5	500	354
-6	-2	6	298	254
-6	-3	0	- 752	- 702
-6	3	-1	1230	1292
-6	3	2	654	644
-6	-3	2	1608	1718
-6	3	-3	- 202	- 236
-6	3	4	- 646	- 620
-6	-3	4	- 328	- 20
-6	-3	5	494	416
-6	4	1	- 492	- 408
-6	4	2	1416	1318
-6	-4	2	778	754
-6	-4	3	822	794
-6	-4	4	- 280	- 270
-6	4	-5	1674	1616
-6	5	0	-1662	-1448
-6	5	-1	- 436	- 374
-6	5	-2	676	664
-6	5	4	- 318	- 266
-6	5	-5	1634	1564
-6	6	-1	1010	908
-6	6	-2	1514	1354
-6	6	-4	382	366
6	-7	-1	336	184
6	-7	3	1460	1946
6	-7	5	- 492	- 738
6	-8	1	250	166
6	-8	2	952	1026
6	-8	4	- 336	- 222
6	-8	6	392	268
6	-9	2	- 346	- 218
6	-9	5	- 552	- 544
-7	0	1	796	794
-7	0	2	-1000	-1050
-7	0	3	- 302	- 320
-7	0	4	810	868
-7	-1	0	738	672
-7	1	-1	804	770
-7	-1	-1	272	184
-7	1	-2	- 410	- 466
-7	-1	3	- 298	- 290
-7	1	-4	414	412
-7	-1	5	906	952
-7	2	0	1154	1282
-6	2	-4	- 252	- 198
-6	2	5	- 786	- 734
-6	-2	5	426	310
-6	3	0	1784	1778
-6	3	1	384	278
-6	-3	1	246	12
-6	3	-2	-1062	-1098
-6	3	3	486	560
-6	-3	3	864	980
-6	3	-4	1206	1296
-6	3	-5	372	334
-6	4	0	226	156
-6	4	-1	524	318
-6	4	-2	- 664	- 624
-6	4	3	1990	1876
-6	4	-4	1668	1616
-6	4	5	- 436	- 478
-6	-4	5	- 310	- 442
-6	5	1	1110	882
-6	5	2	2664	2242
-6	5	3	898	678
-6	5	-4	1280	1202
6	-6	0	- 592	- 646
6	-6	-2	958	988
-6	6	-3	656	540
-6	6	-5	388	348
6	-7	2	1468	2290
6	-7	4	- 602	- 634
6	-8	0	316	240
6	-8	-1	490	450
6	-8	3	700	706
6	-8	5	- 254	- 194
6	-9	1	438	450
6	-9	4	- 328	- 270
-7	0	0	1572	1508
-7	0	-1	442	562
-7	0	-2	492	506
-7	0	-3	322	310
-7	1	0	1804	1788
-7	1	1	550	570
-7	-1	1	612	572
-7	1	2	- 650	- 626
-7	-1	2	- 526	- 484
-7	1	4	454	502
-7	-1	4	1062	1044
-7	1	6	306	374
-7	-2	0	- 808	- 776

-7	2	-1	526	564
-7	2	-2	-1040	-1070
-7	2	3	1362	1412
-7	2	4	- 352	- 292
-7	-2	4	772	846
-7	-2	5	1026	1140
-7	3	1	712	738
-7	3	2	1516	1522
-7	-3	2	514	486
-7	3	-3	- 410	- 334
-7	3	4	- 612	- 608
-7	-3	4	440	432
-7	3	-5	1074	1080
-7	4	1	- 328	- 178
-7	4	2	1464	1590
-7	4	3	692	712
-7	4	-5	896	928
-7	5	-1	- 366	- 170
-7	5	-2	1570	1528
-7	5	-3	1480	1376
-7	5	-5	364	278
-7	6	1	480	454
-7	6	-3	1072	924
7	-7	-1	546	642
7	-7	-2	- 374	- 288
-7	7	-3	884	738
-7	7	-5	- 886	- 816
7	-8	0	686	1352
7	-8	3	478	392
-8	0	0	1702	1674
-8	0	-1	498	420
-8	0	4	510	460
-8	1	-1	616	570
-8	1	2	632	632
-8	-1	2	- 336	- 268
-8	1	4	- 320	- 340
-8	2	1	356	298
-8	2	2	1004	1062
-8	2	3	804	758
-8	3	0	- 852	- 868
-8	3	-1	376	312
-8	3	-2	638	588
-8	3	4	- 266	- 278
-8	4	1	348	490
-8	4	-2	1020	1082
-8	4	-4	358	374
-8	5	-1	430	480

-7	2	2	768	782
-7	-2	2	522	506
-7	2	-3	- 266	- 286
-7	2	-4	838	836
-7	2	5	- 806	- 792
-7	3	0	384	428
-7	3	-1	208	186
-7	3	-2	- 640	- 594
-7	3	3	932	918
-7	-3	3	306	292
-7	3	-4	920	992
-7	3	5	- 418	- 432
-7	4	0	- 810	- 908
-7	4	-1	682	768
-7	4	-2	770	804
-7	4	-4	834	898
-7	5	0	-1340	-1218
-7	5	2	1064	1014
-7	5	3	328	312
-7	5	-4	576	524
-7	6	0	- 450	- 400
-7	6	-2	1772	1600
7	-7	0	550	570
-7	7	-1	584	442
-7	7	-2	1084	1068
-7	7	-4	- 722	- 652
-7	7	-6	408	382
7	-8	1	396	622
7	-9	2	- 260	- 312
-8	0	1	658	562
-8	0	2	- 620	- 674
-8	1	0	654	698
-8	-1	1	518	420
-8	1	-2	- 380	- 262
-8	1	3	900	878
-8	2	0	302	360
-8	2	-1	250	202
-8	2	-2	- 630	- 628
-8	2	4	- 294	- 366
-8	3	1	- 278	- 144
-8	3	2	1466	1558
-8	3	3	990	1002
-8	4	0	- 784	- 794
-8	4	2	928	904
-8	4	-3	888	810
-8	5	0	- 246	- 400
-8	5	-2	1486	1604

-8	5	-3	764	808
-8	6	0	486	504
-8	6	-1	- 252	- 28
-8	6	-2	1002	906
-8	6	-4	- 276	- 318
-8	7	-1	894	688
-8	8	-2	- 454	- 416
-9	2	2	1030	1042
-9	3	2	824	944
-9	4	-2	1002	1026
-9	5	1	434	514
-9	5	-2	838	918
-9	6	-1	306	500

-8	5	-4	- 262	- 328
-8	6	1	770	716
-8	6	2	- 272	- 418
-8	6	-3	1052	1048
-8	7	0	1472	1226
-8	8	-1	376	306
-9	2	0	- 752	- 746
-9	3	0	- 644	- 774
-9	4	1	428	416
-9	5	0	476	484
-9	5	-1	380	386
-9	6	0	894	934
-9	6	-2	286	128

REFERENCES

Arndt, U.W. (1963) Hilger J. 8 4

Arndt, U.W., Faulkner, T.H. and Phillips, D.C. (1960) J.Sci.Instr. 37 68

Arndt, U.W. and Phillips, D.C. (1959) Br.J.App.Phys. 10 116

Arndt, U.W. and Phillips, D.C. (1961) Acta Cryst. 14 807

Barnes, W.H., Przybylska, M. and Shore, V.C. (1951) Am.Min. 36 430

Beattie, I.R., McQuillan, G.P., Rule, L. and Webster, M. (1963) J.Chem.Soc. 1514

Beattie, I.R., Gilson, T., Webster, M. and (in part) McQuillan, G.P. (1964) J.Chem.Soc. 238

Beattie, I.R., Gilson, T.R. and Ozin, G.A.S. (1968) J.Chem.Soc. (A) in press

Beattie, I.T. and Webster, M. (1965) J.Chem.Soc. 3672

Beevers, C.A. and McGeachin, H.McD. (1957) Acta Cryst. 10 227

Binns, J.V. (1964) J.Sci.Instr. 41 715

Bond, W.L. (1951) Rev.Sci.Instr. 22 344

Bradley, A.J. and Jay, A.H. (1933) Proc.Phys.Soc. 45 507

Bragg, W.L., James, R.W. and Bosanquet, C.H. (1921) Phil.Mag. 42 1

Buerger, M.J. (1944) The Photography of the Reciprocal Lattice : A.S.X.R.E.D. Monograph No. 1

Buerger, M.J. (1960) Crystal Structure Analysis, P.123: J. Wiley and Sons.

Calvert, D. (1958) Ph.D. Thesis, St. Andrews.

Campbell-Ferguson, H.J. and Ebsworth, E.A.V. (1967) J.Chem.Soc.(A) 705

Clark, J.P. and Wilkins, C.J. (1966) J.Chem.Soc.(A) 871

Cochran, W. (1950) Acta Cryst. 3 268

Cox, E.G. and Shaw, W.F.B. (1930) Proc.Roy.Soc.(A) 127 71

Cruickshank, D.W.J. (1949) Acta Cryst. 2 154

Cruickshank, D.W.J. (1956) Acta Cryst. 9 747

Cruickshank, D.W.J. (1965) Computing Methods in Crystallography: Pergamon Press.

Cruickshank, D.W.J. et al (1961) Computing Methods and the Phase Problem in X-Ray Crystal Analysis : Pergamon Press

Cruickshank, D.W.J. and Robertson, A.P. (1953) Acta Cryst. 6 698

Darlow, S.F. (1960) Acta Cryst. 3 268

Davies, P.T. (1950) J.Sci.Instr. 27 338

Debye, P. (1914) Annln Phys. 43 49

Delange, J.J., Robertson, J.M. and Woodward, I. (1939) Proc.Roy. Soc. 171 398

Delaunay, B. (1933) Zeit.f.Krist. 84 132

Doyle, P.A. and Turner, P.S. (1967) Acta Cryst. 22 153

Ewald, P.P. (1921) Zeit,f,Krist. 56 129

Evans, H.T., Tilden, S.G. and Adams, D.P. (1949) Rev.Sci.Instr. 20 155

Ferrier, W.G., Killean, R.C.G. and Young, D.W. (1962) Acta Cryst. 15 911

Fisher, D.J. (1952) Am.Min. 37 1036

Fisher, D.J. (1953) Am.Min. 38 399

Furnas, T.C. (1957) Single Crystal Orienter Instruction Manual: General Electric Corporation.

Grant, D.F., Killean, R.C.G. and Lawrence, J.L. (1968) Acta Cryst. in press.

Grdenić, D. (1965) Quart.Rev. (Chem.Soc.Lond.) 19 303

Hamilton, W.C. Acta Cryst. 8 199 (1955)

Hein, Fr. and Wagler, K. (1925) Ber. 58 1499

Hodgson, L.I. and Rollett, J.S. (1963) Acta Cryst. 16 329

Hughes, E.W. (1941) J.Am.Chem.Soc. 63 1737

Hulme, R., Leigh, G.J. and Beattie, I.R. (1960) J.Chem.Soc. 366

Howells, R.G., Phillips, D.C. and Rogers, D. (1950) Acta Cryst. 3 210

Iball, J. (1954) J.Sci.Instr. 31 71

Keith, H.D. (1950) Proc.Phys.Soc. (B) 63 208 1034

Keith, H.D. (1955) Am.Min. 40 530

Kitaigorodskii, A.I. (1957) The Theory of Crystal Structure Analysis; Translation 1961, P.249: New York, Heywood

Lipson, H.S. and Wilson, A.J.C. (1941) Proc.Phys.Soc. 53 245

Miller, P.H. and DuMond, J.W.M. (1940) Phys.Rev. 57 198

Muetterties, E.I. (1960) J.Am.Chem.Soc. 82 1082

Ozin, G.A.S. (1967) D. Phil. Thesis, Oxford.

Pakhomov, V.I. (1966) Acta Cryst. 21 (supp.) A125

Patterson, A.L. (1934) Phys.Rev. 46 372

Patterson, A.L. (1935) Zeit.f.Krist. 90 517

Patterson, A.L. and Love, W.E. (1957) Acta Cryst. 10 111

Pauling, L. (1948) The Nature of the Chemical Bond: Cornell University Press.

Phillips, D.C. (1954) Acta Cryst. 7 746

Renninger, M. (1937) Zeit.f.Krist. 97 107

Robertson, J.M. (1943) J.Sci.Instr. 20 175

Rogers. D. (1954) Acta Cryst. 7 628

Rogers, D. (1965) Computing Methods in Crystallography: Pergamon Press.

Ross, P.A. (1928) J.Opt.Soc.Am. 16 375, 433

Schomaker, V., Shoemaker, D.R., Donahue, J. and Corey, R.B. (1950) J.Am.Chem.Soc. 72 2328

Sim, G.A. (1961) Computing Methods and the Phase Problem in X-Ray Crystal Analysis: Pergamon Press.

Sparks, R.A. (1961) ibid.

Truter, M.R. (1967) Acta Cryst. 22 556

Tunnell, G. (1939) Am.Min. 24 448

Waller, I. (1927) Ann.Physik 83 153

Wegener, H.A.R. (1961) Zeit.f.Krist. 115 185

Weisz, O. and Cole, W.F. (1948) J.Sci.Instr. 25 213

Whittaker, E. and Robinson, G. (1944) The Calculus of Observation: Blackie and Son.

Wiebenga, E.H. (1947) Rec.Trav.Chim. 66 746

Wiebenga, E.H. and Smits, D.W. (1950) Acta Cryst. 3 265

Wilson, A.J.C. (1942) Nature 150 152

Some useful textbooks

not included in the list of references

Arndt, U.W. and Willis, B.T.M. (1966) Single Crystal Diffractometry: Cambridge University Press

Buerger, M.J. (1942) X-Ray Crystallography: J. Wiley and Sons.

Buerger, M.J. (1959) Vector Space: J. Wiley and Sons.

Buerger, M.J. (1964) The Precession Method: J. Wiley and Sons.

Henry, N.F.M., Lipson, H. and Wooster, W.A. (1951) The Interpretation of X-Ray Diffraction Photographs: MacMillan

International Tables for X-Ray Crystallography; Vols. I,II,III

James, R.W. (1948) The Optical Principles of the Diffraction of X-Rays: G. Bell and Sons.

Leeson, D.N. and Dimitry, D.L. (1962) Basic Programming Concepts and the IBM 1620 Computer: Holt, Rinehart and Winston, Inc.

Lipson, H. and Cochran, W. (1966) The Determination of Crystal Structures: G. Bell and Sons.